A first look at monotreme meiotic recombination

Master's thesis

Sonia Horan
Supervisors:
Dr. Frank Grützner
Dr. Enkhjargal Tsend-Ayush
Dr. Tasman Daish

Fall, 2012

Abstract

Recombination is a critical event in meiosis required for proper chromosome segregation; however, despite its importance, crossovers have not yet been analysed in egg-laying mammals, representing an extant species from the most basal of the contemporary mammalian lineage. The platypus is a unique species in that it has a complex system of ten sex chromosomes that form a chain in meiosis, and the segregation of this chain raises many questions regarding the state of meiotic recombination among chain members. This study aimed to set a foundation for recombination studies in the platypus. 15 genes essential for crossover formation were analysed; while most of these genes showed generally high levels of conservation, surprisingly it was found that Mei4 and Rec114 are not expressed during platypus meiosis. This raises several questions about the platypus double-strand break induction mechanism in which these genes have an essential function in other mammals. Furthermore, characterisation of the crossover hotspot-determining protein, Prdm9, shows that the platypus protein differs significantly from the Prdm9 of eutherians, suggesting that the gene underwent rapid evolution after the divergence of monotremes nearly 200 Million years ago. This study also aimed to examine the distribution of crossovers in meiotic cells using Mlh1 as a marker for crossover events. Despite conservation of the protein and expression and some specific staining overall, crossover counts could not be analysed in platypus male meiotic cells. Surprisingly another protein which can be found in earlier meiotic stages, Dmc1, showed a very distinct pattern in platypus pachytene cells. It was observed that an average of 24 Dmc1 foci were present in platypus pachytene, long after Dmc1 is expected to have diminished from chromosome cores. These foci seemed to localise to the ends of chromosomes and were more prominently associated with the sex chromosomes, particularly the pseudoautosomal regions. Together with other evidence this suggests that the Dmc1 antibody may be cross-reacting with Rad51, which plays a structural role in pachytene, holding chromosomes together at the telomeres. Overall this work provides first evidence for a general conservation of genes involved in the recombination pathway but has also identified some genes that may have diversified in their function.

Thesis declaration

This work contains no material which has been accepted for the award of any other degree or diploma in any university or other tertiary institution to Sonia Adeline Horan and, to the best of my knowledge and belief, contains no material previously published or written by another person, except where due reference has been made in the text. I give consent to this copy of my thesis, when deposited in the University Library, being made available for loan and photocopying, subject to the provisions of the Copyright Act 1968.

The author acknowledges that the copyright of published works contained within this thesis (as listed below*) resides with the copyright holder(s) of those works. I also give permission for the digital version of my thesis to be made available on the web, via the University's digital research repository, the Library catalogue, the Australasian Digital Theses Program (ADTP) and also through web search engines, unless permission has been granted by the University to restrict access for a period of time.

X

Sonia Adeline Horan
postgraduate student

* Figure 1 (page 15 Whitby, 2005), Figure 2 (page 21 Shinohara & Shinohara, 2004), Figure 3 A (page 28 Oliver-Bonet, Turek, Sun, Ko, & Martin, 2005), Figure 4 (page 37 Grützner, Deakin, Rens, El-Mogharbel, & Marshall Graves, 2003), Figure 5 (page 38 Daish, Casey, & Grutzner, 2009), and Figure 37 (page 94, Veyrunes et al., 2008).

Acknowledgements

I must first and foremost recognise the efforts of Dr Frank Grützner and Dr Tasman Daish not only for welcoming me into the lab and all their assistance in with experimental design and troubleshooting, but also for their boundless patience editing drafts of this thesis. This thesis would not have been possible without them. Thanks also go out to my mother, Dr Sheila Horan, for all her help in designing a statistical model with which to analyse the data. To all the members of the Grützner lab, especially Aaron Casey, Megan Wright, Shu Lim, David Stevens, Enkhjargal Tsend-Ayush, and Dan Kortschak, thank you for showing me the ropes.

Thanks also go to my family, for all your support, emotional and financial, I am lucky to have to all. To my friends state-side—thank you for ensuring I never went insane. To Fanny, Pete, Loz, Tara, Fiona, Maria, and Nora, you all gave me a true Aussie family and helped me call (R)Adelaide home; thank you all. Thank you to Thea for your phenomenal distractions and in-depth discussions of gender, sex, and sexuality. And last, thanks to Alex, Dylan, and Jackson for being the greatest of pen pals—I swear I will write you back some day!

Chapter 1: Background: Meiosis and the DSB machinery

Introduction to meiosis

Meiosis is a specialised cell division necessary for the formation of gametes. In most instances the complex process of the meiotic division begins in the gonads with the diploid nucleus of a germ cell containing two homologous copies (one paternal and one maternal) of each chromosome. After one round of DNA replication the diploid germ cell undergoes two consecutive cell divisions producing four haploid gametes. In males these progeny cells are termed spermatozoa while in females, three polar bodies and one mature ovum are produced. As meiosis results in the production of gametes, it follows that it is essential for all sexual reproduction, but more to the point, sexual reproduction generally hinges on recombination, the process of forming crossovers between homologous chromosomes. In what has become a somewhat dogmatic perspective, crossovers have three widely-recognised functions. First, they promote genetic diversity by creating new and potentially beneficial allelic combinations (Whitby, 2001). Second, crossovers can remove deleterious mutations that would otherwise decay genetic information (e.g. *Drosophila* Y chromosome preservation) (Carvalho, 2003). Last, the physical connection made by the chiasmata is necessary for proper chromosome segregation (Whitby, 2001; Roeder, 1997).

Unlike mitosis—the process of somatic cellular division—meiosis has a linear directionality; it is not cyclical. At the end of Interphase a diploid number of chromosomes exists, each consisting of a pair of sister chromatids. The second meiotic division (meiosis II, also termed the equational division) is similar to mitosis in that sister chromatids are segregated into daughter cells at anaphase II. It is the first division (meiosis I, also known as the reductional division) that makes meiosis distinct from mitotic division. Meiosis I produces two haploid daughter cells: secondary spermatocytes in males, a secondary oocyte and a polar body in females. Like mitosis and meiosis II, meiosis I is divided into several distinct stages. The first of these, prophase I, is what truly sets meiosis apart. This stage is further divided into five distinct substages that can be characterised by chromosomal events and the status of the proteinaceous synaptonemal complex (SC) (Table 1). Throughout these five stages, three key processes take place: (1) chromosome pairing is the interaction between homologous

chromosomes resulting in their juxtaposition and the formation of bivalents. This includes two major events: chromosomes must first come into close physical proximity and they must also undergo a step of homology recognition (Pawlowski & Cande, 2005). (2) Synapsis is the establishment of the proteinaceous synaptonemal complex (SC) structure between two homologous chromosomes. (3) Meiotic recombination, the intricate series of events spanning a period of DNA double strand break initiation to the completion of the repair process, resulting in the formation of chiasmata via reciprocal chromosome arm exchange. These processes are highly complex and although described here as separate events, their interdependence and precisely orchestrated coordination should not be overlooked (reviewed in Pawlowski & Cande, 2005). The error-free completion of each of these processes is required as any mistakes in meiosis can result in a variety of deleterious consequences ranging from infertility to miscarriage or severe birth defects.

Table 1: Events of prophase I Outlined here is the progression of chromosome pairing, synapsis, and homologous recombination over the five stages of prophase I.

Stage	SC components	Synapsis and chromosome morphology	Bouquet formation	DSB repair	Signs of recombination
Leptotene	Axial elements (SCP3/Cor1, SCP2) begin to form	Single homologues comprised of sister chromatids	Telomeres spread along nuclear envelope	DSBs appear	Early nodules
Zygotene	Axial elements become lateral elements; central region (SCP1/Syn1, Tex12, SYCE1, SYCE2) forms	Partial synapsis, centromeres are closely paired	Telomeres closely clustered	DSBs disappear	Early nodules
Pachytene	Lateral elements persist, central element fully formed	Full synapsis (except XY), compacted bivalents	Telomeres disperse	Double Holliday junctions	Late nodules
Diplotene	All components begin to dissociate	Chromosomes paired at chiasmata only.		Mature crossovers	Chiasmata
Diakinesis	Components dissociated except around the centromere	Further chromosome compactions, chiasmata link persists			Chiasmata

It has been estimated that 10-25% of human foetuses have the “wrong” number of chromosomes (Hunt & Hassold, 2002; Hassold & Hunt, 2001). Furthermore, nearly one third of spermatogenesis is spent in meiosis, and more than 90% of that time is spent in prophase

I—and most of that time is spent in Pachytene finalising crossovers (Cobb & Handel, 1998). This underscores the critical importance of meiosis—and crossing over in particular—to sexual reproduction and, therefore, to the persistence of sexually reproductive organisms.

The double strand break (DSB) repair pathway of meiotic recombination

The proteins catalysing the recombination pathways were first identified in yeast and later in nematode, fly, mouse, and humans; however, while many groups are utilising other model organisms, generally most meiotic recombination studies have been performed in yeast, C. elegans, or mouse. Effectively little is known about the evolution and diversity of recombination mechanisms in reptilian and mammalian lineages, with new variations still being discovered. Recent findings indicate that crossovers and non-crossovers arise from different branches of the same pathway. DSBs seem to be the initiating factor of both routes, as mutations preventing DSB formation and processing also eliminate both COs and NCOs, but new evidence has challenged the hypothesis that NCOs and COs arise from the same double Holliday junction (dHJ)-containing intermediates. First, studies in budding yeast have shown that NCOs and COs do not form in temporal unison; rather, NCOs form before COs (Allers & Lichten 2001). It has also been shown that mutants with reduced SEI or dHJ have consequent reductions in CO, but not NCO, frequencies (Börner, Kleckner, & Hunter, 2004).

While NCO-specific intermediates have not been identified there is a proposed mechanism: Synthesis-Dependent Strand-Annealing (SDSA). An overview of SDSA and its relation to the CO-producing repair pathway can be seen in Fig. 1.

In addition to these two complicated recombination models, there is yet more complexity as there is more than one pathway regulating crossovers. Indeed, there are at least two crossover pathways just in budding yeast: the Msh4-Msh5[1] pathways (also called the ZMM-dependent pathway) and the Mus81-Eme1/Mms4 pathway (Fig. 1). While the former is subject to crossover interference—a phenomenon preventing two crossovers from forming closely together—the latter is not, and both pathways, in addition to the SDSA model, are all initiated by DSBs (Cromie & Smith, 2007).

[1] Note on gene and protein nomenclature: gene names are italicised while protein names are not; additionally, human and chicken gene and protein names are all capitalised (e.g. for a gene: *SHH* and a protein: SHH), while most other eukaryotic genes and proteins are written with only the first letter capitalised (e.g. for a gene: *Shh* and a protein: Shh). Bacterial proteins are written the same as non-human/chicken proteins; however, bacterial and yeast genes are all lower-cased and italicised.

Figure 1: The DSB repair pathways DSBs are initiated and 5′-end resection produces 3′ tails in all pathways. In steps 3a-7a the ZMM-dependent pathway produces crossovers subject to interference. Rad51 catalyses single end invasion as Mer3 extends the newly formed heteroduplex region (3a) as Msh4-Msh5 forms a sliding clamp around the resulting Holliday junctions (3a-6a) as DNA synthesis extends the D-loop (4a) and second end capture (5a) spur on the production of the double Holliday junction (6a). The dHJ is then resolved (7a). The SDSA involves a temporary single end invasion (3b) followed by DNA synthesis (4b). The extended 3′ tail is then unwound (5b) and reannealed, resulting in a non-crossover (6b). The Mus81-dependent pathway (3c-6c) produces interference insensitive crossovers. After single end invasion (3c), the invading strand is cut. DNA synthesis extends the resulting semi-D-loop (4c), allowing for the formation of a single Holliday junction (5c). Resolution of the sHJ results in a crossover. Other, more complex joint molecules consisting of three and four interconnected duplexes are formed between homologues and sister chromatids in the absence of the BLM orthologue, Sgs1 (not shown here) (Figure from Whitby, 2005).

Regulation of meiotic recombination

DSB initiation and 5' resection

DSBs do not form randomly along the chromosomes; rather specific regions, termed "hotspots" tend to be preferential sites of DSB induction (Koehn, Haring, Williams, & Malone, 2009; Gerton et al., 2000; Sun et al., 1989). These hotspots tend to occur in the promoter regions of genes but are generally absent vincinal the centromeres and telomeres (Blat, Protacio, Hunter, & Kleckner, 2002; Petes, 2001; Baudat & Nicolas, 1997). Genome-wide microarray studies have further suggested that hotspots occur preferentially in high GC chromosomal domains, however, no obvious consensus sequence has ever been linked to hotspots (Haring, Lautner, Comeron, & Malone, 2004). A large number of proteins have been shown to govern the recombination pathway, and moreover at least ten proteins (Spo11, Rec102, Rec104, Ski8/Rec103, Rec114, Mei4, Rec107/Mer2, Mre11, Rad50, and Xrs2) have been identified as being essential in initiating meiotic recombination via DSB induction (Keeney, 2001). Null mutations of these ten genes are indistinguishable from one another in an *S. cerevisiae* model—all result in an absence of DSBs or recombination, disrupted synapsis, and unviable spores (Koehn et al., 2009). Other studies have demonstrated that these ten proteins function within three sub-complexes: (1) the Spo11-sub-complex, comprised of Spo11, Ski8, Rec102, and Rec104 (Arora, Kee, Maleki, & Keeney, 2004; Cheng, Liu, Wang, Parker, & Song, 2004; Kee, Protacio, Arora, & Keeney, 2004; Jiao, Salem, & Malone, 2003; Kee & Keeney 2002; Uetz et al., 2000; Salem, Walter, & Malone, 1999); (2) the Rec114-sub-complex, consisting of Rec114, Rec107, and Mei4 (Sasanuma et al., 2008; Maleki, Neale, Arora, Henderson, & Keeney, 2007; Henderson, Kee, Maleki, Santini, & Keeney, 2006; Li, Hooker, & Roeder, 2006; Arora et al., 2004); and (3) the MRX-sub-complex, made up of Mre11, Rad50, and Xrs2 (Borde, 2007). While it has been suggested these ten proteins function as a holocomplex, the exact mechanism by which they collectively form DSBs has been challenging to define.

Among the first meiotic recombination-associated proteins to be identified was Spo11 (Klapholz, 1985; Esposito, 1969). The original DSBs that initiate all the recombination repair branches are made by Spo11, a meiosis-specific protein with homology to an archeal type II topoisomerase (Bergerat et al., 1997). The Spo11-initiated DSBs have further been implicated as necessary for synapsis and sex body formation (Bellani, Romanienko, Cairatti, & Camerini-Otero, 2005). *Spo11* is evolutionarily extremely well conserved, with orthologues

present in yeast (Lin & Smith, 1994), fly (McKim & Hayashi-Hagihara, 1998), *C. elegans* (Dernburg et al., 1998), mouse and humans (Shannon, Richardson, Christian, Handel, & Thelen, 1999). Several studies aiming to retard recombination showed that when DSBs were induced (with all subsequent resolution was prevented) Spo11 was found covalently linked to the 5′ terminus of the broken DNA (Keeney, Giroux, & Kleckner, 1997). Cytological studies show that Spo11 forms foci on chromatin during leptotene in mouse, *Sordaria macrospora,* and *S. cerevisiae* (Prieler, Penkner, Borde, & Klein, 2005; Storlazzi et al., 2003; Romanienko & Camerini-Otero 2000), but strangely enough, Spo11 is present in greater quantities than what is simply required for DSB formation (Neale, Pan, & Keeney, 2005), and the Spo11 foci persist on chromatin at hotspots well into Pachytene (Prieler et al., 2005; Storlazzi et al., 2003; Romanienko & Camerini-Otero, 2000). It is still unknown what, if any, purpose the persistence of Spo11 has (Keeney, 2007).

In contrast to Spo11, the role of Mei4 and Rec114 in mammalian DSB formation was only recently discovered. To date, the mammalian Mei4 and Rec114 protein structures have only been characterised in a series of short signature sequence motifs (SSMs) located mostly in the N- and C-termini of the proteins (Kumar, Bourbon, and de Massey, 2010). Altogether the SSMs only constitute approximately 20% of the total protein sequences, which has been interpreted as a reflection of the overall low amino acid sequence identity of the proteins across species (Kumar et al., 2010). Kumar et al. (2010) found that the six SSMs of yeast Mei4 form alpha-helical or coiled coil structures, which they propose are indicative of protein-protein interactions. In contrast, they also predicted SSMs 1-6 of Rec114 form beta-sheet structures of unknown biochemical functions. Using these data, they were able to identify orthologues of *Mei4* and *Rec114* in most eukaryotes (excluding Sordariomycetes, *C. elegans*, and *Drosophila*), including mammals. This study also found that the N-terminal region of Mei4, but not the C-terminal, is necessary for interaction with Rec114. Furthermore, both the N- and C-terminal regions of Rec114 are needed for this interaction. Kumar et al. also tested mouse *Mei4* mutants finding that in the absence of Spo11, Mei4 foci are present in wildtype numbers; however, in *Mei4* mutants DSBs are not induced. They thus concluded that Mei4—and by extension Rec114—play a structural role in DSB induction (while Spo11 actually makes the DSB), yet the mechanisms of this function are still not known.

After DSB induction, the 5′ termini are resected via 5′-to-3′ exonucleolytic action of the MRX-sub-complex. It has since been observed that mutations in *rad50*, *mre11*, and *com1/sae2* result in failure to resect DSBs (McKee & Kleckner, 1997; Nairz & Klein, 1997; Prinz, Amon, & Klein, 1997; Alani, Padmore, & Kleckner, 1990). In cases of *rad50* and

mre11, null mutations also result in failure to induce DSBs, suggesting they are intimately involved in the formation and processing of DSBs (Nairz & Klein, 1997; Johzuka & Ogawa 1995; Alani et al., 1990). Looking into the evolution of Rad50 and Mre11 it was found that Rad50 is homologous to the *E. Coli* SbcC protein while Mre11 is homologous to SbcD (Sharples & Leach, 1995). In *E. Coli*, SbcC/SbcD acts as an exonuclease of dsDNA. The observed homologies, therefore, further support the role of Rad50 and Mre11 in 5′ end resection (Connelly & Leach, 1996).

DSB induction seems to be conserved between yeast and mammals; however, the resolution of recombination intermediates differs slightly, most notably in terms of regulation. While both use the RecA homologues Rad51 and Dmc1, additional proteins are required in mammals. RecA homologues and other proteins are relegated to distinct recombination nodules that, in higher eukaryotes, far outnumber matured sites of crossing over. This overabundance of recombination nodules seems to be unique to higher eukaryotes as in yeast generally all early nodules mature into crossovers. Over the course of prophase I in mammals, the protein composition of recombination nodules changes as their numbers decline, suggesting that there is a temporal order to resolving recombination (reviewed by Cohen & Pollard 2001).

RecA homologues, early recombination nodules, and strand invasion

In 1992 *rad51*, a *recA* homologue was identified in yeast (Aboussekhra, Chanet, Adjiri, & Fabre, 1992; Shinohara, Ogawa, H., & Ogawa, T 1992). Since then, *Rad51* has been found in most eukaryotes (Brendel, Brocchieri, Sandler, Clark, & Karlin, 1997) as well as archaea (Sandler et al., 1999). Additionally, eukaryotes contain a family of *Rad51* paralogues (Sung, Krejci, Van Komen, & Sehorn, 2003), although the number of paralogues differs between organisms. Also in 1992, Bishop et al. identified a meiosis-specific RecA homologue, Dmc1. Like Rad51, Dmc1 is also well conserved in eukaryotes, and both proteins seem to be required for meiotic recombination (Bishop, Park, Xu, & Kleckner, 1992).

Rad51 has been shown to be necessary for both mitotic and meiotic recombination and is essential for cell viability in vertebrates. In mitosis, Rad51 is the only recombinase expressed and recombination occurs predominantly between sister chromatids; however in meiosis, where both *Rad51* and *Dmc1* are expressed, recombination occurs preferentially between homologues (Sheridan et al., 2008). Rad51 is very well conserved; between yeast and humans

there is ~50% sequence identity (Shinohara et al., 1993, 1992). Rad51 forms a right-handed helical filament on ssDNA (Fig. 2) that catalyses strand exchange (Egelman, 2001; Ogawa, T., Yu, Shinohara, & Egelman, 1993).

Unlike Rad51, Dmc1 is typically described as being meiosis-specific—though it is worth noting studies in plants have shown somatic Dmc1 activity (e.g. Doutriaux, Couteau, Bergounioux, & White, 1998). Dmc1 shares about 50% sequence identity with Rad51 and (like Rad51) is highly conserved (Habu, Taki, West, Nishimune, & Morita, 1996; Bishop et al.,1992). Indeed, despite the high identity between Rad51 and Dmc1, it has been suggested that this is due more to convergent evolution than common origins. It is also thought that Dmc1 evolution was driven primarily by the advantages of sexual reproduction (Marcon & Moens 2005). In humans, DMC1 forms an octameric ring with itself (Fig. 2), binding as a ring to DNA (Masson et al., 1999; Passy et al., 1999); however, it has also been shown that conditions stimulating DMC1 recombinase activity also stimulate its ability to form filaments like those of RAD51 and RecA (Bugreev, Golub, Stasiak, Stasiak, & Mazin, 2005; Lee et al., 2005; Sauvageau et al., 2005; Sehorn, Sigurdsson, Bussen, Unger, & Sung, 2004). Ultimately, whether or not the octameric ring plays a role in meiotic recombination has yet to be shown (Sheridan et al., 2008). Recent studies have shown that the Dmc1 filament is essentially identical to the Rad51 filament with respect to structural parameters including persistence length, helical pitch, filament diameter, DNA bp per helical turn, and helical handedness (Sheridan et al., 2008). This suggests the functional differences between Rad51 and Dmc1 are the result of accessory proteins; Dmc1 function requires Mei5-Sae3, Hop2-Mnd1, and Tid1/Rdn54 while Rad51 functions in association with Rad52, Rad55-Rad57, and Rad54 (Sheridan et al., 2008). In both yeast and humans, Dmc1 catalyses *in vitro* strand exchange and D-loop formation (Gupta, Golub, Bi, & Radding, 2001; Hong, Shinohara, & Bishop, 2001; Masson et al., 1999). Despite the conservation and the critical role of Dmc1 in many species, fruit flies, nematodes, and Neurospora all lack a Dmc1 homologue (Shinohara & Shinohara, 2004).

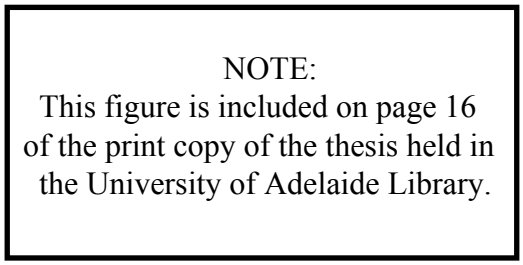

Figure 2: Dmc1 and Rad51 assembly After DSB initiation and 5′-end resection, RPA and Rad52 bind to a 3′ tail, prompting Rad51 to assemble, forming a right-handed helix along the ssDNA. Dmc1 then forms an octameric ring on the opposing 3′ tail. Following Rad51 and Dmc1 assembly, single end invasion is catalysed (Figure from Shinohara & Shinohara 2004).

Despite their structural and functional similarities, Dmc1 and Rad51 each play a unique role in the formation of crossovers. Many researchers (Zickler & Kleckner, 1999; Schwacha & Kleckner, 1997; Shinohara et al., 1997) have suggested that cooperation between Dmc1 and Rad51 is critical to the development of meiosis-specific recombination. Cytological studies in yeast, lily, and mouse have all shown that Rad51 and Dmc1 form foci on meiotic chromosomes in Zygotene and that Rad51 foci co-localise with Dmc1 (Tarounas, Morita, Pearlman, & Moens, 1999; Terasawa, Shinohara, Hotta, Ogawa, H., & Ogawa, T., 1995; Bishop, 1994), supporting the claim that the two act cooperatively. In mouse and yeast *Dmc1* mutants, RAD51 foci still form, suggesting that RAD51 assembly on chromosomes is independent of DMC1 function (Pittman et al., 1998; Yoshida et al., 1998; Bishop, 1994). However, *rad51* mutants in yeast are also defective in Dmc1-focus formation (Bishop, 1994; Shinohara et al., 1997), implying that Rad51 promotes Dmc1 foci. In 2000, Shinohara et al. used high resolution immunostaining to reveal a side-by-side staining of Rad51 and Dmc1 foci (Shinohara, M., Gasior, Bishop, & Shinohara, A., 2000). Consistent with this finding, two-hybrid studies show homotypic, but not heterotypic, interactions of Dmc1 and Rad51 (Catlett & Forsburg, 2003; Dresser et al., 1997). These findings support the proposed hypothesis that Dmc1 and Rad51 function independently rather than forming heteromeric

filaments (Shinohara et al., 2000; Zickler & Kleckner, 1999). Immuno-EM imaging of Dmc1 and Rad51 in mice further suggests an independent assembly of the two proteins (Tarsounas et al., 1999) and identified the proteins within the early recombination nodule. Shinohara et al. proposed that Dmc1 and Rad51 would be asymmetrically distributed at either end of the DSB, thus resulting in functionally differentiated DSB ends. In 2001, Hunter and Kleckner reported the two ends of a DSB do indeed act independently; at the Zygotene/Pachytene transition only one DSB end is engaged in forming SEI (Hunter & Kleckner, 2001). It is still unclear, however, how Dmc1 and Rad51 are distributed at DSBs.

HORMA-domain proteins and recombination partner selection

While most reviews of meiotic recombination assume that crossovers form between homologous chromosomes, this is not always the case. Observed intermediates in budding yeast indicated that inter-homologue recombination was greatly favoured (Schwacha & Kleckner, 1997); however, in fission yeast, hot spots exist where inter-sister recombination occurred at a higher frequency than inter-homologue interactions (Cromie et al., 2006). The difference between the two seems to be an inter-sister barrier that presents in budding, but not fission, yeast. While the mechanism of the barrier is not fully understood, it is thought that Mek1, Hop1 and Red1 of the axial elements play a role; mutations in these genes remove the meiotic block to inter-sister recombination in budding yeast (Niu et al., 2005; Wan, de los Santos, Zhang, Shokat, & Hollingsworth, 2004; Peciña et al., 2002; Bishop et al., 1999; Schwacha & Kleckner, 1997; Mao-Draayer, Galbraith, Pittman, Cool, & Malone, 1996; Rockmill & Roeder, 1990). Comparisons of joint molecule formation in 2D gel analysis of *dmc1* and *rad51* mutants suggests that Dmc1 promoted interhomologue over inter-sister recombination (Schwacha & Kleckner, 1997). In yeast, in which the Red1 block to inter-sister recombination was defective, *rad51* deletions had no effect on the number of interhomologue interactions while *dmc1* deletions eliminated such interactions, leaving only inter-sister recombination. In yeast, the ATR and ATM homologues, Mec1 and Tre11, are required along with Hop1 (a HORMA domain protein) for the prophase checkpoint (Carballo, Johnson, Sedgwick, & Cha, 2008; Aravind & Koonin, 1998). Hop1 is necessary for SC and DSB formation and, when phosphorylated by Mec1 and Tre11, is essential for the maintenance of the meiotic prophase checkpoint and the interhomologue bias (IH bias) of crossovers (Carballo et al., 2008; Niu et al., 2005; Bailis, Smith, & Roeder, 2000; Woltering et al., 2000; Schwacha & Kleckner, 1994). HORMA domain-containing proteins have been shown to be

conserved evolutionarily and have similar roles in other organisms from plants and nematodes to mammals (Wojtasz et al., 2009; Goodyer et al., 2008; Martinez-Perez et al., 2008; Sanchez-Moran, Santos, Jones, & Franklin, 2007; Couteau & Zetka, 2005; Martinez-Perez & Villeneuve, 2005; Nonomura et al., 2004; Caryl, Armstrong, Jones, & Franklin, 2000; Zetka, Kawasaki, Strome, & Muller, 1999). In 2009, Wojtasz et al. showed that Hormad1 and Hormad2 accumulate on unsynapsed chromosome axes in mouse, and that Hormad1/2 deplete from the chromosomes in response to SC formation in an ATP-dependent fashion (Wojtasz et al., 2009), making them an interesting candidate when looking at sex chromosome recombination (as much of the paired sex chromosomes do no synapse). It is possible that this depletion downregulates IH bias and the prophase checkpoint at completion of the chromosome homology search and formation of SCs between aligned homologues, thus Hormad1/2 may be at the centre of coordination between homologue pairing, synapsis, and crossing-over.

The fate of SEI: Rpa and Blm

RPA is a heterotrimeric complex (consisting of Rpa1, Rpa2, and Rpa3) that binds ssDNA (Wold, 1997). In somatic cells, Rpa recruits Rad51 (McIlwraith et al., 2000), however in meiotic cells, *Rpa* expression increases as Rad51 and Dmc1 leave chromosome cores (Oliver-Bonet, Turek, Sun, Ko, & Martin, 2005; Moens et al., 2002). Rpa foci are associated with transition nodules (TN) that initially contain Rad51/Dmc1 but later are comprised of Msh4, Blm and topoisomerases (Marcon & Moens, 2005). It is debatable whether or not Rpa is associated with recombination nodules (RNs, a.k.a. crossovers) due to temporal separation between Mlh1 and Rpa, though immunofluorescent studies have shown some co-localisation (Plung et al., 1998). It has thus been suggested that Rpa, along with Msh4/Msh5 (and possibly Mlh3) may be involved in conformational changes necessary to convert TNs to RNs, further suggesting meiotic-specific roles for Rpa and evolutionary modifications in the development of sexual reproduction (Marcon & Moens, 2005). It has also been suggested that Rpa phosphorylation is the key to the proteins' differential functions during these various processes (Clifford, Marinco, & Brush, 2004; Brush, Clifford, Marinco, & Bartrand, 2001; Wang, Guan, Perrault, Wang, & Iliakis, 2001; Brush & Kelly, 2000; Brush, Anderson, & Kelly, 1994). The phosphorylation of Rpa may explain its persistence in prophase, allowing Rpa to displace Rad51/Dmc1 and provide the necessary DNA conformation for interaction with Blm, Msh4/Msh5, and topoisomerases.

BLM is a helicase belonging to the well-conserved RecQ family which is responsible for genome maintenance from bacteria to humans (We & Hickson, 2006). Blm has been shown to interact with Rad51 along with a host of other proteins involved in DNA-damage repair, including Mus81, Mlh1, Rpa, and Atm (Sharma, Doherty, & Brosh, 2006; Beamish et al., 2002). In 2000, Karow et al. described that Blm can reorganise Holliday junctions and promote branch migration, and *in vitro* studies have shown that Blm acts to unwind D-loops and resolve HJs (Bachrati, Borts, & Hickson, 2006; Wu & Hickson, 2003; Karow, Constantinou, Li, West, & Hickson, 2000; van Brabant, 2000). Yet, the activity of Blm has been somewhat controversial: several studies have indicated that Blm may repress homologous recombination or promote it (Adams, McVey, & Sekelsky, 2003; Gonzalez-Barrera, Cortes-Ledesma, Wellinger, & Aguilera, 2003; Sonoda et al., 1999). Blm likely acts as a mediator in crossover formation. The Blm homologue, Sgs1, prevents aberrant CO formation by suppressing joint molecule (complexes comprised of 3 and 4 interconnected DNA duplexes) formation. Sgs1 and pro-crossover factors Msh5 and Mlh3 are antagonistic, as Sgs1 prevents dHJ formation in *msh5* mutants and *sgs1* mutants alleviate CO defects in *msh5/mlh3* mutants (Oh et al., 2007). It is in disrupting any aberrant junction molecules (JMs) that Blm maximised efficient repair while minimising deleterious COs (Oh et al., 2007).

Mismatch repair proteins

In yeast, Msh4 and Msh5 were identified to be meiosis-specific MutS homologues, the two forming a heterodimeric complex—a sliding clamp—with one another (Svetlanov & Cohen, 2004). However, due to a deletion, they are missing the appropriate residues necessary for mismatch detection (Svetlanov & Cohen, 2004). The structure of the Msh4-Msh5 heterodimer is such that it allows heteroduplex-like structures to pass through it. Yeast studies had suggested their role in recognising HJs, perhaps involved in resolving recombination intermediates. Msh4-Msh5 have also been linked to a large number of vital functions in meiotic recombination including chromosome pairing (Kneitz et al., 2000; de Vries et al., 1999; Edelmann et al., 1999) crossover interference (Novak, Ross-Macdonald, & Roeder, 2001; Zalevsky et al., 1999) and the stabilisation of HJs *in vitro* (Snowden, Acharya, Butz, Berardini, & Fishel, 2004).

MLH1, MLH3, and PMS2 (Pms1 in yeast) are the major eukaryotic MutL homologues active in meiosis, though none of them are meiosis-specific. MLH1 forms a heterodimer with either MLH3 or PMS2, with both dimers having different functions. Yeast studies show *mlh1* and

mlh3 mutants have defective crossover formation, thus suggesting the Mlh1-Mlh3 heterodimer plays a vital role in crossover formation (Svetlanov & Cohen, 2004). Further, in mice and humans MLH1 and MLH3 form foci in pachytene with number and distribution matching that of the chiasmata (Moens et al., 2002; Anderson, Reeves, Webb, & Ashley, 1999). These finding have led to the interpretation of MLH1 and MLH3 as markers of crossovers. Moreover, biochemical and immunofluorescent studies have implied a functional interaction between MLH1 and MLH3. Indeed, the recruitment of MutL homologues to MutS homologue complexes seems to require the heterodimerisation of MLH1 and MLH3 (Svetlanov & Cohen, 2004); however, this does not necessarily mean the two universally co-localise. It has been shown that MLH3 foci are occasionally found in the absence of MLH1. This could mean that MLH3 localises at crossovers before (and recruits) MLH1 and/or MLH3-exclusive foci may be a novel class of meiotic nodule involved in non-reciprocal recombination.

Temporal progression of recombination

As implied by the changing composition and number of recombination nodules, the machinery regulating meiotic recombination is subject to temporal and spatial expression. In 2005, Oliver-Bonet et al. characterised the temporal expression of meiotic DSB repair proteins (Fig. 3) in human spermatogenesis (Oliver-Bonet et al., 2005). Oliver-Bonet's study began with the localisation of RAD51, first seen in late leptotene / early zygotene. RAD51 initially is visible as foci along the axial elements, having a fixed number until mid-zygotene. At this point, the foci numbers decline until virtually all RAD51 foci are gone in mid-pachytene. However, they found a heavy concentration of RAD51 persists on the axial elements of the X chromosome and on the pseudoautosomal region well into late pachytene. Overall, RAD51 foci number declined with an increase of synapsis, and during pachytene RAD51 foci localised to asynaptic regions. While RAD51 co-localised briefly with MSH4 during zygotene, it never co-localised with MLH1. MSH4 expressed shortly after RAD51, first appears in early zygotene. Unlike RAD51, though, MSH4's temporal expression follows somewhat of a bell curve, increasing until it reaches its maximum at late zygotene / early Pachytene (in human males this amounts to nearly 200 foci). After peaking, MSH4 numbers decline until they plateau from mid-to-late Pachytene. During this plateau, MSH4 co-localises with MLH1 and MLH3. MSH4 was also detected on the sex body, present on the axes of the X and Y chromosomes in early Pachytene, even if the sex chromosomes existed as univalents. Like RAD51, MSH4 also localises on the AEs of some asynapsed regions of the autosomes,

though not all asynapsed regions had MSH4 foci. The persistence of Msh4 through Pachytene has also been reported in mouse (Santucci-Darmanin et al., 2000). The interaction of MSH4 with RAD51, RPA, MLH1, and MLH3 in human and mice (Neyton et al., 2004; Moens et al., 2002; Santucci-Darmanin et al., 2002, 2000) has influenced the hypothesis that MHS4 has diverse functions in meiosis. One of these roles may be structural in nature as *Msh4* mutants in mice initiate synapsis but cannot maintain it, implying that Msh4 is essential for proper synapsis (Kneitz et al., 2000). MSH4 has been detected at nascent sites of synapsis, as well as at asynapsed regions in Pachytene, further suggesting a structural role of MSH4 (Oliver-Bonet et al., 2005).

MLH3 first appears at early Pachytene, co-localising with MSH4; the appearance of MLH3 further coincides with a decrease in MSH4 foci. MLH1 foci follow shortly after, supporting the hypothesis that MLH3 can attach to recombination nodules in the absence of MLH1 (Lipkin et al., 2002) as well as supporting the hypothesis that MLH3 recruits MLH1. On the sex chromosomes, one—and only one—foci was identified, positive for MSH4, MLH3, and MLH1, localised in the pseudoautosomal region in humans (Oliver-Bonet et al., 2005).

Figure 3: Temporal progression of recombination machinery in prophase I A. Graphical representation of temporal expression of RPA, MSH4, MLH1, MLH3, and RAD51 foci. See text for review (Figure from Oliver-Bonet et al., 2005). B. Breakdown of events of DSB repair; proteins governing each stage are indicated via arrows. See text for further review.

Regulation of crossover frequency and position

Recent studies have begun to characterise the temporal and spatial activities of recombination proteins, and there is increasing evidence that chromosome morphology (e.g. size, centromere position) and chromatin conformation play an important role in the process of meiotic recombination (Kleckner et al., 2004; Nabeshima, Villeneuve, & Hillers, 2004; Hillers & Villeneuve, 2003; Meneely, Farago, & Kauffman, 2003). Spatial regulation of crossovers has also been demonstrated in a number of species. In chicken, MLH1 foci appear in late Zygotene and persist through Pachytene. The number of foci has a linear, direct relationship with SC length as well as DNA content and SC number (Pigozzi, 2001). Generally speaking, the longer an SC, the more DNA is present, and therefore more MLH1 foci. The exceptions to this trend are the microbivalents. The number of foci on microbivalents in relation to the amount of DNA and SC length is higher (proportionally) than in the larger bivalents. The microbivalents invariably have one MLH1 focus each while the longer bivalents can have anywhere from two to nine foci. The distribution of these foci was further shown to be non-random, and although no specific localised position was identified, there was a noticeable reduction of foci near the kinetochores (Pigozzi, 2001). Interestingly, it has been shown that centromere location can influence crossover position in humans as the metacentric chromosome 16 typically has two chiasma each located on one opposing arm and each distal to the centromere. In contrast, the acrocentric chromosome 15 has anywhere from one to three chiasmata located across the long arm (with none on the short arm), and in the event of trichiasmates, the third crossover is positioned adjacent to the centromere (Saadallah & Hulten, 1983).

In 2002, Froenicke et al. used immunofluorescent staining against MLH1 combined with fluorescence in situ hybridisation of chromosome specific DNA probes in order to construct a physical recombination map for mouse meiotic chromosomes. In general, they observed the same trend Pigozzi had seen in chicken. There were, however, some notable exceptions. In mouse, chromosomes 5, 7 and 11 had SCs that were 10-20% longer than would be predicted by this trend while chromosomes 3, 16 and 18 were 10-14% shorter. SC length accounted for 96% of the variation in foci number, with the longer SCs having more MLH1 foci. However, the three shortest SCs (chromosomes 16, 18 and 19) did not follow this relationship. Each of these short SCs had one MLH1 focus per bivalent, rather than the expected frequency

(predicted to be less than one focus per bivalent). This observed MLH1 foci has been termed the "obligate crossover."

The location of the MLH1 foci also followed a set pattern. On all SCs, foci were severely repressed within 0.5-1 μm of the centromere. In the longest SCs (chromosomes 1, 2, 4, 5, 7 and 11) two MLH1 foci were typically present. When two foci were present, they had a bimodal distribution: one focus near the centromere while the other was near the distal end. If the longest SCs had only one foci, its distribution tended to be more spread out over the area between the locations of the double-foci SCs. Mid-length SCs (chromosomes 3, 6, 8, 9, 10 and 12) generally had one focus. However, in the instances where they had two, distribution was more bimodal than the longer SCs with foci being relegated to more extreme ends. When shorter SCs had only one MLH1 focus a more wide-spread localisation was observed than was seen on longer SCs. The short SCs (chromosomes 13-19) rarely had two foci, though when present these foci were at extreme opposing ends. More typically, these chromosomes had only one foci which had a unimodal distribution for chromosomes 14 and 18, but a bimodal distribution for chromosomes 13, 15, 16 and 17. In all shorter chromosomes, the MLH1 focus could localise anywhere along the SC length, though it appeared most frequently at the distal ends of the SC. As a result of the recombination mapping, Froenicke et al. concluded that there were "hot" and "cold" regions of recombination as well as crossover interference present in mouse (2002).

It has thus been demonstrated that many species have a non-random distribution of crossovers (de Massy, 2003), but what regulates the number and position of these crossover events? Using ChIP analysis, a Spo11-based ChIP-chip approach was used to detect sites of DSBs in budding yeast. These studies found that DSB hotspots tend to occur in promoter regions while being repressed in centromeric and telomeric domains (Mieczkowski et al., 2006; Borde et al., 2004; Gerton et al., 2000), confirming previous conclusions of Southern blot analysis (Baudat & Nicolas, 1997). However, similar experiments in fission yeast have revealed more widely distributed DSB sites (Cromie et al., 2007; Young, Schreckhise, Steiner, & Smith, 2002). Other studies in yeast have shown that Spo11 activity is restricted to hotspot domains. A specialised form of Spo11 made to target UAS sites only acted on targets integrated into hotspots while it failed to act on targets integrated outside of hotspots (Fukuda, Kugou, Sasanuma, Shibata, & Ohta, 2007). In mouse, variants of the *Dsbc1* (Double-strand break control 1) locus were found to influence DSB and CO formation at hotspots on chromosomes (Grey, Baudat, & de Massy, 2009). Located in the *Dsbc1* locus is the *Prdm9* gene (Baudat et

al., 2010). *Prdm9* is a member of the PR-domain family and encodes a protein, Prdm9, present in prophase of meiosis and has been shown to trimethylate lysine 4 of histone H3 (Hayashi, Yoshida, & Matsui, 2005). This is significant because in yeast and mice, the trimethylation of H3K4 is an indicator of DSB initiation sites (Buard, Barthès, Grey, & de Massy, 2009). In 2010, Baudat et al. demonstrated that variations in the PRDM9 zinc finger array were associated with hotspot usage in mouse and humans (Baudat et al., 2010). Indeed, they showed that PRDM9 specifies DSB induction sites in mammals via direct binding to specific sequences in the genome. This was expanded upon through the findings that *Prdm9* has also been shown to be a hybrid sterility gene; the number of zinc fingers encoded by *Prdm9* directly affects hybrid sterility (Mihola, Trachtulec, Vlcek, Schimenti, & Forejt, 2008). In a recent study, Oliver et al. found that the *Prdm9* gene has been subject to rapid evolution across many Metazoan taxa (Oliver et al., 2009). They found that positive selection and concerted evolution directly and profoundly altered the DNA-binding specificity of PRDM9 in primates and rodents. However, the influence of positive selection was not universal across taxa and was not observed in ray-finned fish or tunicates. There are examples of lineage specific changes of the Prdm9 gene which include loss of all zinc finger domains in *C. elegans Prdm9,* pseudogenisation in dog, and duplication in platypus (Oliver et al., 2009).

The phenomenon of crossover interference also has a major impact on meiotic recombination regulation. Interference, as its name implies, is a repression of adjacent crossovers—it prevents crossovers from being formed within a certain distance of one another. Previously it was thought that interference was mediated by the SC, after all, fungi known to lack SCs also lacked interference (Cromie & Smith, 2007). In budding yeast, a mutation in Zip1—an SC component—knocks out both the SC and interference (Sym & Roeder, 1994). However, it now seems interference is established prior to synapsis. The Zip2 and Zip3 proteins are part of the ZMM group that are required to form interference-sensitive crossovers (Börner et al., 2004). Msh4 and Msh5 are also members of the ZMM group of proteins that co-localise with Zip1 and Zip2 (Novak et al., 2001). Zip1 and 2 form as foci in meiosis that have a frequency and display interference matching that of COs (Fung, Rockmill, Odell, & Roeder, 2004; Henderson & Keeney, 2004; Rockmill, Fung, Branda, & Roeder, 2003); these foci also mark sites of synapsis initiation (Agarwal & Roeder, 2000; Chua & Roeder, 1998), suggesting that interference not only precedes synapsis but that synapsis may be initiated at sites of interference-sensitive COs.

Recent evidence in *C. elegans* shows that the physical structure of chromosome axes influences interference. Only the ZMM pathway exists in nematode, meaning a high level of

interference is exhibited (typically only one CO occurs per bivalent) (Meneely et al., 2002). Yet when two or three chromosomes are fused end-to-end, still only one crossover is observed between the fused homologues, instead of two or three COs (Hillers & Villeneuve, 2003). Continuity of the axis is essential; when a fused chromosome recombines with two unfused chromosomes (such that one has a "broken" axis and the other does not) CO number between the two increases (Nabeshima et al., 2004). It has since been suggested that meiotic COs are promoted to relieve stress locally in chromosome axes, which then suppresses further CO formation (Kleckner et al., 2004). However, this hypothesis still does not explain the specific roles of ZIP2-ZIP3 or MSH4-MSH5.

Given the critical importance of meiotic recombination, it follows that the number and position of crossovers are tightly regulated yet, genome-wide and regional recombination rates differ between males and females, as well as between individuals of each sex (Sun et al., 2006; Hassold et al., 2004; Lynn et al., 2002; Kong et al., 2002; Broman, Murray, Sheffield, White, & Weber, 1998). In 2008, Kong et al. showed that sequence variance in the human *RNF212* gene was associated with sex-based differences in recombination rate (Kong et al., 2008). This was further substantiated when *RNF212* variants were specifically shown to influence male recombination rates (Chowdhurry, Bois, Feingold, Sherman, & Cheung, 2009). *RNF212* is a putative orthologue of the *C. elegans ZHP-3* gene, a homologue of the yeast *Zip3* gene (Jantsch et al., 2004). The Zip3 gene, as part of the ZMM recombination pathway, is involved in SC formation, yet the conservation between *RNF212* and *ZHP-3* is low (Kong et al., 2008). This may suggest an alternate function of the RNF212 protein in humans and other mammals, though the Kong et al. 2008 study clearly indicates that *RNF212* still plays a role in recombination, and it's possible that *RNF212* influences different recombination rates via crossover interference.

It has been observed that the degree of interference does not depend only on species but also on sex. In humans, the female recombination map is 1.7 times longer than that of males (Broman et al., 1998; Donis-Keller et al., 1987). In mice, the female map is 1.3 times longer (Roderick, Davisson, & Doolittle, 1996). Petkov et al. proposed that interference underlies the sex differences in recombination frequency (2007); looking at crossovers on mouse chromosome 1, they found that females averaged 1.97 chiasmata per bivalent while males only had 1.60. Furthermore, females had approximately 1.5 times higher frequency of double crossovers and ~14 times higher frequency of triple crossovers. Indeed, they also found that males had a larger interference distance than females. In females, complete interference

extends up to 40 Mb and fades between 40 and 77 Mb while in males complete interference extends to 57 Mb, fading between 57 and 112 Mb. Given that chromosome 1 is only 197 Mb; females have plenty of space for 3 COs, while males would require nearly the entire length of the chromosome to accomplish this. Overall it has been concluded that interference is correlated with bivalent length in Pachytene. Differences in the bivalent length have been reported between males and females in humans and mice (Tease & Hulten, 2004). In female mice, chromosome 1 was measured to be 13.7 μm long while in males it was only 10.2 μm (Petkov et al., 2007). It has now been suggested that the position of crossovers is dependent (to a degree) on interference distance, which is then related to SC length.

Sex chromosomes and queering the crossover paradigm

What is the crossover paradigm?

Crossing over between homologues has been recognised as a necessity for proper meiotic segregation and progression (Page & Hawley, 2003). Crossovers are tightly controlled such that every bivalent makes at least one "obligate" CO, with multiple COs on the same chromosome being widely spaced (Jones & Franklin, 2006; Hillers, 2004). In eutherian mammalian males, recombination between the X and Y chromosomes is further restricted to the small pseudoautosomal region (PAR). Because a crossover is generally necessary for proper segregation of sex chromosomes, the crossover frequency per Mb of DNA is orders of magnitude higher in the PAR compared to the rest of the genome. Recent studies have shown that the serine/threonine kinase, ATM, is necessary for sex chromosome synapsis and the formation of the X-Y obligate crossover (Barchi et al., 2008). Many studies have further linked aneuploidy to male infertility (Calogero et al., 2003; Aran et al., 1999; Moosani et al., 1995) and reduced XY crossovers, specifically, have been correlated with increased aneuploidy of sex chromosomes (Sun et al., 2008). Overall, the crossover paradigm describes the necessity of crossovers for correct meiotic segregation and progression.

Sex chromosomes: exceptions to the rules?

The hypothesis of X-Y crossovers goes back to Koller and Darlington who, in 1934, concluded that rat sex chromosomes always undergo one crossover in their paring segment (Koller & Darlington, 1934). It had been shown that X and Y chromosomes form end-to-end associations, and in 1959, Ohno, Kaplan, & Kinositar supported the obligate sex chromosome crossover hypothesis (Ohno, Kaplan, & Kinositar, 1959), and electron microscopy confirmed that the sex chromosomes undergo partial synapsis followed by chiasma formation (Solari, 1974). Since then, an X-Y crossover model has been proposed. First, sex chromosome pairing is possible due to homologous pairing segments. It has since been demonstrated in many species that PARs exist and are instrumental in sex chromosome pairing, synapsis, recombination and segregation—in humans, the PAR exists between Xp and Yp (Pearson & Bobrow, 1970). Second, a single obligatory crossover is made in the PAR, supporting the hypothesis that all chromosomes require at least one CO (Hulten, 1974). It is widely thought that the X-Y PAR in humans was too small to accommodate more than one crossover (Burgoyne, 1982), and this idea was supported when it was observed that chromosomes 21 and 22 q arms—which are about four times the length of the PAR—have one and only one CO (Hulten, 1974). Furthermore, it has been demonstrated that COs in the PAR are strongly restricted to the proximal third of the pairing region (Solari, 1980). This evidence suggests that crossover location and number is highly regulated in the PAR. A summary of meiotic recombination in sex chromosomes (for some vertebrates) can be found in Table 2.

Table 2: Summary of meiotic recombination in sex chromosomes Outlined below are known details regarding the pseudoautosomal regions (PARs), synapsis and the formation of axial elements (AEs), and meiotic recombination and the formation of recombination nodules (RNs) of the heterogametic sex in birds and mammals Pigozzi & Solari, 2005, 1997).

	Aves			**Mammalia**		
	Palaeonathae		**Neognathae**	**Monotremes**	**Marsupials**	**Eutherians**
	Ratites	**Tinamiformes**				
	R. americana	*N. maculosa*	*G. gallus*	*O. anatinus*	*T. elegans*	*M. musculus*
Sex Chromosomes	ZZ (♂), ZW (♀)	ZZ (♂), ZW (♀)	ZZ (♂), ZW (♀)	5X5Y (♂), 10X (♀)	XY (♂), XX (♀)	XY (♂), XX (♀)
PARs	Large PAR spaning most of the length of the sex chromosomes	Large diversity of PAR sizes (some span large portions of chromsomes, some are small)	Small terminal PAR	Large diversity of PAR sizes, some PARs have yet to be identified.	Hypothesised absence of PAR	Small terminal PAR
Synapsis	Synapsis along vast majority of axial length	Synapsis along PAR	Full heterologous synapsis	Unknown	Asynaptic; sex chromosomes form AEs and associate via a dense plate	Synapsis along PAR
Recombination in the PAR of heterogametic sex	2-3 RNs freely distributed along 80% of SC	Single RN freely distributed along 25% of W chromosome	Single RN strictly located at the synaptic terminus	Hypothesised meiotic chain held together via terminal chiasmata	Achiasmate	Single RN

However, studies in birds have shown some variation in the regulation of CO placement in the PAR. Neognaths have a single crossover that is strictly localised near the synaptic telomeres of the Z-W chromosomes, contrasting with the more wide-spread range of the single CO in *N. maculosa*, a bird belonging to more basal avian taxa of Ratites (Pigozzi & Solari, 2005). *R. americana*, has multiple COs along most of the SC of the ZW bivalent (Pigozzi & Solari, 1997). This free recombination observed in the ratites has been partly attributed to low W heterochromatin content, the nearly equivalent size of their Z and W chromosomes, and an interference distance of 25% the length of the W axial length (Pigozzi & Solari, 1997), although it is very likely this is also a function of PAR size. Though these species of birds show multiple sex chromosome COs, they are unique in that their PARs are considerably larger than those of mammals and Neognaths. Nonetheless, double-crossovers have been observed in humans and mice. In humans, the Xp-Yp PAR has a recombination frequency of 50% (meaning it always recombines) in male meiosis, and recombination across the PAR is an order of magnitude higher in males vs. females (Henke, Fischer, & Rappold, 1993; Page et al., 1987; Rouyer et al., 1986). In 1994, a double CO was described in the human PAR (Rappold, Klink, Weiss, & Fischer, 1994), and though exceptionally rare, the finding challenged Burgonye's assertion that one and only one CO forms between sex chromosomes (Burgonye, 1982). The possibility of double PAR crossovers was confirmed using sperm-typing (Schmitt et al., 1994). Also identified was a relatively strong interference with a coefficient of coincidence (ratio of observed to expected) of 0.26, where 0 is complete interference and 1 is no interference (Schmitt et al., 1994). Interestingly, PAR1 in human was subject to less interference than was once thought, as it was originally hypothesised that recombination would occur at a frequency of 0.018 in PARs (observed ~0.4) and that interference would be complete. In fact the value of 0.26 coincidence is similar to the 0.35 estimated for the autosomes (Shields, Collins, Buetow, & Morton, 1991; Morton & Collins, 1990; Pascoe & Morton, 1987). The mouse PAR, which is only 700 Kb long (Perry, Palmer, Gabriel, & Ashworth, 2001), is vastly shorter than the human PAR (about 2.5 Mb), but nonetheless can have double COs. Moreover, double COs seem to occur at a higher frequency in mouse than in human and with no significant interference (Soriano et al., 1987). Double recombinants are still rare, as Soriano et al. reported only three in a sample population of 127 (1987).

Crossing over, then, has been recognised to be required at least once in the PAR, and recombination outside the PAR does not occur. Theories of sex chromosome evolution propose that the sex determining locus was established on sex chromosomes in a region of

reduced recombination, perhaps due to inversions (Charlesworth & Charlesworth, 1978; Ohno, 1970). It has been shown that DNA sequence divergence increases with distance from the PAR—a feature that has been called evolutionary strata (Lahn & Page, 1999). It is thought that strata may be the result of multiple Y inversions that disrupted recombination (Lahn & Page, 1999). Furthermore, strata resembling those on the human X have also been observed in the chicken Z (Lawson-Handley, Ceplitis, & Ellegren, 2004).

Throughout this review the position that crossovers are necessary for meiosis has been repeatedly expressed, however, Drosophila males and Lepidoptera females (Turner & Sheppard, 1975) do not undergo meiotic recombination at all. In mammals, exceptions to the obligate crossover paradigm seem to be restricted to sex chromosomes. Marsupial sex chromosomes (like those of eutherian males) pair later than the autosomes and form a dense sex body, thought to be an effect of chromosome condensation and transcriptional inactivation (Solari, 1974). Unlike eutherians, marsupial sex chromosomes do not form a synaptonemal complex. Instead their sex chromosomes develop axial elements that do not associate via an SC, but rather a dense plate (DP) attached to the chromosome ends (Seluja, Roche, & Solari, 1987; Roche et al., 1986; Solari & Bianchi, 1975). Balloon-like structures have also been observed between sex chromosomes (Roche et al., 1986; Sharp, 1982), and it has been thought that these structures are related to the DP (Page et al., 2003; Roche et al., 1986). Using immunofluorescence studies, it was determined that the DP was made up of Sycp3 (Page et al., 2003), and it was further observed that no central element forms between marsupial sex chromosomes, suggesting that the two never synapse. In 2005, it was shown that the DP is conserved across marsupial species (Page et al., 2005). Moreover, because the sex chromosomes of marsupials do not have a PAR, they are achiasmate (Page et al., 2006; Toder, Wakefield, & Graves, 2000; Graves, 1996). The pairing and association of achiasmate sex chromosomes raises interesting questions. It was observed that the sex chromosomes paired in early Pachytene, perhaps as part of a secondary polarisation, correlated with the adjacent location of the Golgi and centrioles, causing a late bouquet stage in which the sex chromosomes find one another (Page et al., 2003; Roche et al., 1986; Solari & Bianchi, 1975). The actual mechanism of recognition is unclear as chromosome ends associate, but this association is not specific to a given arm (Page et al., 2003). The DP begins to form as the axial elements (AEs) of the sex chromosomes thin, seeming to be derived from an expansion of the AE ends along the nuclear envelope and both the DP and AEs are continuous (Page et al., 2003). The DP then holds the sex chromosomes together until their segregation at late metaphase / anaphase I (Page et al., 2006).

Achiasmate sex chromosomes are not unique to marsupials, and have also been identified in rodents (gerbils and voles) (Wolf, Baumgart, & Winking, 1988; Ratomponirina, Viegas-Péguignot, Dutrillaux, Petter, & Rumpler, 1986; Ashley & Moses, 1980; Solari & Ashley, 1977). It had been proposed that sex chromosomes in these species use telomeric or distal heterochromatic associations to remain paired (Wolf et al., 1988; Ashley & Moses, 1980; Solari & Ashely, 1977). In 2007 the behaviour of these eutherian achiasmate sex chromosomes was investigated. It was observed that the sex chromosomes did not synapse, as evidenced by the lack of Sycp1 (de la Fuente et al., 2007). Instead, the sex chromosomes associated along the nuclear periphery, each forming its own distinct axial element (AE). In Pachytene, the X and Y AEs were juxtaposed, but never in contact, and by Diplotene the AEs of the X and Y had folded and become entangled, such that by diakenesis the X and Y were indistinguishable (de la Fuente et al., 2007). As with the marsupial DP, the gerbil sex chromosomes were connected via their AEs (SYCP3) until their segregation at anaphase I (de la Fuente et al., 2007). Furthermore, Mlh1 was never observed between the sex chromosomes; instead, the X and Y accumulate a considerable number of Rad1 foci, persisting into late Pachytene (de la Fuente et al., 2007). De la Fuente et al. proposed that the lack of Mlh1 was due to the absence of a PAR, although confirmation of this was never provided.

The complex monotreme sex chromosome chain raises more questions about PAR crossovers

The above-mentioned findings of crossing over within PAR (or in the case of marsupials, gerbils, and voles the complete absence of crossovers) underscores both the rigid control of recombination in the sex chromosomes during spermatogenesis as well as the breadth of flexibility afforded in these systems. The extent of this flexibility may be challenged yet again as monotremes (platypus and echidna) question preconceived notions that suggest extensive meiotic multiples are hindrances to fertility and rarely observed in mammals (Grützner, Ashley, Rowell, & Marshall Graves, 2006). Since the 1950's the platypus karyotype has generated controversy. Initially it was thought that the platypus had micro- and macrochromosomes like birds and reptiles (Van Brink, 1959), but later reports of the discovery of ten unpaired mitotic chromosomes and a male meiotic chain resulted in the hypothesis of a sex-linked or an autosomal translocation system (reviewed by Grützner et al., 2006). Recently, however, the controversy has been resolved to reveal a complex system of ten sex chromosomes (five X and five Y) in the platypus and nine (five X and four Y) in the

echidna (Rens et al., 2007, 2004; Grützner, Deakin, Rens, El-Mogharbel, & Marshall Graves, 2003). During spermatogenesis the 10 platypus (Fig. 4) sex chromosomes (and the 9 in echidna) form an alternating chain such that all Y chromosomes are oriented towards one meiotic pole and the X chromosomes are oriented to the opposing pole (Rens et al., 2007; Grützner et al., 2003).

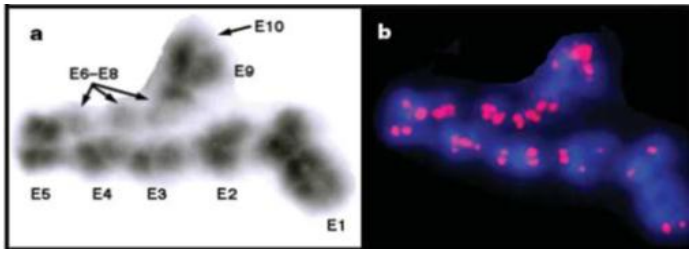

Figure 4: The platypus sex chromosome chain a) Inverted DAPI stain of the male meiotic chain and b) the same chain hybridised with a telomeric repeat (red). The elements of the chain ordered for oriented segregation. (Figure from Grützner et al., 2003).

The discovery of the monotreme sex chromosome chains has raised a number of questions about sex determination, evolution (reviewed by Grützner et al., 2006), fertility, and meiotic behaviour. In sex chromosome evolution studies it was found that while the platypus, like all mammals, has an XY sex chromosome system, the platypus and therian X chromosomes share no homology (Veyrunes et al., 2008). The platypus orthologues of genes found on the human X (e.g. *SOX3*) all map to the platypus autosome 6, indicating that this is the ancestor of the therian X and Y chromosome (Veyrunes et al., 2008). Furthermore, the platypus X chromosome shares extensive homology with the chicken Z chromosome (Veyrunes et al., 2008; Rens et al., 2007; Grützner et al., 2004). The platypus and echidna chains are results of reciprocal translocations between autosomes and sex chromosomes (Grützner et al., 2006), and studies of other fixed chromosomal heterozygotes show a propensity for terminal and subterminal chiasmata (Stack & Soulliere, 1984; Lin, 1980). Based on these findings, it has been assumed that translocation chromosome chains cannot be held together via proximal chiasmata because only terminal and subterminal chiasmata would permit the chain flexibility required for the zigzag confirmation at metaphase (Grützner et al., 2006; Rickards, 1983), although this rule is not universal (Rowell, 1991). In the platypus, sex chromosomes in the chain show a tandem arrangement; furthermore, given the small, shared terminal paring regions of many of the sex chromosomes, it has been suggested that the chain is held together by terminal chiasmata (Grützner et al., 2006). The exceptions to this are the X1 and Y1 long arms, which share extensive homology (Grützner et al., 2004; Rens et al., 2004).

Many PARs have been identified in the echidna and the platypus (Fig. 5). In the platypus, nine PARs are predicted between the ten sex chromosomes, though only seven have been identified: PAR 1 encompasses the entire long arm of X1 and Y1, but PAR 7 (between X4 and Y4) and PAR 9 (between X5 and Y5) have yet to be identified (Veyrunes et al., 2008). Likewise, eight PARs are expected in echidna, though only six have been identified; yet to be detected are PAR 5 (between X3 and Y3) and PAR 6 (between Y3 and X4) (Rens et al., 2007). It was recently shown that the platypus meiotic chain assembles in a stepwise fashion such that X1-Y1 pair first, then X2 and Y2, and so on until the chain is fully paired (Daish, Casey, & Grützner, 2009). Left unanswered, however, are questions concerning synapsis and recombination.

NOTE:
This figure is included on page 34 of the print copy of the thesis held in the University of Adelaide Library.

Figure 5: Platypus pseudoautosomal regions PARs 1-6 and PAR8 have been identified, but PAR 7 (between X4 and Y4) and PAR 9 (Between X5 and Y5) are still unidentified. (Figure from Daish et al., 2009).

The current proposal for recombination in the monotreme meiotic chains suggests that each member of the chain (with the exception of the two terminal chromosomes) must have two crossover events each, one per PAR. This feat, while possible (as evident in other species with smaller meiotic multiples) is still quite an undertaking, as most of these sex chromosomes are extremely small. In order for most of them to have two chiasmata would seem to require an extremely low (if not non-existent) level of crossover interference. Given the unidentified PARs on some chromosomes, some members of the chain may be achiasmate and form a DP-like structure as observed in marsupials. Interestingly, the major histocompatibility complex (MHC) was recently mapped to the platypus sex chromosome chain; however, the MHC in monotremes is not contiguous, rather it is located on two different PARs (Dohm, Tsend-Ayush, Reinhardt, Grützner, & Himmelbauer, 2007). Using gene mapping it was found that the MHC core class I and II genes were located on the platypus X_3/Y_3 (PAR 5) while the MHC class III genes were located on the Y_4/X_5 (PAR 8) (Dohm et al., 2007). This is a particularly important finding as the MHC is a recombination hotspot in the human genome (Dohm et al., 2007) and its localisation in the PARs of the platypus chromosome chain could be indicative of recombination hotspots being utilised to ensure proper segregation of the chain via homologous recombination.

Other factors of interest in monotremes are the divergence between the platypus and the echidna sex chromosome chains. In both species X_1, Y_1, X_2, Y_2, and X_3 are homologous; however, the platypus Y_3 and X_4 are autosomal in echidna and likewise the echidna X_5 is autosomal in platypus. Furthermore, the platypus Y_5 has partial homology to the echidna Y_3, suggesting the two had been fused (Rens et al., 2007). These neo-sex chromosomes in echidna may make for an interesting comparison of crossover frequency between sex chromosomes and their autosomal orthologues. Also of interest is the considerable size discrepancy present in monotreme karyotypes. Platypus and echidna have a few large chromosomes and several small chromosomes (Warren et al., 2008), and a comparison of crossover frequency and position between the different sizes of chromosomes will provide interesting insights in mammalian meiotic recombination. Currently nothing is known about monotreme meiotic recombination, and an in-depth investigation of whole-cell crossover frequencies, crossover spatial and temporal arrangements, and recombination in the sex chromosome chain will be instrumental to further understanding the diversity existing in meiotic recombination systems.

Project aims:

Aim 1: Identification and characterisation of recombination machinery in platypus

In order to gain first insights into the molecular basis of monotreme meiotic recombination, major players in the recombination pathway were identified and characterised. To this end, this study aims to bioinformatically analyse a broad range of genes critical to the initiation and processing of DSBs into crossovers. This involves 15 key genes: *Spo11, Mei4, Rec114, Rad50, Rad51, Dmc1, Hormad1, Rpa1, Blm, Msh4, Msh5, Mlh1, Mlh3, Rnf212,* and *Prdm9*. Platypus orthologues[2] will be identified and evolutionary conservation analysed. This includes multiple alignment analyses comparing the platypus protein sequence to protein sequences from other taxa, prediction of protein domains in platypus, and phylogenetic

[2] Orthologues are determined via two methods. Initially nucleotide BLASTs using a known mouse gene sequence are used to search for platypus orthologues; if, following a reciprocal BLAST using the platypus gene sequence, the original mouse sequence is re-obtained as first match, then the platypus sequence is deemed a putative orthologue. If the platypus gene further demonstrated conserved genomic context with the mouse gene, then the platypus gene is a likely orthologue (Jun, Mandoiu & Nelson, 2009).

analyses to examine evolutionary differences in the platypus genes and signs of positive selection. Furthermore, this research will determine gene expression in platypus.

Aim 2: Visualisation of crossover events in platypus

In addition to the bioinformatics analysis of recombination genes in platypus it was a major aim of this study to gain insight into the distribution of crossovers *in situ* in platypus using immunofluorescent imaging. If successful, visualisation of mature crossovers by an Mlh1 antibody in platypus would provide first estimates of recombination rates in platypus. A diploid male platypus pachytene cell has 52 chromosomes organised into 21 autosome pairs and ten sex chromosomes in the meiotic chain, i.e. a total of 21 autosomes plus 9 PARs. Assuming the obligate crossover paradigm is upheld in the platypus, it is hypothesised that there will be a minimum of 30 Mlh1 foci per cell, though it is certainly possible that any given cell may have significantly more foci than that as some autosomes may be likely to have more than two crossovers per homologous pair. Depending on the success using these antibodies across species, visualisation of other stages of the meiotic recombination was attempted using Rad51/Dmc1 antibodies. In the case of Rad51 or Dmc1 it would be expected that hundreds of foci would be present in zygotene, with foci numbers decreasing until they approach zero in pachytene. In order to stage cells in pachytene, antibodies against members of the synaptonemal complex will be used. In other platypus immunofluorescence experiments it has been established that Smc3 and Scp1 antibodies stain platypus cells well (A. Casey pers. comm. 2010; Daish et al., 2009). Either of these antibodies can easily be used to estimate the cell stage as zygotene cells are not fully synapsed but pachytene cells are. In this study, antibody epitopes were compared against the database protein sequences in order to ensure the best chance of reactivity. Western blots were then used to test the accuracy of antibody reactivity.

Aim 3: Analysis of crossover localisation in the platypus sex chromosome chain

Contingent on the success of Aim 2, it is the goal of this study to specifically demonstrate whether or not crossovers occur between members of the platypus sex chromosome chain. The sex chromosome chain has provoked several questions about platypus meiosis, namely how the chain is faithfully segregated into daughter cells. Visualising crossovers between members of the chain is an essential step in answering these questions, and to that end this

study aims to use genomic clones (BAC clones) for specific regions of the chain and comparative analysis with immunofluorescence data to demonstrate recombination between sex chromosomes. This investigation aims to examine the X-specific and shared regions of X_1, as the X_1 chromosome and PAR1 both represent a large percentage of the chromatin in the chain and, furthermore, PAR1 spans almost an entire arm of the X_1 chromosome, making it likely that any crossovers present in that PAR would be easily detected. Additionally this research will examine PARs of other members of the chain, one in a more central position (Y_2 PAR) and one at the terminal of the chain (Y_5). A probe for a known hotspot in other organisms, the MHC domain, will also be used because it is hypothesised that this region will also be likely to be a hotspot in platypus. Lastly, as a comparative control for the PARs, this analysis will examine recombination on chromosome 6, a mid-length autosome. Again, assuming the obligate crossover paradigm, it is hypothesised that each of the PARs and chromosome six will have crossovers while the X_1-specific region will not.

Chapter 2: Identification and characterisation of DSB repair machinery in platypus

As a representation of a group of extant mammals most distantly related to eutherians, the platypus is a critical species to understand the evolution of meiotic recombination pathways in mammals. As more has been learned about the diverse dynamics of meiotic recombination in marsupials and chickens, the status of platypus meiotic recombination machinery has become an increasingly important link to understanding the evolution of regulating factors in this complex process. Moreover, the extensive platypus sex chromosome chain poses a unique set of problems to the crossover pathway, specifically, how can a chain consisting of ten sex chromosomes—most of which are very small in size—undergo faithful segregation in meiosis? It is possible the platypus recombination pathway has undergone changes to specifically handle the dynamics of extensive meiotic chains. Through a series of multiple alignments, protein domain predictions, and phylogenetic analyses, this study represents a first bioinformatic characterisation of fifteen genes critical to meiotic recombination in yeast and mouse (*Spo11, Mei4, Rec114, Rad50, Rad51, Dmc1, Hormad1, Blm, Rpa1, Msh4, Msh5, Mlh1, Mlh3, Rnf212,* and *Prdm9*).

This study began with an identification of platypus orthologues of meiotic recombination genes (a full list of materials and methods is available in the supplemental data on the accompanying CD). Orthologues of all fifteen genes were successfully identified in platypus and most showed a conserved genomic context with mouse and human; the only observed exceptions were *Msh4* and *Mlh3* (Table 4). While a lack of conserved genomic context is problematic, it is important to note that the platypus genome assembly is patchy despite being sequenced to 6X coverage, and as a result the annotation and assembly is fraught with errors (Warren et al., 2008). These errors often manifest as gaps in the assembly or, occasionally, incorrect gene sequence. Thus, it was reassuring to observe a conserved genomic context for thirteen of the genes studied; furthermore, with additional bioinformatics characterisation, it was possible to say with a high degree of certainty that the observed *Msh4* and *Mlh3* are orthologous with the mouse genes (for an overview of the characterisation of the fifteen genes examined in this study, see Tables 4 and 5).

Table 3: Summary of characterisation of meiotic recombination machinery in platypus

Function	Gene names	Conserved genomic context in platypus	Platypus orthologue	Expression in platypus testis	Expression in mouse testis	Comments
Hotspot determination	*Prdm9*	+	+	+	+	Duplicated gene; missing eutherian domains
Double strand break initiation	*Spo11*	+	+	+	+	Complete assembly; predicted functional domains present
	Mei4	+	+	-	+	Complete assembly; predicted functional domains absent
	Rec114	+	+	-	+	Complete assembly; predicted functional domains absent
5′-end resection	*Rad50*	+	+	+	+	Complete assembly; predicted functional domains present
CO partner selection	*Hormad1*	+	+	+	+	Complete assembly; predicted functional domains present
Single-end invasion	*Rad51*	+	+	+	+	Assembly extended; predicted functional domains absent
	Dmc1	+	+	+	+	Assembly extended; predicted functional domains present
Transition Nodule	*Rpa1*	+	+	+	+	Apparent complete assembly; functional domains present
Disrupts aberrant junction molecules	*Blm*	+	+	+	+	Predicted incomplete assembly; predicted functional domains absent
Processing intermediates, stabilising Holliday junctions	*Msh4*	-	+	+	+	Predicted incomplete assembly; predicted functional domains absent
	Msh5	+	+	+	+	Predicted incomplete assembly; predicted functional domains present
Establishing and stabilising crossovers	*Mlh1*	+	+	+	+	Complete assembly; predicted functional domains present
	Mlh3	-	+	+	+	Complete assembly; predicted functional domains present
Sex-biased recombination rates	*Rnf212*	+	+	+	+	Complete assembly; predicted functional domains present

After platypus orthologues were identified, their expression in platypus adult testis was examined using RT-PCR (for methods and primer list see supplemental materials and methods section on accompanying CD). It was found that all the genes examined in this study except for *Mei4* and *Rec114* are expressed in platypus meiotic cells (Table 3) (It should be noted that RT-PCR experiments used in this study used echidna genomic DNA in addition to platypus genomic DNA; however, no echidna cDNA was used and the echidna genomic DNA was not sequenced. In effort to make gel images as simple as possible, the echidna genomic lanes have been included). Moreover, most of these genes are very well conserved across taxa (Table 4). There were, however, notable exceptions. Mei4 and Rec114 both have a number of protein motifs that, while conserved across most mammals, are not conserved in platypus. Along with their apparent lack of expression in platypus testis, this data seems to conflict with findings in mouse that implicate *Mei4* and *Rec114* as essential for DSB formation (Kumar, Bourbon, & de Massy, 2010). Likewise, *Blm*, *Msh4, Prdm9,* and *Rad51* all appear to be missing one or more domains that are predicted to be critical to protein function. *Prdm9,* in particular, yielded interesting results; and evidence presented here indicates the existence of a *Prdm9* paralogue in platypus. Identification of a domain shared with other mammalian lineages which is absent in non-mammals suggests that this domain and significant changes to Prdm9 function occurred early in mammalian evolution. In addition, this analysis has identified and corrected assembly artefacts for a number of genes, in particular a key gene in meiotic recombination and DSB repair, *Rad51*.

Last, phylogenetic analyses were performed on each of the fifteen genes studied using a Bayesian analysis. This study first looked at Ensembl gene trees for phylogenetic assessment. This database-focused analysis usually resulted in the expected phylogenetic tree topology for each gene; however, trees for *Rec114* and *Rad51* showed some aberrations from the expected model. In the case of *Rad51* sequencing of PCR products corrected the database sequence which was then used for further analysis (Section S1.2 of Supplemental Data (pg. 16) on accompanying CD). It is suggested that the unexpected topology of the *Rec114* tree is due in large part to a lack of sequence conservation across species (chicken, platypus, opossum, mouse, and human).

Eight of the genes examined in this study (*Spo11, Rad50, Hormad1, Rpa1, Msh5, Mlh1, Mlh3,* and *Rnf212*) are highly conserved in platypus, and detailed data can be found in the supplemental data section S1 on the accompanying CD (pg. 9). The following discusses a set of genes that showed unexpected divergences in platypus.

Table 4: Conservation of protein sequence of genes investigated Detailed here are calculations of percent identical amino acid sites across taxa (column 2) and pairwise percent identity between mouse and chicken (column 3) and mouse and platypus (column 4). Also provided is a summary of predicted protein domain (column 5). "+" symbols indicate all domains are predicted to be present while a "-" indicates one or more domains are predicted to be absent.

Protein	Pairwise identity across taxa*	Pairwise identity between chicken and mouse	Pairwise identity between platypus and mouse	Functional protein domains predicted to be conserved**:
Spo11	57.1%	65.6%	**71.9%**	+
Mei4	17.3%	45.2%	**36.0%**	-
Rec114	32.2%	51.6%	**56.7%**	-
Rad50	63.7%	74.5%	**83.2%**	+
Rad51	64.6%	96.2%	**96.5%**	-
Dmc1	90.0%	95.3%	**95.6%**	+
Hormad1	34.7%	58.4%	**59.5%**	+
Rpa1	65.9%	71.6%	**82.5%**	+
Blm	76.1%	57.4%	**91.6%**	-
Msh4	62.4%	76.4%	**80.7%**	-
Msh5	49.8%	66.2%	**71.6%**	+
Mlh1	54.5%	77.7%	**65.1%**	+
Mlh3	48.9%	46.0%	**42.8%**	+
Rnf212	40.2%	52.0%	**53.8%**	+
Prdm9	51.9%	77.9%***	**31.7%**	-

* taxa include chicken, platypus, opossum, mouse, and human

**A summary of InterPro domain scans is outlined in column 3 with a (+) indicating all functional domains are present in platypus while a (-) represents one or more domains are missing in platypus.

***comparison is between opossum and mouse, as there is no chicken Prdm9

Mei4 and Rec114

Recently it has been suggested that Mei4 and Rec114 are necessary for the formation of DSBs and may mediate Spo11 activity (Maleki et al., 2007; Prieler et al., 2005). Because of the limited information regarding the conservation or functional domains of Mei4 and Rec114, analysis of these proteins in platypus proved challenging. To investigate the expression in meiotic cells, RT-PCR experiments were conducted. Confirming initial expression results (Table 3), repeated RT-PCR experiments performed at varying annealing temperatures (53°C, 55°C, and 57°C) yielded no amplified product using platypus testis cDNA and primers specific for *Mei4* and *Rec114* (Fig. 6 and 7 respectively). RT-PCR did not, however, yield any amplification in the platypus controls for either *Rec114* (Fig. 6) or *Mei4* (not shown). It is unlikely that the lack of expression data in these experiments is due to corrupted or denatured cDNA, as these RT-PCRs were run with positive controls (i.e. other RT-PCR experiments for genes examined in this study) that confirmed the good quality of the template cDNA and reagents. It is possible that the genomic control products (estimated at over 1.7 kb) were too large to be amplified given the extension times used in these experiments; however, extension

time was predicted to be adequate enough to amplify the expected product sizes in the cDNA samples. It is not likely that the primers were an issue, as each primer was designed specifically for each gene and have optimal features (no hairpins, dimers, palindromes—each primer scored a 100 on Netprimer). These results indicate that *Mei4* and *Rec114* may not be expressed in platypus adult testis.

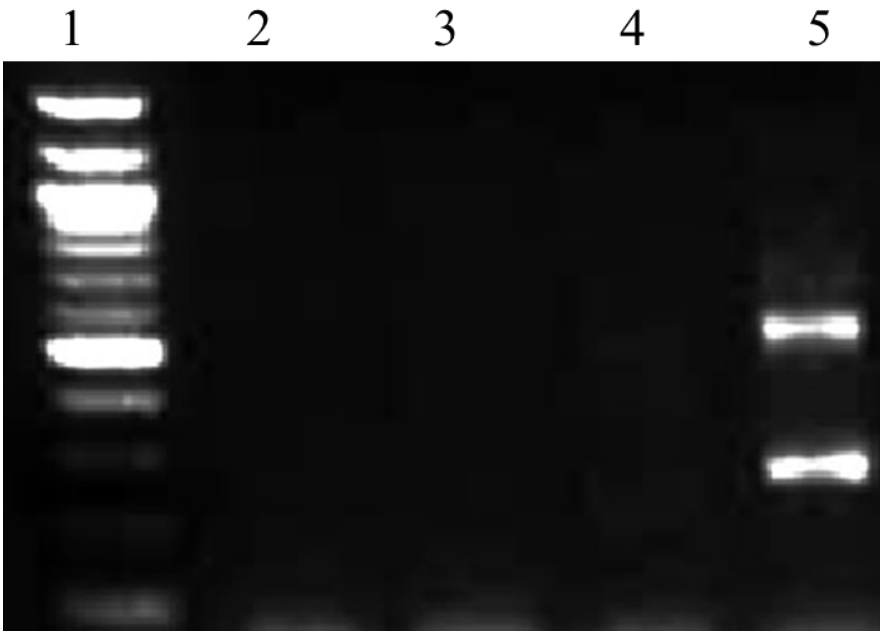

Figure 6: RT-PCR gel for *Mei4* The results of a *Mei4* RT-PCR experiment using a 57°C annealing temperature. In this gel, lane 1 corresponds to a standard 100bp ladder; platypus testis cDNA samples were run in lanes 2 and 3 while platypus genomic and echidna genomic DNA was run in lanes 4 and 5 respectively. No *Mei4*amplification could be obtained for any of the platypus samples; however, some amplification was obtained using the echidna genomic DNA (not sequenced). A negative control (blank) was also run, but is not shown in this image (the two RT-PCR experiments were run on the same gel, and the blank was run at the far end of the gel).

Unexpectedly, protein sequence alignments revealed that (relative to mouse) the platypus Mei4 protein sequence is less conserved than the chicken orthologues (Table 4). Between chicken and mouse Mei4 there is a 45.2% pairwise identity while between platypus and mouse this number is only 36.0% (Table 4). As expected, the platypus Rec114 protein sequence shows a higher degree of conservation (56.7% pairwise identity with mouse) than the chicken (51.6%) (Table 4). Neither protein sequence is well conserved across taxa, and no InterPro domains were identified in the mouse or platypus protein sequence; however, in 2010 Kumar, Bourbon, and de Massy identified a series of conserved regions in mouse Rec114 and Mei4 that, they proposed, were essential to the proteins' function in DSB initiation. These domains, called short signature sequence motifs (SSMs), are concentrated predominantly in the N- and C-termini of the proteins and comprise approximately 20% of each protein (Kumar et al., 2010). In mouse Mei4, all six SSMs adopt a primarily α-helical secondary structure.

Alignment of the Mei4 SSMs of *S. cerevisiae*, chicken, platypus, opossum, and mouse (Fig. 7) showed that these α-helical motifs are largely conserved across taxa; however, SSM4-6 are missing in platypus and chicken, and platypus SSM2 adopts a coil-turn motif. These missing motifs suggests that in some respects the platypus Mei4 is more similar to the chicken orthologue than the mouse; yet, chicken SSM2 is far more similar to the mouse motif than it is to distinctly diverged platypus sequence (this is thought to account for the higher percent identity between the chicken and mouse Mei4 proteins).

The motif alignment results for Rec114 were very similar (Fig. 8). Overall SSMs 1-5 of Rec114 adopt a β-sheet motif while SSMs 6 and 7 adopt α-helical motifs. The platypus Rec114 appears to be missing SSM2 and SSM3, and the platypus Rec114 SSM4 adopts a predominantly α-helix motif, much like the chicken SSM4. According to Kumar, Bourbon, and de Massy, the SSMs of Mei4 and Rec114 are essential for the two proteins ability to interact; specifically the N-terminal SSMs of Mei4 (particularly SSM1) and the C-terminus of Rec114 (SSM7) were necessary for their functional interaction (Kumar, Bourbon, & de Massy, 2010). Despite the lack of conservation in platypus Mei4 and Rec114, the aforementioned critical SSMs are conserved in the platypus orthologues. These data imply, from a bioinformatics perspective, that it is conceivable that the proteins' ability to interact is conserved. However, between missing motifs and diverged sequences, these alignments strikingly reflect the pairwise percent identity results: platypus *Rec114* and *Mei4* appear to have dramatically diverged from other mammals, and the respective chicken sequences appear to be more conserved than their platypus counterparts. In light of the poor sequence conservation, the missing domains, and expression data, this study indicates that Mei4 and Rec114 are not functional in platypus meiosis.

Figure 7: Mei4 SSMs motif prediction using InterPro Protein motifs were analysed for the 6 SSMs of Mei4. Red tubes represent α-helixes while yellow arrows indicate β-sheets, blue arrows are turns, and grey waved lines represent coils. Above each alignment is a graphical representation of the % identity between the protein sequences—% identity is measured on a scale of 0 to 1, where a value of 1 represents a site that is identical in all sequences. The platypus SSM2 domain (predicted to adopt a coil-turn-coil motif) appears to have been dramatically different than that of other species (which are largely comprised of α-helixes), and both the platypus and chicken proteins are missing SSM4-6.

Figure 8: Rec114 SSMs motif prediction Using InterPro domain predictions the SSM domains of Rec114 were analysed (as in Fig. 7). Overall the SSM domains of Rec114 appear to be conserved; however, the platypus protein is missing SSM2 and 3.The absence of an Isoleucine residue in the platypus Rec114 SSM4 appears to have disrupted β-sheet formation, resulting in a continuous α-helix motif, while therian protein sequences with the Isoleucine reside are predicted to adopt a helix-sheet motif.

Phylogenetic analyses of *Rec114* (Fig. 9) and *Mei4* (Fig. 10) supported prior observations of poor conservation of the proteins. For *Rec114* species tend to be clustered tightly with similar taxa (e.g. eutherians cluster separately from marsupials, which are set apart from platypus), while in *Mei4*, the platypus has been grouped away from other mammals, corresponding with the overall high divergence observed in platypus *Mei4*. In each phylogenetic tree, branch lengths tended to be longer than would be expected for well-conserved meiotic proteins, but the platypus distance is longer in *Mei4*, indicative of the greater number of missing or altered motifs in the platypus protein.

The lack of expression and predicted loss of function of *Mei4* and *Rec114* is surprising. Specific mechanisms of Mei4 and Rec114 activity are still elusive, making it difficult to predict what their absence in platypus meiosis could specifically signify; yet, in mouse mutant studies, *Mei4* has been shown to be critical for fertility. In male meiosis, *Mei4* mutations result in a failure to form DSBs, defective synapsis, and, ultimately, cells undergo apoptosis prior to the first meiotic division (Kumar et al., 2010; Ward et al., 2007). It has also been reported that *rec114* mutants in *S. cerevisiae* show an inability of Spo11 to associate with DSB hotspot DNA, while *mei4* mutants show a retarded dissociation of Spo11 at uncleaved hotspots (Maleki et al., 2007; Prieler et al., 2005). Additionally it has been shown that in *rec114* mutants, Mei4 is unable to associate with Rec102-Rec104—part of the Spo11-subcomplex (Maleki et al., 2007). These past studies strongly imply that *Mei4* and *Rec114* expression are necessary for proper DSB formation and regulation in meiosis from yeast to mouse; however, this current study indicates that platypus meiosis may not be dependent on Mei4 or Rec114 function.

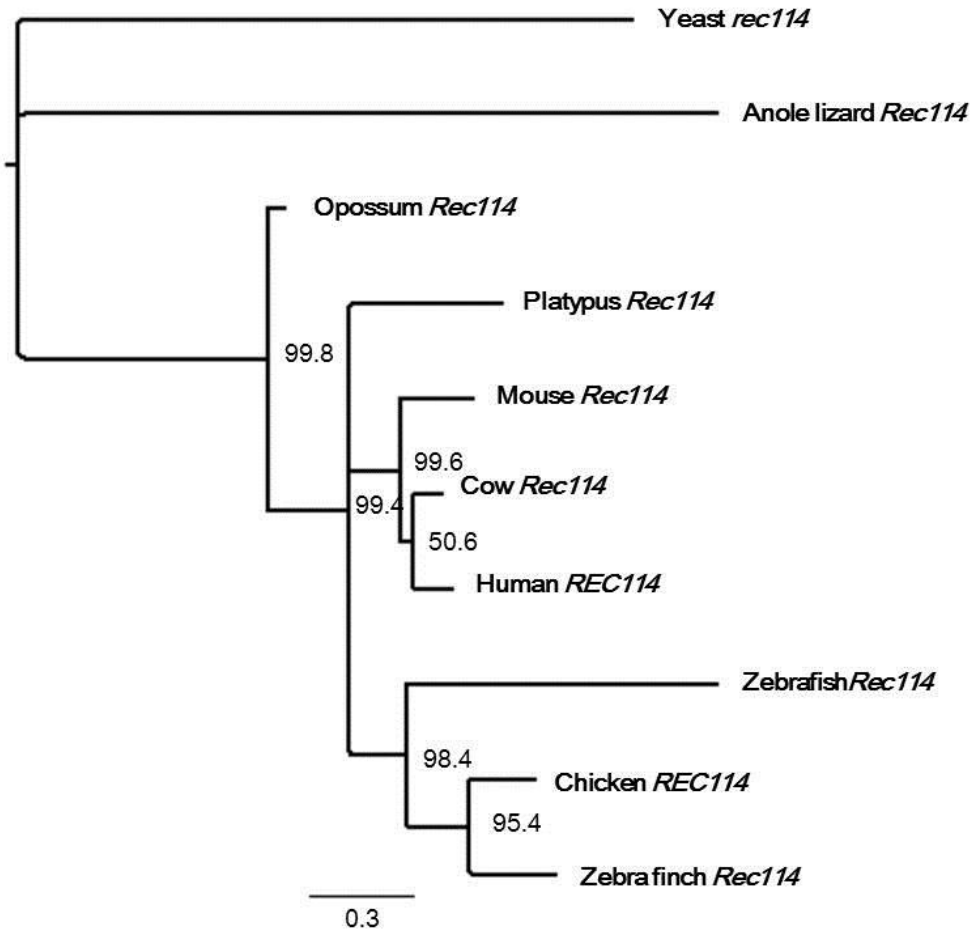

Figure 9: Phylogenetic tree for *Rec114* MrBayes (Ronquist & Huelsenbeck, 2003) generated phylogenetic tree using a translation alignment of cDNA sequences. The numerical values marked at the nodes represent the posterior probability (the proportion of sampled trees containing the nodes). The scale bar of 0.3 represents the branch length, measured in expected changes per site.

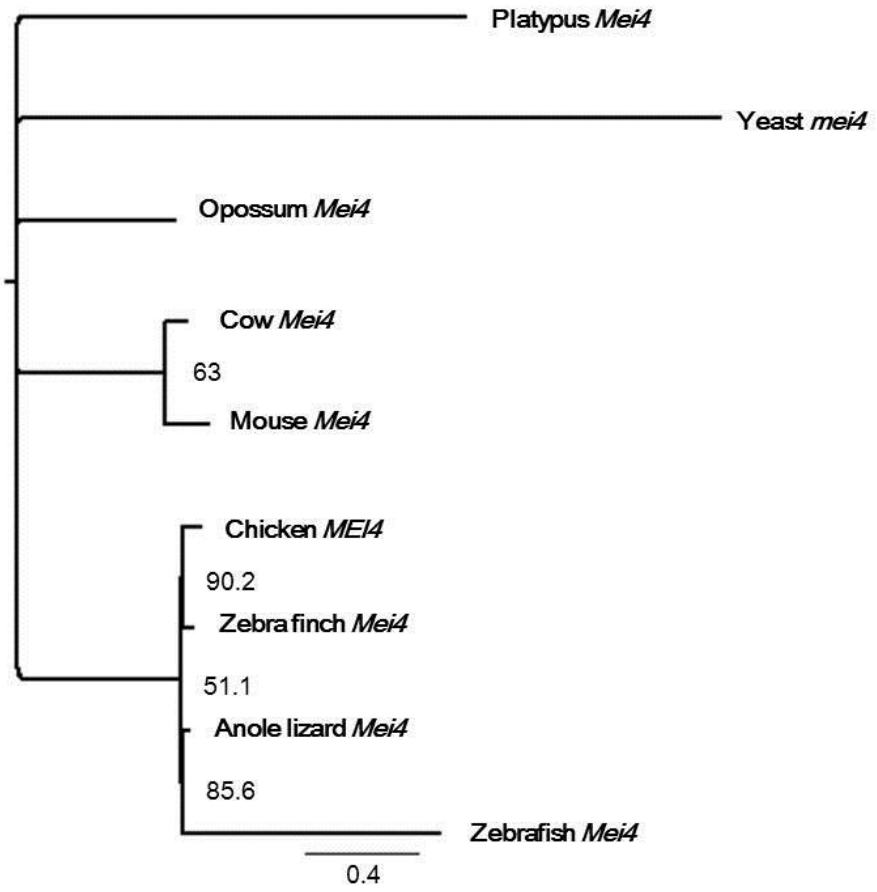

Figure 10: Phylogenetic tree for *Mei4* MrBayes (Ronquist & Huelsenbeck, 2003) generated phylogenetic tree using a translation alignment of cDNA sequences. The numerical values marked at the nodes represent the posterior probability (the proportion of sampled trees containing the nodes). The scale bar of 0.4 represents the branch length, measured in expected changes per site.

Rad51

The Rad51 protein is well known for its role in single-end invasion and the formation of Holliday junctions. Partial sequence of a putative platypus orthologue of mouse *Rad51* was identified on Contig7495, and while this gene did show a conserved genomic context with mouse, the platypus sequence in the database covered only about one third of the mouse sequence (only 225 bp and 2 exons in the platypus genome database versus the 3368bp and 10 exons in mouse, data from Ensembl assemblies, v5.0.1). RT-PCR using *Rad51* primers with platypus adult testis cDNA amplified a ~165 bp cDNA product (Fig. 11). The PCR also amplified several non-specific bands that were not further investigated. The genomic controls amplified a band of the expected size (~700 bp), and sequencing of the 165bp cDNA confirmed amplification of *Rad51* (Fig. 11). Thus RT-PCR analysis indicates that *Rad51* is expressed.

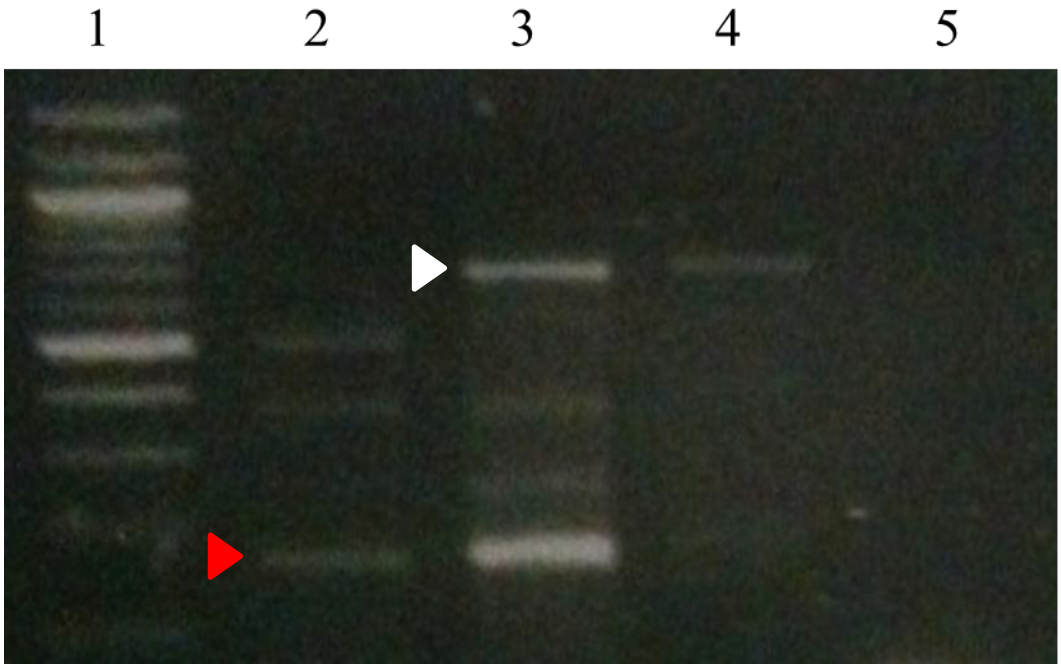

Figure 11: Expression analysis of *Rad51* in platypus RT-PCR Primers specific for *Rad51* amplified a band of ~165 bp in platypus testis cDNA samples (lanes and 3) that sequencing reactions confirmed to be *Rad51* (red triangle indicates the 165 bp *Rad51* cDNA product). These same primers also amplified several unspecific bands of unknown identity. Lane 4 contains a platypus genomic DNA control with the expected size genomic amplification (the white triangle indicates the expected ~700 bp product). Lane 5 represents an echidna genomic DNA sample (which resulted in no amplification), and lane 6 represents the negative control (a blank sample containing only reagents and primers).

To obtain the full *Rad51* sequence a tBLASTn using the mouse Rad51 protein sequence uncovered additional platypus *Rad51* sequence on Contig14268, which also had conserved genomic context with the mouse *Rad51* on murine chromosome 2 (Fig. 12). It appeared as though the two platypus contigs were actually contiguous, with Contig14268 containing the

3′-end of the gene. Yet, joining the two *Rad51* sequences revealed that there was some sequence still missing between the two contigs.

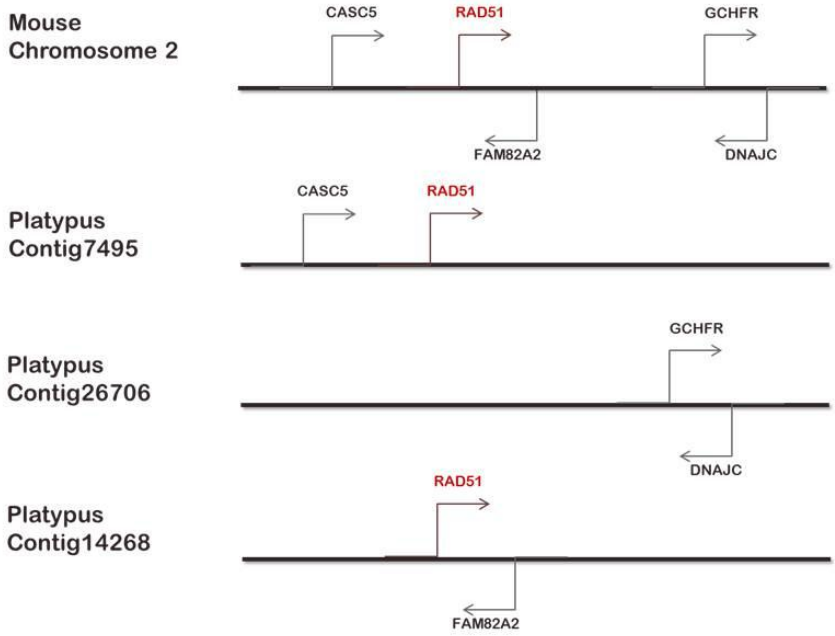

Figure 12: Synteny analysis of *Rad51* in platypus and mouse using Ensembl The platypus *Rad51* gene appears to be divided across two contigs, 7495 and 14268. Both *Rad51* fragments show conserved synteny with the mouse gene.

Primers were designed to span the two contigs which yielded the predicted missing cDNA sequence (Fig. 13). Both platypus cDNA samples (from animals PIII and P07) resulted in the same product; however there was a greater product yield observed from PIII. This is possibly due to a slightly lower concentration of cDNA present in the P07 sample. Nonetheless, both RT-PCR products were identical and therefore it is not thought that the difference in product concentration is a major issue. Sequencing the RT-PCR cDNA product revealed that the forward sequencing reaction matched Contig7495, while the reverse sequencing reaction contained DNA sequences from Contig14268. Alignment of the two sequencing reactions revealed a small, additional 118bp sequence (Fig. 13). This novel sequence linked the two contigs, and was incorporated into the cDNA sequence. After translating the completed platypus *Rad51* sequence (S1.2 on accompanying CD), a multiple alignment was performed against chicken, opossum, mouse, and human peptide sequences. Between those five species there were 64.6% peptide sequence identity, and between the complete platypus protein sequence (including the translated 118bp of novel DNA) and mouse there was a 96.5% pairwise identity, indicating the platypus Rad51 protein is well conserved (Table 4).

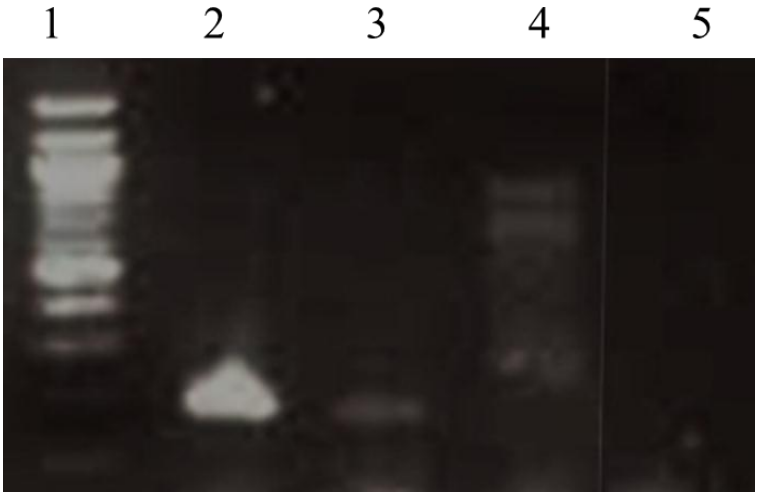


```
Rad51_Forward      --------------------CTATGATCATAGCATGACCTGA-AGAAGCGGTTCGCTTCG 39
Rad51_Reverse      ATCAAGGGCATCAGCGAAGCCAAAGCCGATAAGAT--CCTGACGGAGGCGGCTAAGCTCG 58
                               * * *   ***  **  *****  ** **** *    ***

Rad51_Forward      TCCCGATTAGGGCTTCACCACCGCCACCGAATTCCACCAGCGGCGGTCGGAGATCATCCA 99
Rad51_Reverse      TCCCGAT--GGGCTTCACCACCGCCACCGAATTCCACCAGCGGCGGTCGGAGATCATCCA 116
                   *******  ************************************************

Rad51_Forward      GATCACCACGGGCTCCAAAGAGCTGGACAAGCTGCTGCAAGGGGGCATCGAGACGGGCTC 159
Rad51_Reverse      GATCACCACGGGCTCCAAAGAGCTG-ACAAGCCTACGTA-------------------- 154
                   ************************* ******    * *

Rad51_Forward      CATCACGG 167
Rad51_Reverse      -------- 
```

Figure 13: RT-PCR reveals the missing *Rad51* sequence Primers designed to span the gap between the two predicted platypus *Rad51*-containing contigs amplified a cDNA product of ~200 bp in two platypus testis cDNA samples (lanes 2 used cDNA from PIII and lane 3 used cDNA from P07). Lane 4 is a platypus genomic DNA control (from P07) and lane 5 is a blank negative control. Sequencing of the product revealed sequences specific for Contig7495 (in red), Contig14268 (in blue), as well as a novel cDNA sequence (in green).

Performing a scan for functional domains, however, revealed that the platypus Rad51 is missing the RecA monomer-monomer interface (IPR020587) on the C-terminal, necessary for the assembly of the Rad51 filament (Fig. 14). Given the high evolutionary conservation of the Rad51 filament and the expression of Rad51 in platypus it seems unlikely that this essential monomer-monomer interface is missing, and further attempts to obtain additional sequence were not possible due to the unavailability of contig-specific primers. It is more likely that the observed C-terminal divergence is either an artefact of the assembly or due to errors in the assembly sequence. RACE PCR was attempted to complete the sequence data; however, while bands were amplified in RACE experiments, no sequence data corresponding to the *Rad51*could be obtained at this time (data not shown). Aside from this missing domain, the platypus Rad51 protein has every other essential functional domain and is nearly identical to the mouse protein.

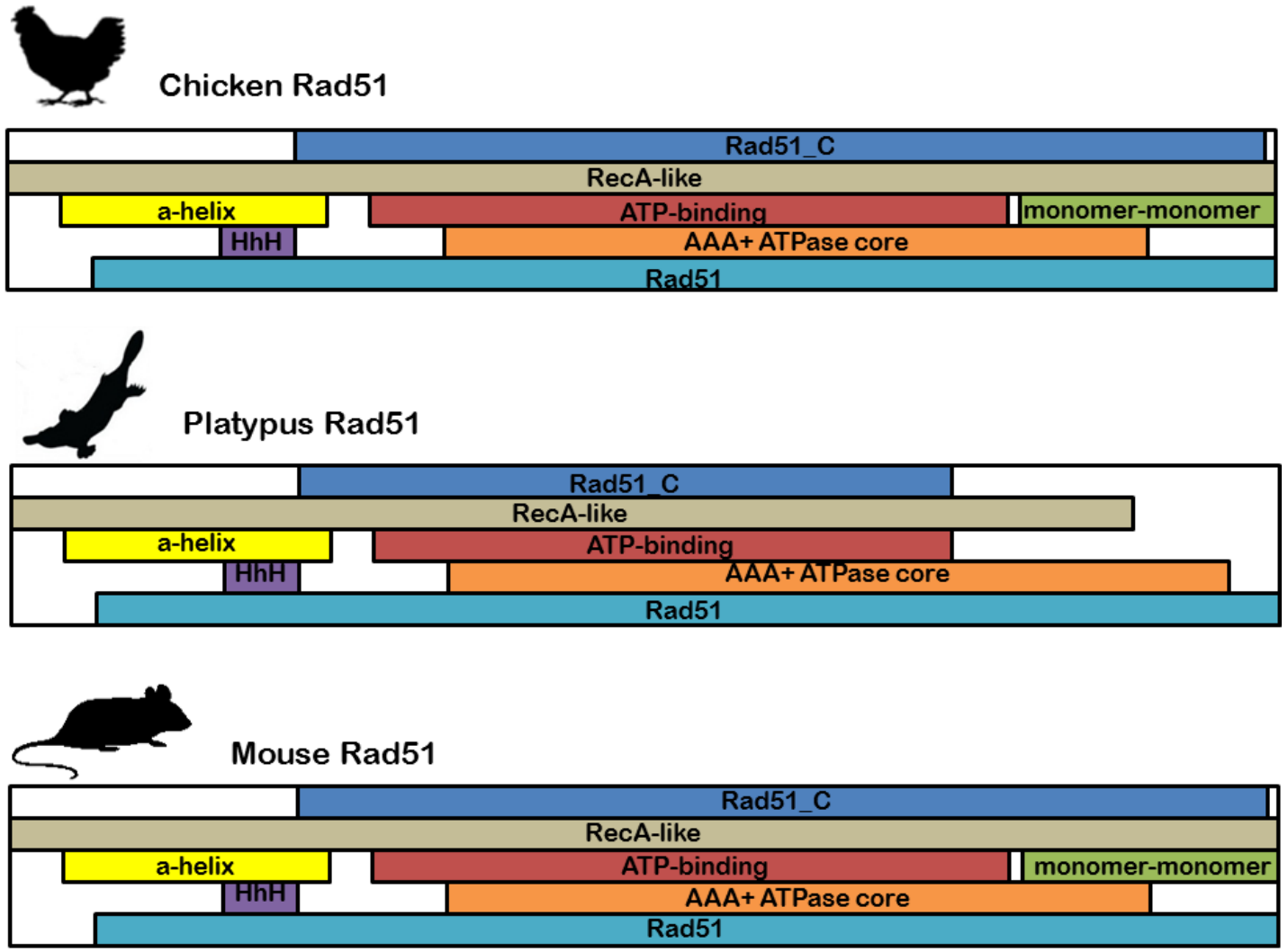

Figure 14: Protein domain alignment of chicken, platypus, and mouse Rad51 The platypus Rad51 protein domains appear to be nearly identical to those of mouse and chicken with the sole exception that the platypus protein seems to be missing the monomer-monomer interface on the C-terminus.

The clustering of taxa on the *Rad51* phylogenetic tree (Fig. 15) overall produces expected species distribution; however, the position and branch length for platypus is much longer than would be typical for such a well-conserved gene. It is unclear why the phylogenetic analysis resulted in such long branch lengths as gaps in gene sequences were omitted. A cursory examination of the Ensembl-generated *Rad51* (not shown) clearly shows the expected phylogenetic topology and branch lengths, suggesting that the utilised Geneious Baysian analysis was faulty. Omega analysis[3] of the *Rad51* sequences does not indicate any positive selection. Based off the corrected assembly sequence, expression data and domain prediction, it appears that Rad51 has a conserved function in platypus meiosis; however, more work is needed to confirm the C-terminal sequence data of the peptide sequence. With more time and optimisation it is likely a RACE PCR will be able to complete the platypus gene sequence.

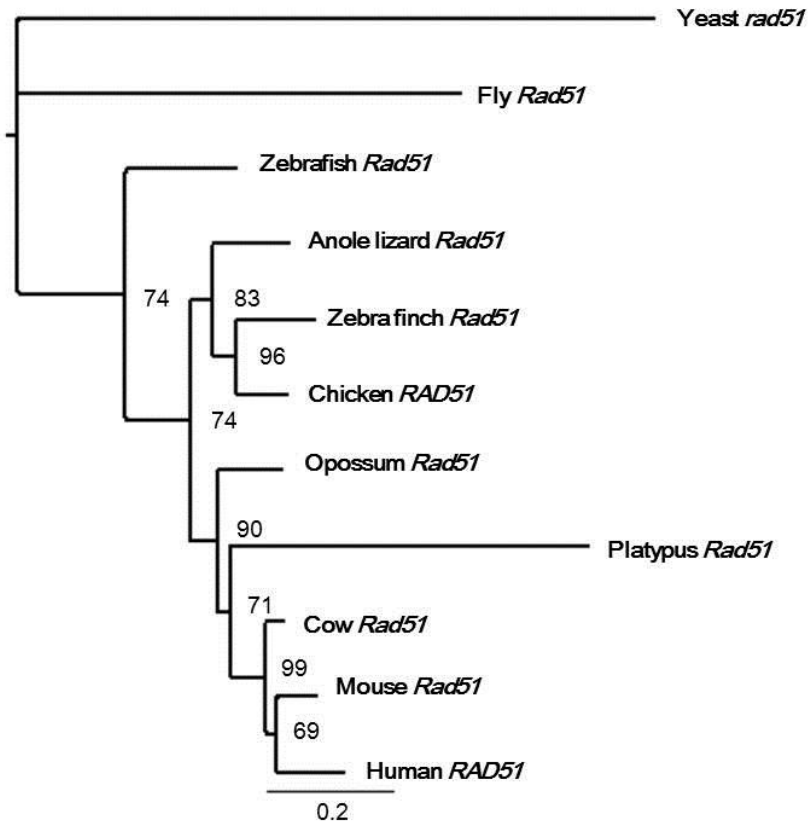

Figure 15: *Rad51* phylogenetic tree MrBayes (Ronquist & Huelsenbeck 2003) generated phylogenetic tree using a translation alignment of cDNA sequences. The numerical values marked at the nodes represent the posterior probability (the proportion of sampled trees containing the nodes). The scale bar of 0.2 represents the branch length, measured in expected changes per site.

[3] Omega analysis uses translation alignments of cDNA sequences from related species to estimate the influence of positive selection on a given sequence. Sequences are aligned codon-by-codon and gaps and deletions are excluded in order to analyse specific base changes, and comparing these changes to the Molecular Clock to estimate whether or not positive selection or other factors are driving observed sequence divergences (Personal correspondence with Dr Dan Kortschak, 2010).

Dmc1

Like Rad51, Dmc1 is important to single end invasion and the formation of Holliday junctions. The platypus copy of *Dmc1* had conserved genomic context with mouse. Expression analysis based off RT-PCR experiments (Table 3) using platypus adult testis cDNA amplified a product of ~130 bp that was confirmed by DNA sequencing analysis to be *Dmc1* (Fig. 16). Conservation studies using a multiple alignment of chicken, platypus, opossum, mouse, and human DMC1 protein sequences revealed 90% identical sequences; moreover the pairwise identity between mouse and platypus was calculated to be 95.6% (Table 4), indicating a high level of conservation.

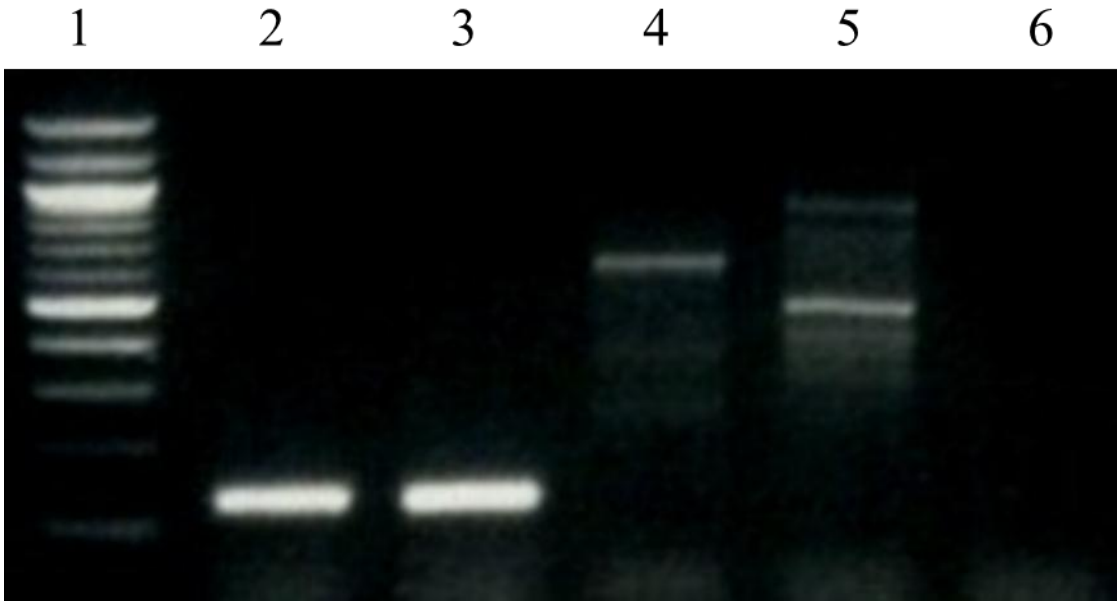

Figure 16: RT-PCR expression analysis of platypus *Dmc1* A *Dmc1* RT-PCR amplified cDNA products just over 100 bp. Lane 1 is a 100 bp maker; lanes 2 and 3 are platypus testis cDNA samples; lane 4 is a platypus genomic DNA control; lane 5 is an echidna genomic DNA control; in lane 6 is a blank negative control.

Initial domain predictions, however, indicated that the platypus Dmc1 protein was missing a critical Helix-Hairpin-Helix (IPR000445) motif that is required for the interaction of Dmc1 with single-stranded DNA. To further investigate if platypus is missing the domain, primers were designed adjacent to the prospective motif sequence. PCR experiments amplified a cDNA product of the expected size, and DNA sequencing and additional domain prediction analysis revealed the missing motif (Fig. 17; Full gene sequence in S1.3 on accompanying CD). Comparing the protein domains of the mouse, chicken, and platypus Dmc1, the three proteins are virtually identical (Fig. 18).

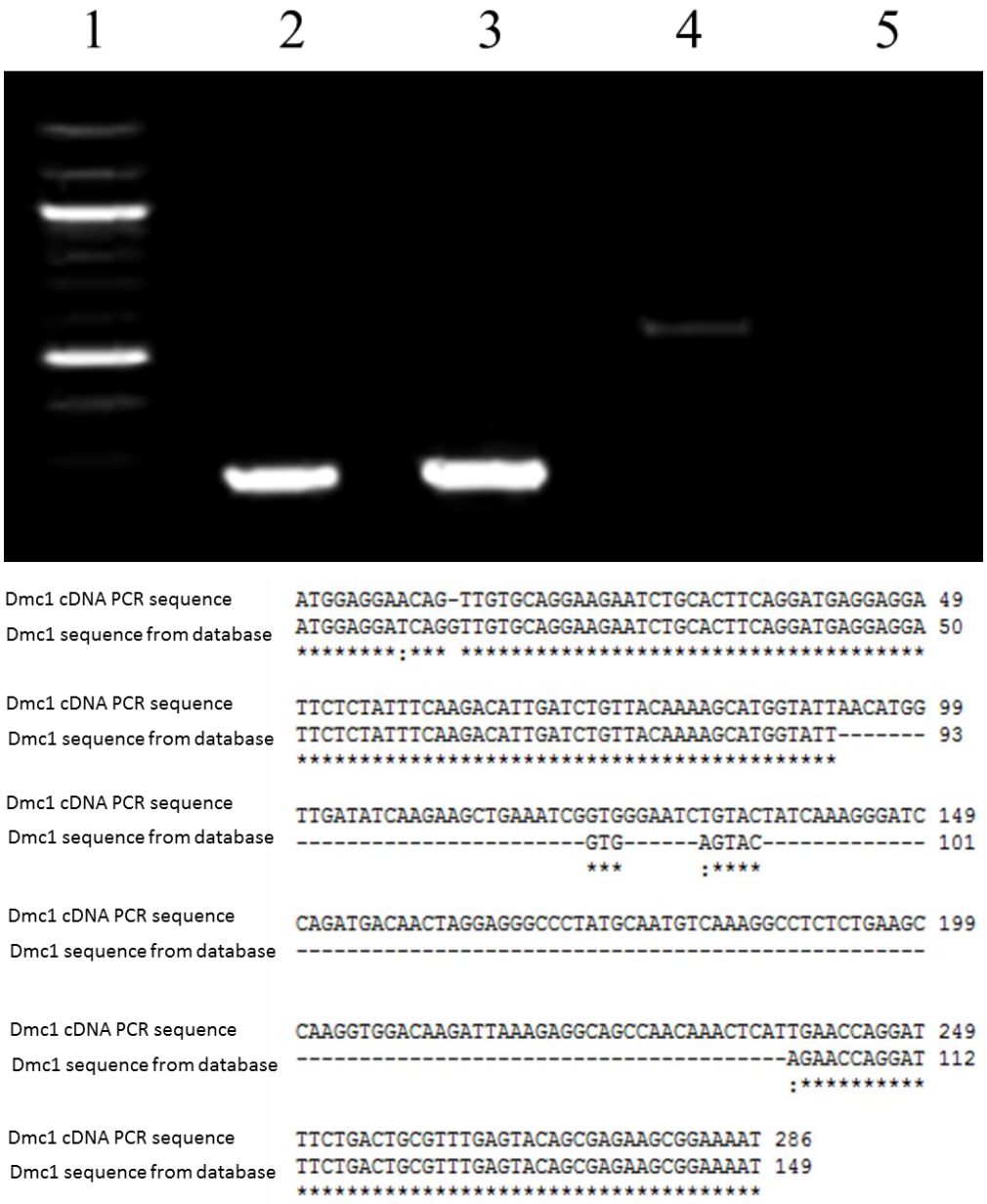

Figure 17: RT-PCR analysis amplified cDNA coding the HhH domain of platypus *Dmc1* (A) To confirm the presence of the HhH domain, primers were designed in the 5′ end of the *Dmc1* gene. Lanes 2 and 3 are platypus testis cDNA samples while lane 4 is a platypus genomic DNA control. In lane 5 is a blank negative control. (B) Sequencing of the resulting cDNA product from (A) was aligned with corresponding Dmc1 sequence in the Ensembl platypus database. Starred bases represent identical sites while colons indicate substitutions. Gaps in sequence are indicated by dashed lines.

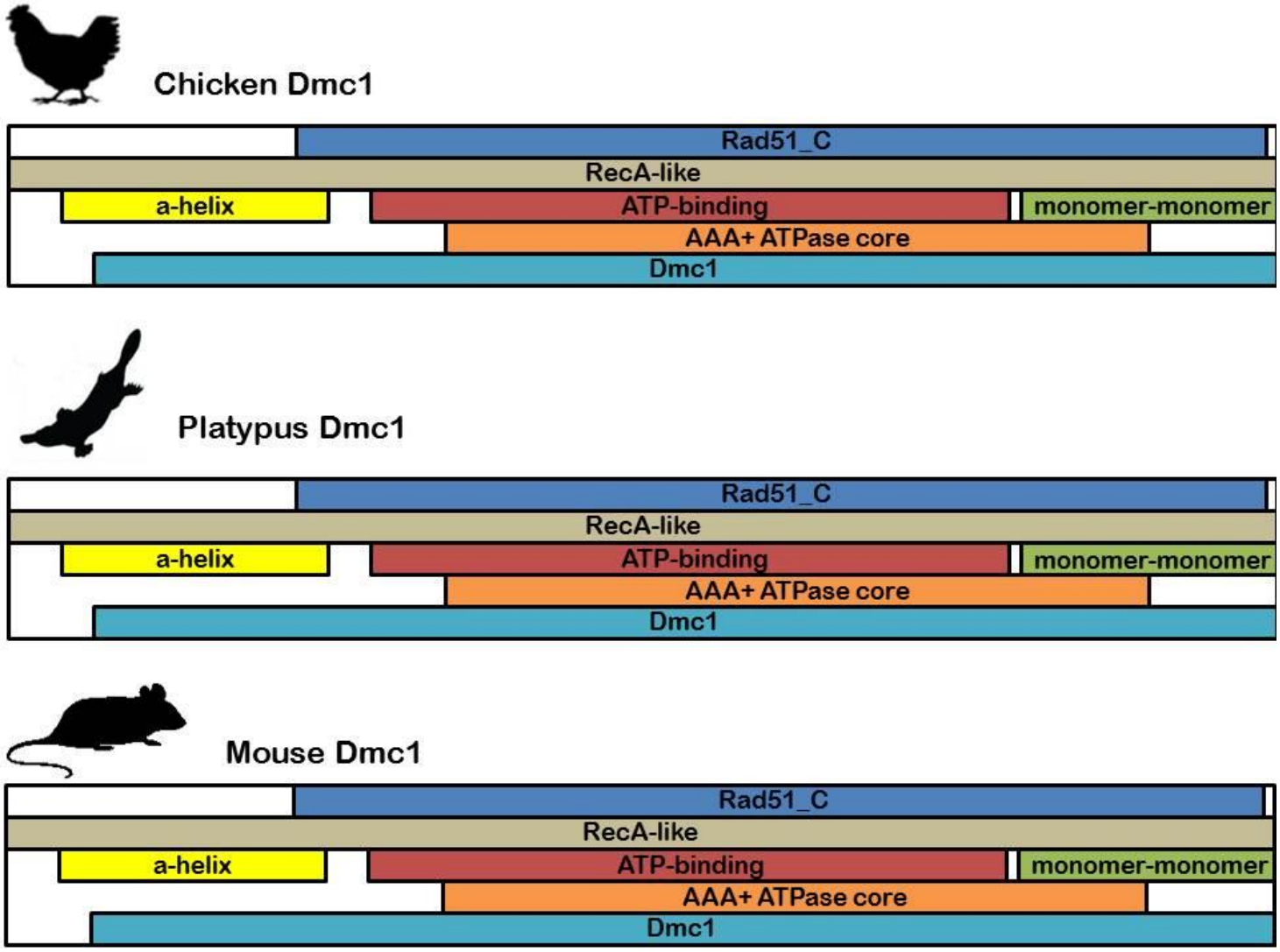

Figure 18: Dmc1 domain prediction in chicken, platypus, and mouse using InterPro This prediction shows that the same domains are present in platypus as in chicken and mouse. Platypus Dmc1 protein domains appear to be indistinguishable from those of mouse and chicken.

Corresponding with these results, the branch lengths on the *Dmc1* phylogenetic tree (Fig. 19) tend to be remarkably short. This result along with Omega analysis indicated that *Dmc1* has been extremely well conserved across taxa.

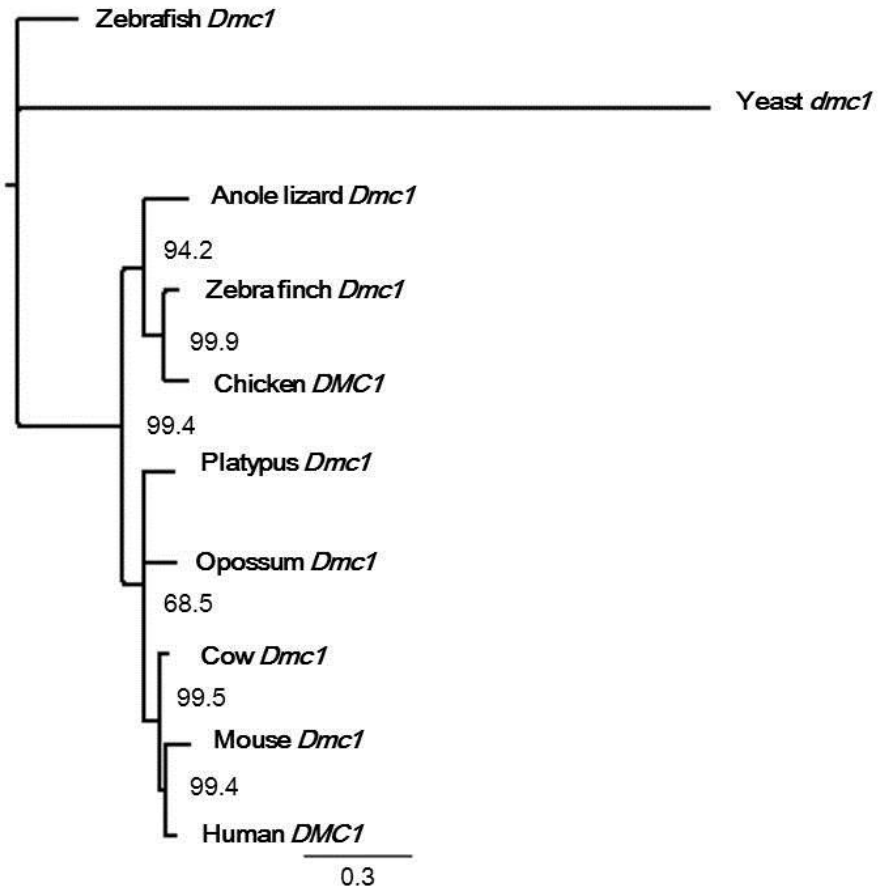

Figure 19: *Dmc1* phylogenetic tree MrBayes (Ronquist & Huelsenbeck, 2003) generated phylogenetic trees using a translation alignment of cDNA sequences. The numerical values marked at the nodes represent the posterior probability (the proportion of sampled trees containing the nodes). The scale bar of 0.3 represents the branch length, measured in expected changes per site.

Blm

Blm is an important protein that is critical for the prevention of aberrant crossover formation. *Blm*, like *Rad51*, proved to be one of the more difficult genes to analyse in platypus. On first inspection the platypus *Blm* gene did not appear to have conserved genomic context with mouse *Blm* (on chromosome 7); however, sequence downstream of *Blm* in platypus corresponded with mouse chromosome 7 in a nucleotide BLAST. The platypus *Blm* database sequence also seemed to be incomplete. When the translated protein sequences were aligned, platypus Blm appeared to be missing the N- and C-termini. RT-PCR expression analysis and sequencing of the expected ~250 bp product (Table 4, Fig. 20) confirmed the presence of *Blm* transcripts in adult platypus testis. This experiment could not, however, amplify any product

using the genomic DNA control. It is thought that the expected genomic product (~1.4 kb) was too large to amplify under these conditions.

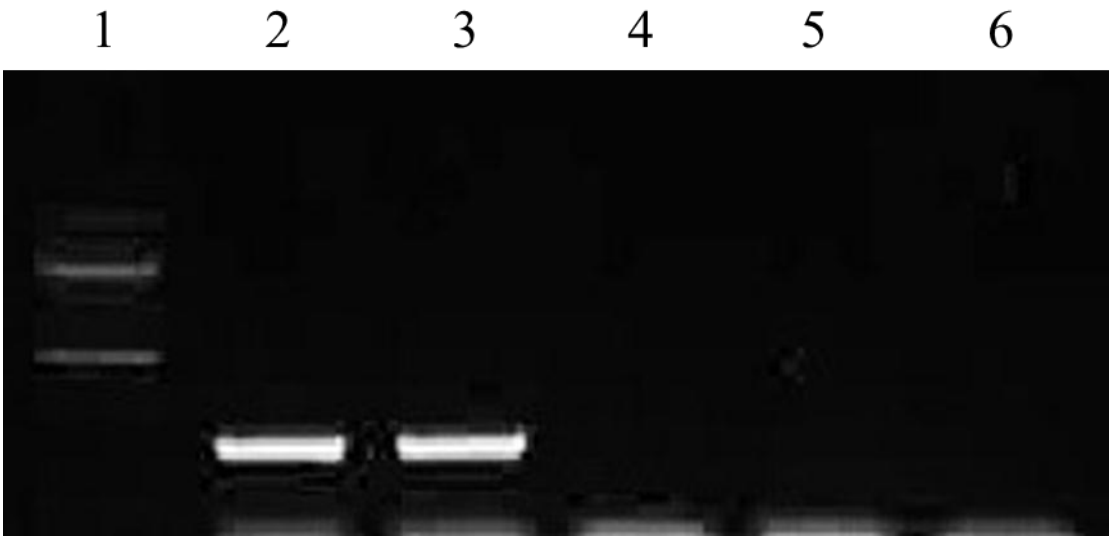

Figure 20: RT-PCR expression analysis of *Blm* A *Blm* RT-PCR amplified cDNA products ~250 bp. A 100 bp marker was used and lanes 2 and 3 are platypus testis cDNA samples (from animals PIII and P07 respectively); lane 4 is a platypus genomic DNA control (the expected product size, ~1.4 kb, was not successfully amplified in this experiment); lane 5 is an echidna genomic DNA control; and in lane 6 is a blank negative control. The cDNA products are both of the expected size (~250 bp).

Conservation analysis between platypus and mouse there is a 91.6% pairwise identity (excluding gaps in database sequence, as they were considered likely artefacts of an incomplete assembly) (Table 4). This indicates that the *Blm* sequence present in the database is highly conserved across species. According to protein domain scans (Fig. 21) the platypus *Blm* gene appears to be missing four key domains: BDHCT (IPR012532), RecQ_C (IPR018982), Helicase/RNaseD_C (IPR002121), and HRDC (IPR010997). Further analysis using alternate domain search software (MotifScan using Prosite on ExPASy, Pfam, and InterPro databases) predicted RecQ_C, Helicase/RNaseD_C, and HRDC domains to be present in the platypus Blm peptide; however, there is no evidence for the presence of the BDHCT domain (IPR012532). This is a potentially significant result as the BDHCT domain anticipates DNA repair and unwinds DNA in a 3′-to’5′ direction. As such, it is critical to Blm’s helicase function in meiosis. Attempts to further investigate were hampered by lack of sequence conservation which did not allow for the design of degenerate primers adjacent to the BDHCT domain using chicken, opossum, and/or mouse sequences. In future studies, RACE PCR could be used to further investigate the terminal *Blm* gene sequence in platypus.

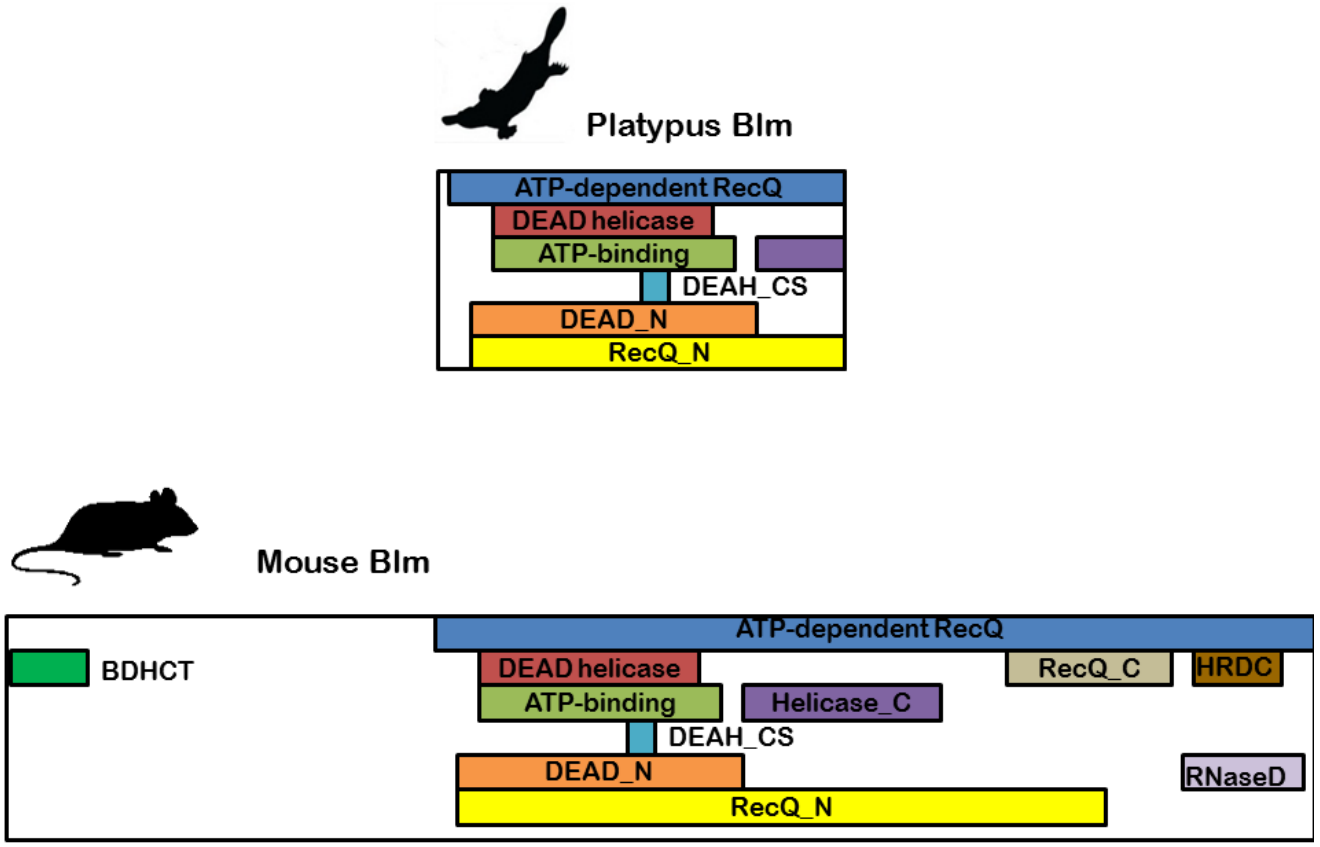

Figure 21: Blm protein domain alignment InterPro domain scans of the platypus Blm protein indicate that the platypus is missing both the N- and C-terminal ends, resulting is a loss of the BDHCT, RecQ_C, HRDC, and RNaseD domains. Further analysis has identified potential platypus RecQ_C, HRDC, and RNaseD domains, but not the BDHCT domain (not shown here as more experimentation is required to confirm their presence).

Despite these differences between the platypus, mouse and chicken Blm peptide sequences, the phylogenetic tree for *Blm* resembles what would be expected for a well-conserved gene (Fig. 22). Most branch lengths among vertebrates are short (under 0.3 amino acid substitutions per site), and the platypus *Blm* is positioned closer to other mammals than might be expected given the predicted missing BDHCT domain sequence. Omega analysis does not provide any evidence of positive selection acting to differentiate platypus *Blm* from other vertebrates. This along with the bioinformatics and expression data seems to suggest a conserved role for Blm in platypus meiosis, though additional sequencing work is needed to complete the assembly.

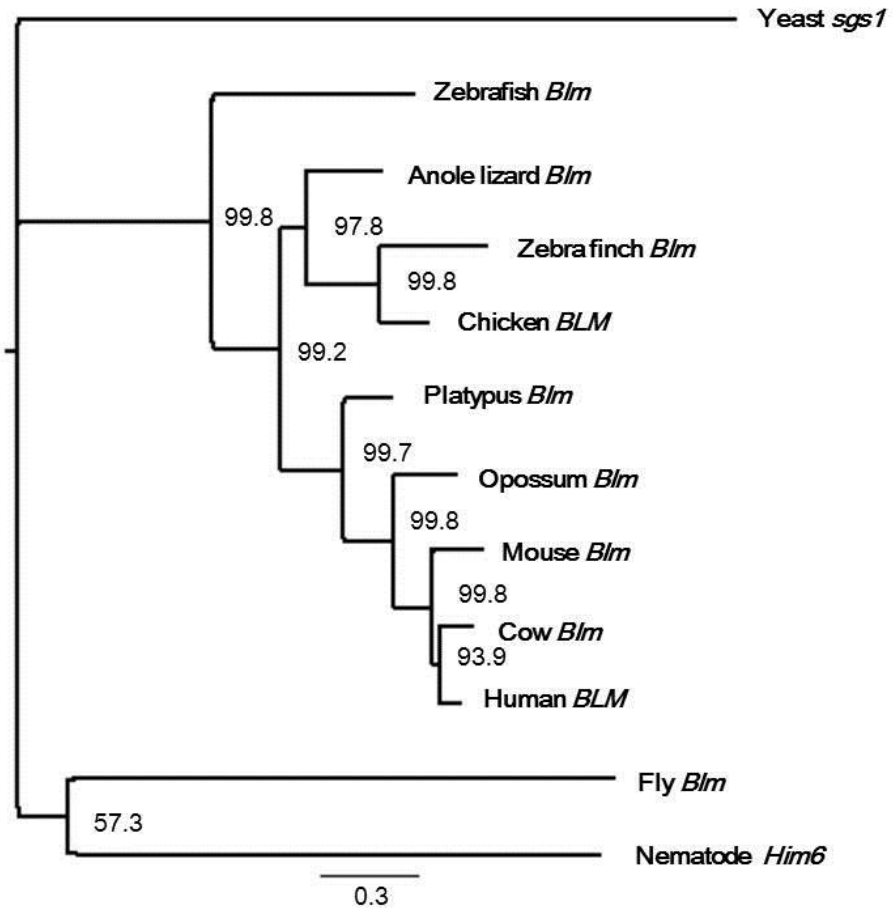

Figure 22: *Blm* phylogenetic tree MrBayes (Ronquist & Huelsenbeck, 2003) generated phylogenetic trees using a translation alignment of cDNA sequences. The numerical values marked at the nodes represent the posterior probability (the proportion of sampled trees containing the nodes). The scale bar of 0.3 represents the branch length, measured in expected changes per site.

Msh4

MutS homologues have recombinase properties and play vital roles in recombination nodules. Msh4 and Msh5 are both structurally similar proteins, though they are not syntenic (in mouse, *Msh4* maps to chromosome 3 while *Msh5* maps to chromosome 17). The platypus copy of

Msh4 was identified, but there was no evidence to confirm conserved gene context with mouse *Msh4*; however. RT-PCR experiments demonstrated *Msh4* expression in platypus adult testis (Table 3) amplifying a ~200 bp product (Fig. 23). Sequencing results further confirmed the identity of this product to be *Msh4*.

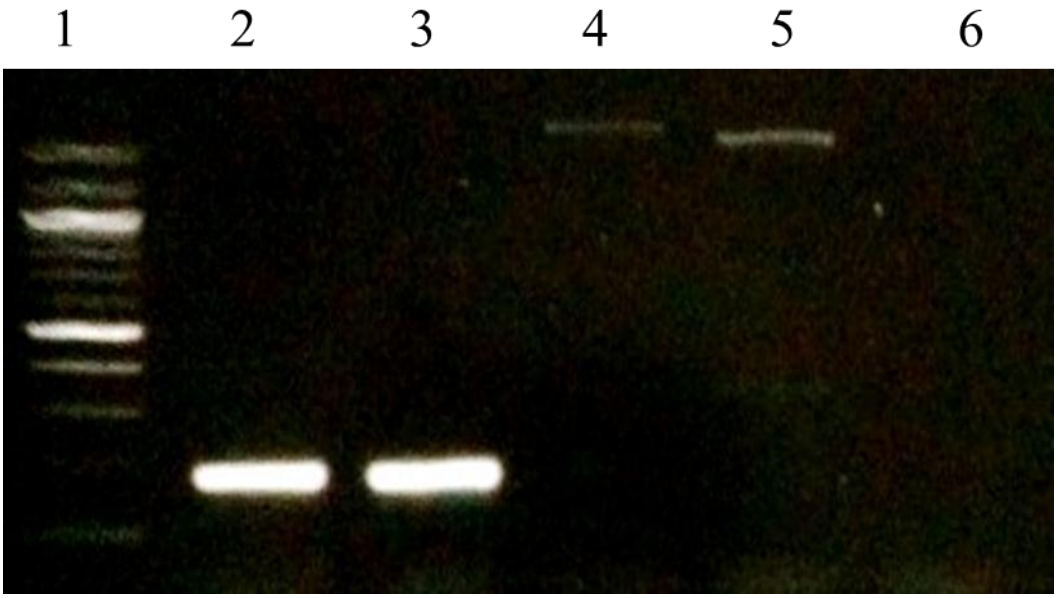

Figure 23: RT-PCR expression analysis of *Msh4* A *Msh4* RT-PCR amplified cDNA products of the expected ~200 bp. Lane 1 is a 100 bp marker; lanes 2 and 3 are platypus testis cDNA samples (from PIII and P07 respectively); lane 4 is a platypus genomic DNA control; lane 5 is an echidna genomic DNA control; and lane 6 is a blank negative control.

The platypus *Msh4* sequence appears to be incomplete in the database, but Msh proteins derived from the partial sequence tend to be well conserved across taxa; Msh4 has a 62.4% identical sites. Excluding gaps in the database sequence, Msh4 has an 80.7% pairwise identity between platypus and mouse (Table 4), and given this high percent identity, it is very likely that the identified platypus gene is a *Msh4* orthologue.

Msh4 has four critical domains: the clamp (IPR007861), the core (IPR007696), the connector (IPR007860), and the MutS-C terminal domain (IPR000432). An InterPro scan (Fig. 24) of the platypus Msh4 protein predicts the presence of all these domains except the connector domain, a Holliday junction resolvase located on the N-terminus of Msh4 that has been hypothesised to interact with Mlh1. The absence of this domain could have dramatic consequences on Msh4's functionality during meiotic recombination. To investigate the potential absence of the connector domain, degenerate primers were designed using chicken, opossum and mouse sequences adjacent to the domain. RT-PCR, was unable to amplify a specific product from platypus testis cDNA which is likely due to divergence of sequence

adjacent to the connector domain. Further analysis is needed to confirm the loss of the connector domain in platypus Msh4, though as of this writing there was not sufficient time to optimize the necessary RACE PCR.

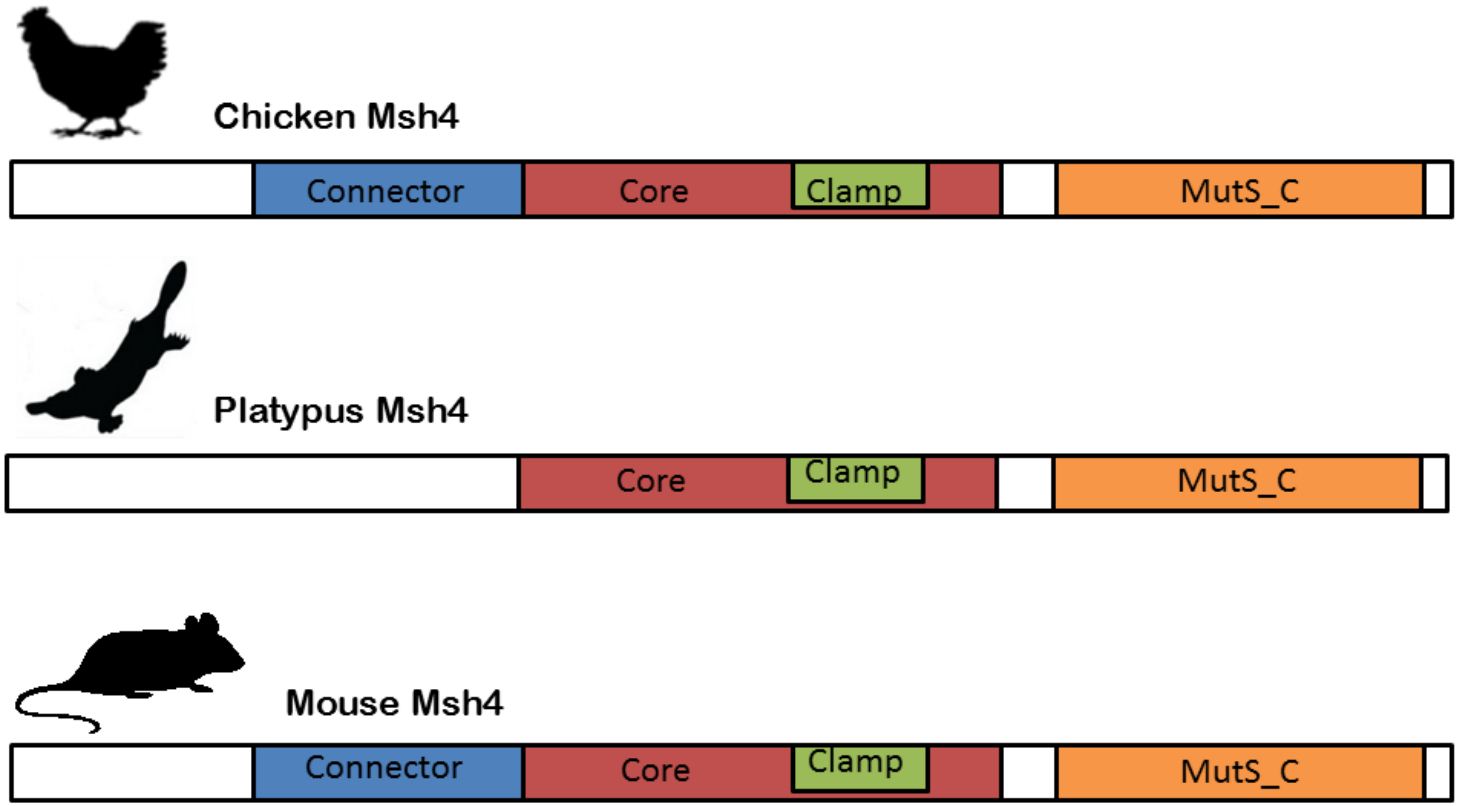

Figure 24 : Msh4 protein domain alignment Using InterPro protein domain scans reveal that the platypus Msh4 is missing the connector domain5.

The phylogenetic tree for *Msh4* (Fig. 25) is characteristic of a well conserved protein, most notably it tends to have very short branch lengths with a tight clustering of mammalian taxa and a shorter branch length for platypus. Omega analysis of *Msh4* further does not support the hypothesis that positive selection is acting on the platypus gene; therefore, aside from the prospective missing connector domain in Msh4, the protein is well conserved in platypus.

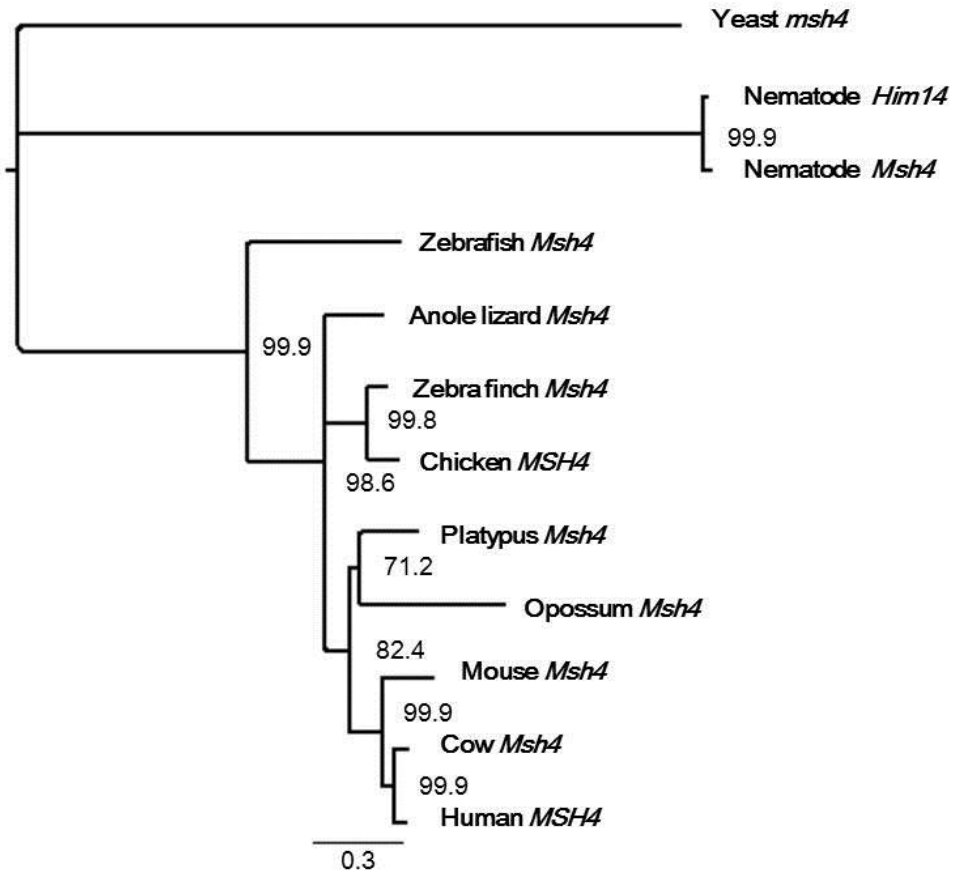

Figure 25: *Msh4* phylogenetic tree MrBayes (Ronquist & Huelsenbeck, 2003) generated phylogenetic trees using a translation alignment of cDNA sequences. The numerical values marked at the nodes represent the posterior probability (the proportion of sampled trees containing the nodes). The scale bar of 0.3 represents the branch length, measured in expected changes per site.

Prdm9

Prdm9, a histone methyltransferase, plays a role in dictating the position of crossover hotspots. The *Prdm9* gene has several paralogues in many species, each with similar protein domains, making identification of orthologues of the mouse *Prdm9* gene difficult. Initial BLAST searches for the platypus orthologue uncovered seven genes. Upon further analysis, two of these were found to be *Prdm9* paralogues (*Prdm12* and *Prdm14*) based on one-to-one orthology with mouse. Two of the five remaining possible genes failed to produce mouse *Prdm9* as a hit on a BLAST search while a third did not have any of the characteristic

functional domains of a Prdm protein. The two positive genes (henceforth termed *Prdm9a* and *Prdm9b*) are located adjacent to one another on platypus X5 and they do have conserved genomic context with mouse, human, rat, and opossum *Prdm9*. There is an overall lack of conserved gene order (Fig. 26) between mammals, suggesting that while *Prdm9* synteny is conserved between mammals, there is also a high degree of intra- and interchromosomal rearrangement. This is reflected more in a break of gene context regarding the *Aco1* and *Prdm6* genes in mouse and human, a possible interchromosomal exchange. In human and mouse, Aco1 is mapped to chromosome 9 and 4 respectively, suggesting that there has been a synteny break between *Prdm9* and *Aco1* after the divergence of platypus from therians. Additionally, the mouse*Prdm6* gene has been mapped to chromosome 18, showing another synteny break around *Prdm9*. Interestingly, while there is no predicted *Prdm9* in chicken, the *Prdm6* and Aco1 genes on the chicken Z show conserved genomic context with platypus X5 and human chromosome 5 (Fig. 26), reflecting previously reported homology between the platypus X and the chicken Z (Veyrunes et al., 2008). These data suggest that the region around *Prdm9* is unstable.

To confirm the predicted duplication of *Prdm9* in platypus, primers specific for each *Prdm9a* and *Prdm9b* were designed. Genomic PCR amplified bands from both primer sets (Fig. 27) and subsequent DNA sequencing confirmed the identity of both *Prdm9* genes from the platypus database. Peptide alignments of the two translated proteins show that each protein has a distinct sequence, further indicating the gene underwent a duplication event in platypus. Additionally, RT-PCR expression (Table 4) analysis demonstrated that *Prdm9a* is expressed in adult platypus testis. Using publicly available sequences it was impossible to identify a *Prdm9* orthologue in chicken, lizard, or frog; however there is a *Prdm9* in zebrafish. Multiple alignment results suggest that Prdm9 is not well conserved across species; among mammals (rat, mouse, human, opossum, and platypus) there are only 51.9% identical sites (Table 4). When only platypus and mouse are compared, the pairwise identity is calculated to be 30.7% (Table 4), and between the two platypus Prdm9 peptides there is a 41% pairwise identity.

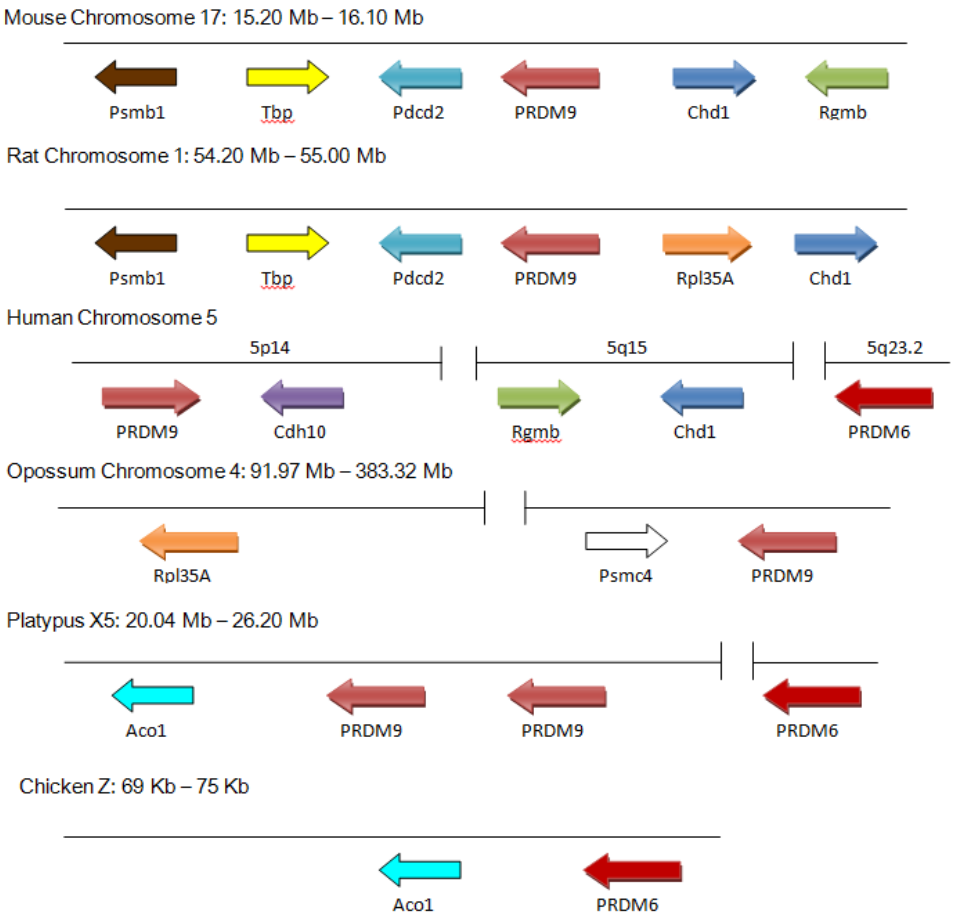

Figure 26: *Prdm9* genomic context in amniotes Arrows signify the orientation of genes while interruptions (gaps) in the lines represent long stretches of chromosome which are not relevant to this figure. Gene arrangements around *Prdm9* have changed dramatically between species, although conserved synteny is present in therians. In mammals there has been significant change in gene order; however, the platypus gene does show conserved synteny.

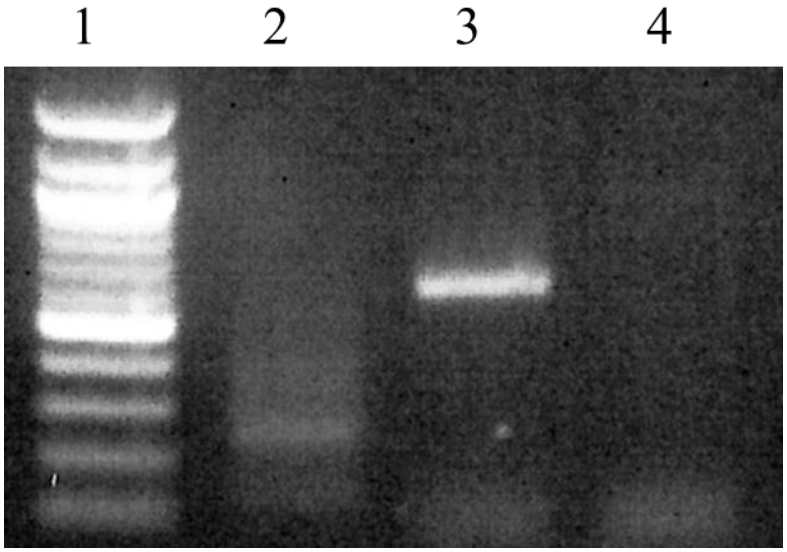

Figure 27: PCR confirms the duplication of *Prdm9* in platypus Lane 1 contains a 100 bp makrer; lanes 2 and 3 used genomic PCR primers specific for platypus *Prdm9a* and *Prdm9b* (amplifying the expected products of ~250bp and ~700bp respectively). Sequencing confirmed the identity of the product *Prdm9a* and *Prdm9b*. Lane 4 is a blank negative control.

Domain scans for functional domains (Fig. 28) revealed interesting results. All eutherian Prdm9 proteins had a similar domain profile consisting of a Krueppel-associated box (IPR003655), a SET domain (IPR001214), an SSXRD domain (IPR019041), and a zinc finger array (IPR007087). In contrast, the platypus Prdm9a is missing the Krueppel-associated box and the SSXRD domains while the opossum only has the SSXRD and SET domains. Platypus Prdm9b, on the other hand, is missing all domains except the zinc finger array, indicating that it has diverged considerably and is not likely to have a conserved function. The zebrafish Prdm9 is remarkably similar to the platypus; both consist only of SET domains and a zinc finger array. These data suggest that the SSXRD domain is a recent development in therians, while the Krueppel-associated box may be a specific feature of eutherian Prdm9. It appears that the opossum, and possibly other marsupials, lost the zinc finger domain sometime in their evolutionary history. Prdm9 seems to be a rapidly-evolving protein, and the lack of pairwise identity across species and these protein domain profiles seem to suggest that the platypus represents the early mammalian stages of the *Prdm9* genes and that the Krueppel box and the SSXRD domains likely evolved after the platypus diverged from the therians.

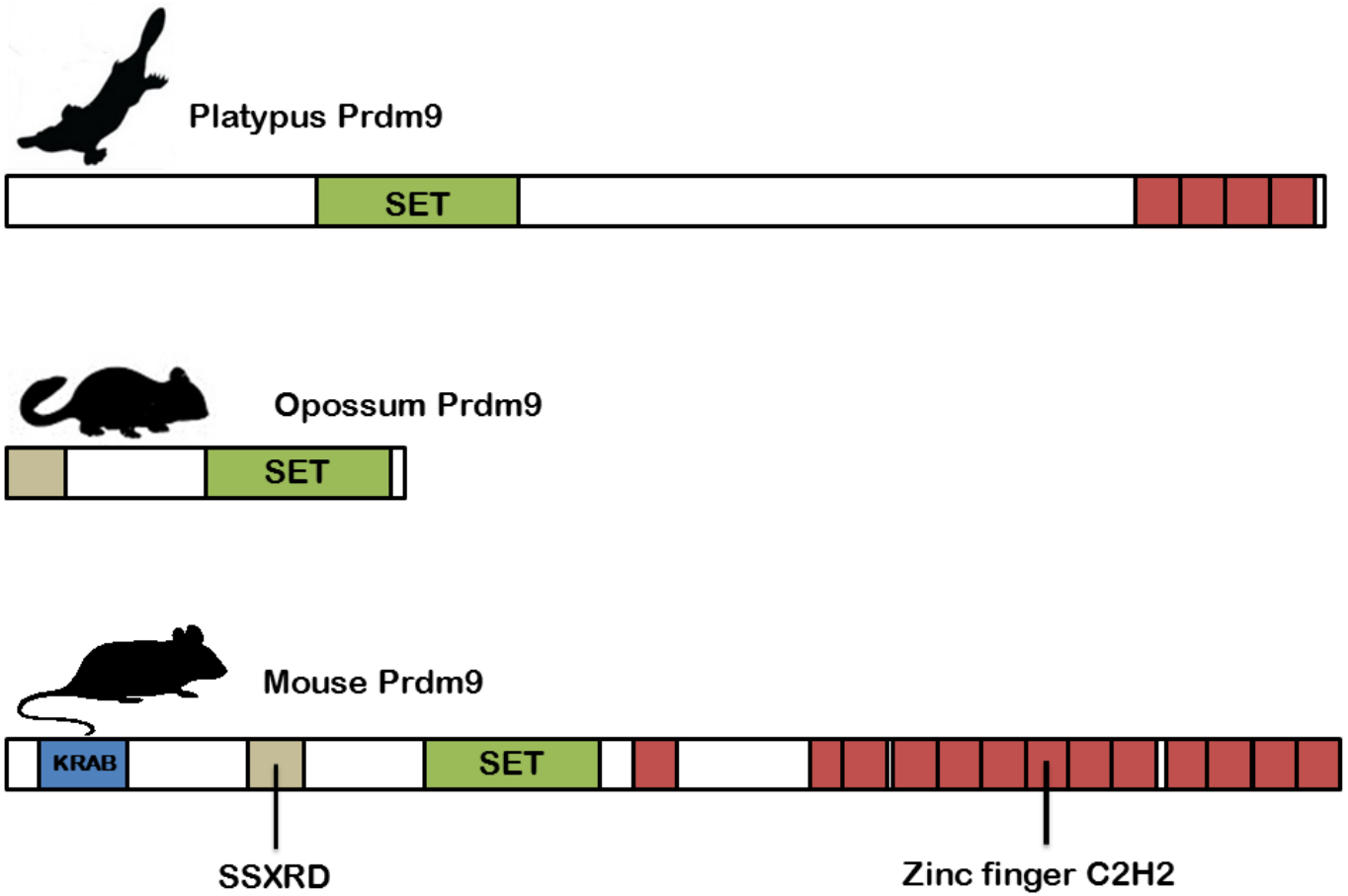

Figure 28: Prdm9 protein domain alignment Protein domains of Prdm9 vary between mouse, opossum, and platypus. All species have the SET domain, necessary for methyltransferase activity; however, the opossum does not have zinc fingers, the platypus does not have an SSXRD domain, and neither the platypus nor the opossum has the KRAB domain, a transcription repressor domain.

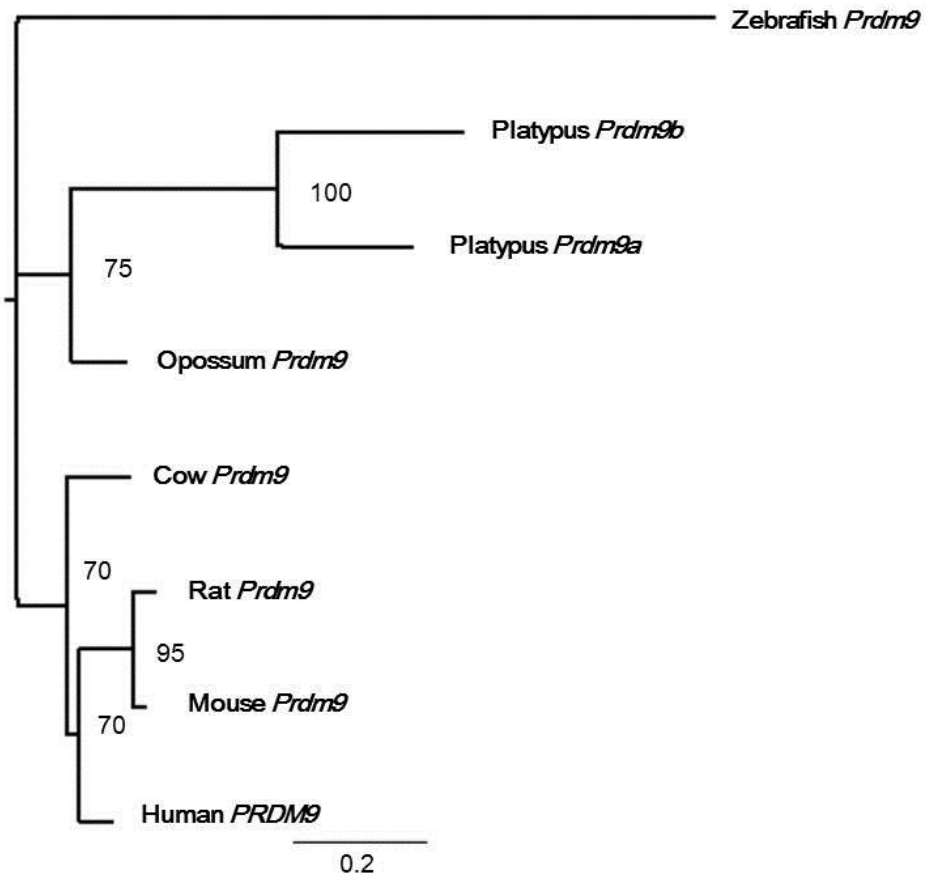

Figure 29: *Prdm9* phylogenetic tree MrBayes (Ronquist & Huelsenbeck, 2003) generated phylogenetic tree using a translation alignment of cDNA sequences. The numerical values marked at the nodes represent the posterior probability (the proportion of sampled trees containing the nodes). The scale bar of 0.2 represents the branch length, measured in expected changes per site.

A Bayesian phylogenetic tree (Fig. 29) was constructed using translation alignments of cDNA sequences. The results of the analysis groups the mammals into two different clusters: the eutherians and the platypus and opossum. While this distribution might suggest that eutherian *Prdm9* and platypus *Prdm9* are divergent, omega analysis was unable to find any evidence of positive selection in platypus. The dramatic differences between opossum *Prdm9* and the eutherian *Prdm9*—and most notably the missing SET domain in opossum—suggest that opossum *Prdm9* is not functional. Conversely, given the protein domain prediction analysis the platypus Prdm9 protein appears to have functional capabilities similar to those of other mammals and zebrafish; the platypus protein has both a zinc finger array and a SET domain, indicating that it is capable of DNA binding and histone methyltransferase activity, with both domains being critical to Prdm9's ability to govern crossover hotspots in meiosis. Yet, whether or not the platypus *Prdm9* gene does influences hotspots has yet to be demonstrated.

Chapter 3: Visualising crossovers in platypus meiosis

The immunolocalisation of proteins during meiosis has been an invaluable tool in the analysis of various aspects of meiotic recombination. Immunofluorescence studies have been instrumental in revealing protein interactions with chromosome cores as well as the temporal progression of meiotic recombination; however, there have not yet been any such studies investigating meiotic recombination in monotremes. In addition to the sequence analysis of genes involved in major steps of the meiotic recombination pathway, it was an aim to visualise recombination events *in situ* in the platypus. As the platypus diverged from therian mammals nearly 200 Million years ago, it is imperative that any antibodies used in immunofluorescent studies react to a conserved epitope. In order to increase chances of cross hybridisation, commercial antibody epitopes sequences were aligned with platypus peptide sequences to determine conservation of the epitope. Using this method, commercial antibodies with platypus-conserved immunogen sequences were identified for Spo11 Rad51, and Mlh1; additionally, considering the high degree of conservation, Dmc1 antibodies were also considered. Of these four antibodies, Mlh1 was the preferred choice as Mlh1 foci in pachytene are markers of crossovers; alternatively, Rad51 would also represent a favourable choice as many other meiotic studies in other organisms have used Rad51 data, and thus would provide a comparable standard. There are two well-established rabbit polyclonal antibodies for platypus synaptonemal complex proteins, Smc3 and Sycp1. For the purposes of this study, Smc3 and Sycp1 were used to identify the pachytene stages.

Examining the specificity of antibodies

Western blot analysis was used to determine the reactivity and specificity of Smc3, Dmc1, Mlh1, and Rad51 antibodies in both mouse and platypus testis and kidney tissue samples. The control, anti-Smc3 antibody detected a ~145 kDa band in both platypus and mouse somatic and meiotic tissue (Fig. 30A). This is an expected result, matching both the ubiquitous expression and predicted size of the Smc3 protein. Several additional smaller bands of varying sizes were observed; however, it is unclear what these bands represent. In immunofluorescence studies the Smc3 antibody does often stain additional, unidentified,

extra-nuclear structures, and it is possible that these extra bands on the Western represent this non-specific binding. A similar result was observed in the Mlh1 Western (Fig. 30C) whereby 84 kDa bands were clearly visible in mouse testis and platypus kidney and testis samples while a faint band of similar size was present in mouse kidney. This, again, is the expected size and expression profile for Mlh1, which is expressed in both meiotic and somatic tissues; however, like Smc3, other, unspecific bands were visible, particularly in the platypus kidney sample. In contrast to the relative specificity of Smc3 and Mlh1, anti-Rad51 Western blot (Fig. 30D) showed a high number of non-specific bands in addition to the expected 37 kDa band in both platypus and mouse somatic and meiotic samples. Interestingly bands of the expected ~37 kDa were observed in the Dmc1 Western (Fig. 30B) in both platypus and mouse kidney and testis samples. 37 kDa is the expected size of the Dmc1 protein; however, Dmc1 is a meiosis-specific protein (except in plants), and the bands in the somatic samples are unexpected. To confirm the expression profile of *Dmc1*, RT-PCR using platypus Dmc1-specific primers was performed with testis and kidney cDNA samples. As expected *Dmc1* expression was observed in testis but not kidney (Fig. S3.1 on accompanying CD). Thus it appears the Dmc1 antibody was not binding to Dmc1 protein in mouse and platypus kidney tissues. A different Dmc1 antibody was used to repeat the Western blot which yielded the same result. It is possible that the antibodies are cross-reacting with Rad51, which would explain the expression observed in somatic tissues as Rad51 is ubiquitously expressed. Additionally, Rad51 and Dmc1 are both 37 kDa and share ~50% sequence homology, making cross-reactivity the most likely explanation of the observed results.

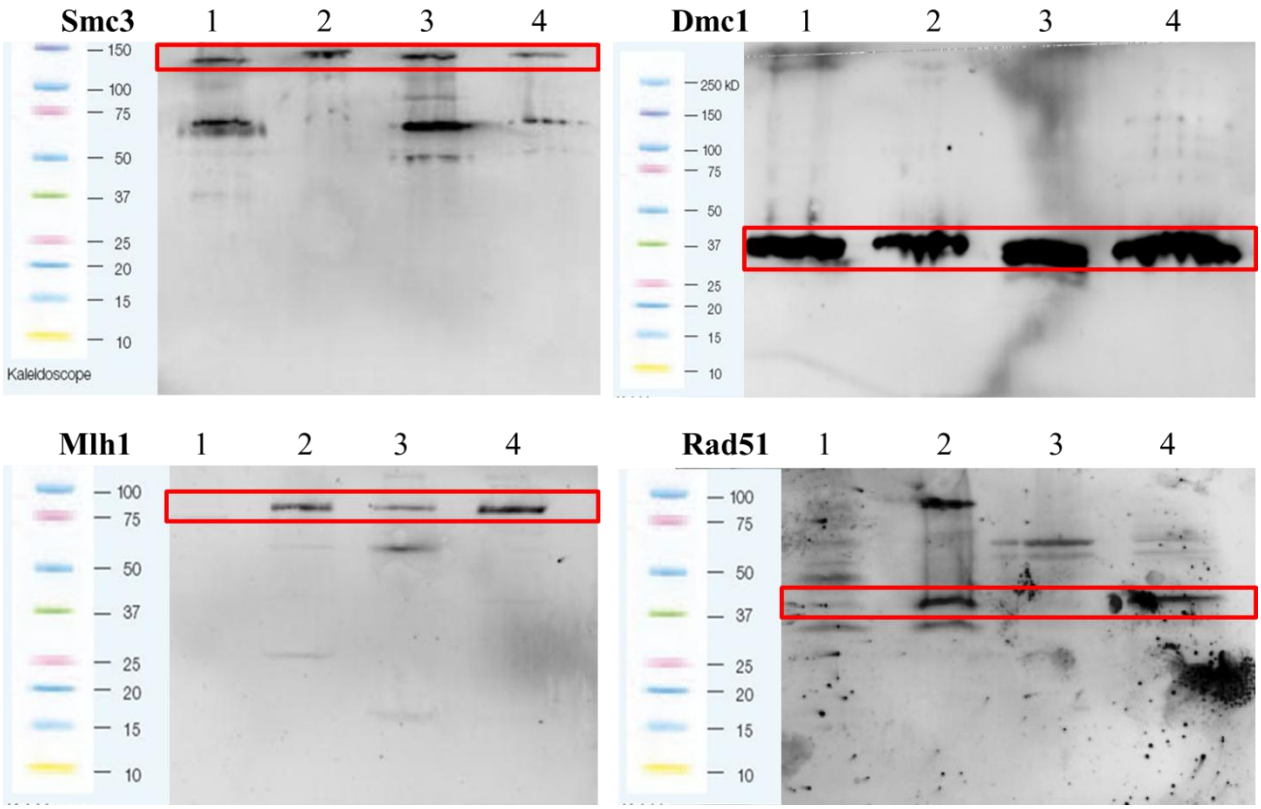

Figure 30: Western blot analysis of Smc3, Dmc1, Mlh1, and Rad51 in platypus Each sample was run in the following order going from left to right: mouse kidney (1), mouse testis (2), platypus kidney (3), platypus testis (4). Red boxes highlight the expected bands. Smc3: Bands were observed at the expected size, 145 kDa in each sample; however some smaller bands of unknown identity were also detected. Dmc1: As expected a 35 kDa band was detected in both mouse and platypus testes; however the same band was also present in the kidney samples. Mlh1: The expected Mlh1 band at 84 kDa was observed in each sample, but several bands of unknown identity were also observed. Rad51: In addition to the expected 37 kDa band, a number of nonspecific bands were detected.

Visualising crossovers in platypus meiosis

The Sycp3 antibody used in this study did not work in platypus immunofluorescence staining experiments; thus, while this study successfully uses a mouse monoclonal Sycp3 antibody in mouse experiments, it is restricted to using a rabbit polyclonal Sycp1 or Smc3 antibodies in platypus experiments. In initial immunofluorescence experiments Mlh1 antibodies were used in both platypus and mouse; despite the disadvantage that both the Mlh1 and Sycp1 antibodies were raised in rabbit (thus making simultaneous staining impossible), the Western blot results were promising and Mlh1 has long been used as an indicator of mature crossover sites. In mouse experiments Mlh1 and Sycp3 were co-stained. As expected, clear, distinct Mlh1 foci were observed along the chromosome cores (Sycp3) in mouse; however, background staining prevented accurate scoring of the foci numbers (Fig. 31). A similar issue was observed in the platypus experiments where, unlike mouse, antibody staining had to be done sequentially. Using this method, what appeared to be distinct Mlh1 foci along the SCs were observed in

pachytene cells amid heavy background staining (Fig. 31). In platypus, as in mouse, the background staining prohibited any scoring of foci numbers; however, these experiments nonetheless yielded foci that appeared likely to be true Mlh1 foci and not artefacts of nonspecific staining. Typically, a minimum of 51% of a focus needs to co-localise with the SC in order for it to be scored as an actual focus (personal correspondence with Dr. Pat Hunt and Dr. Terry Hassold, 2008). Additionally confounding efforts in platypus experiments, the sequential staining proved to be damaging to the integrity of the SC, as Sycp1 staining revealed the transverse filaments to appear frayed and broken. Despite efforts to remove or reduce the background staining (including decreasing antibody concentration and extended washes and using various surface spreading and cytospin protocols, see Supplemental Data section S0.3, page 4 on accompanying CD), it proved impossible to achieve scorable Mlh1 staining in platypus.

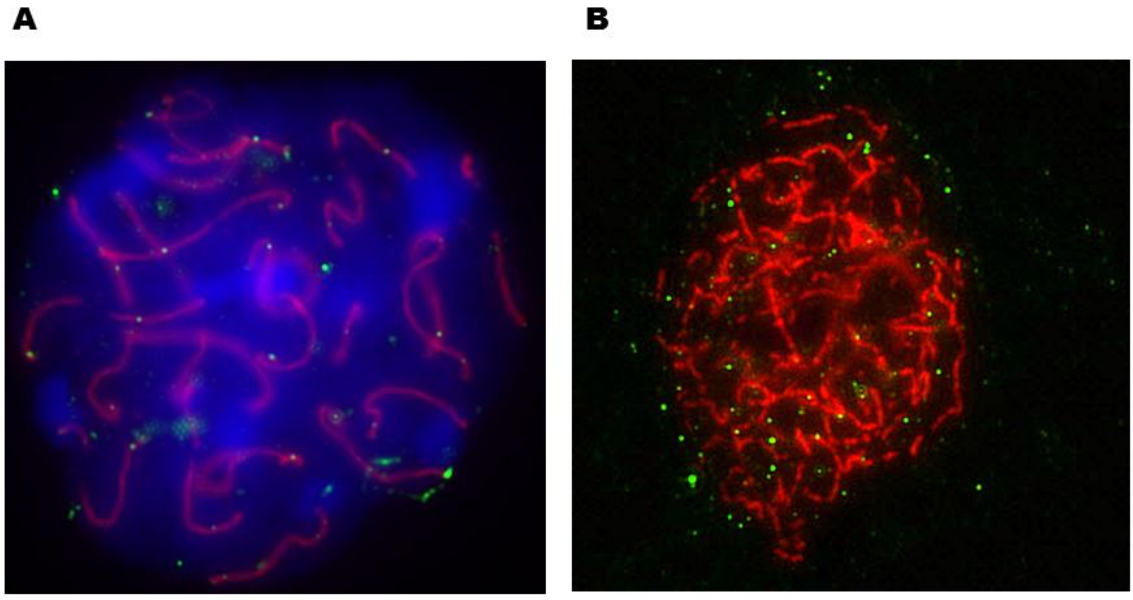

Figure 31: Mlh1 staining in mouse and platypus pachytene cells A) Mouse Mlh1 (green) and Sycp3 (red) staining. B) Platypus Mlh1 (green) and Sycp1 (red) staining. While there do appear to be some specific Mlh1 foci (defined by co-localisation on the SC) in the platypus cell, there is too much nonspecific staining to accurately count Mlh1 foci.

As it was not possible to reduce background of Mlh1 staining, Dmc1 was considered as alternative to visualise crossovers. Due to its extensive sequence conservation, Dmc1 was expected to produce a similar phenotype in platypus as in mouse, namely hundreds of distinct foci in zygotene with diminishing numbers in late zygotene and a near-absence of Dmc1 by the start of pachytene. Initial attempts at immunofluorescent visualisation of Dmc1 expression in prophase cells in mice was inconsistent; with ubiquitous nuclear background staining

common, there were occasional cells that featured distinct Dmc1 foci along the SC. Unfortunately, because the mouse serves as a control system, these results made it difficult to make a comparative assessment in platypus.

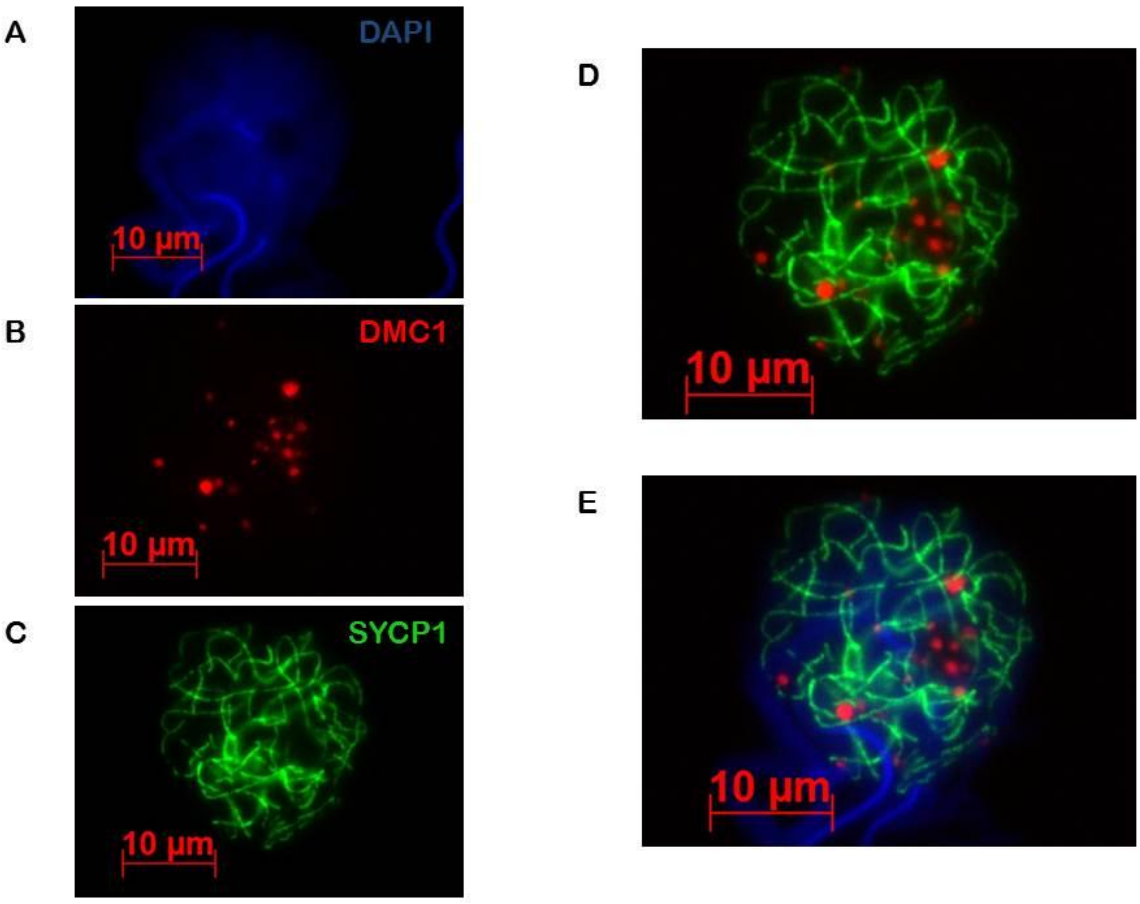

Figure 32: Pachytene expression of Dmc1 and Scyp1 in platypus Immunofluorescent imaging of A) DAPI, B) Dmc1, C) Sycp1, D) merged Dmc1 and Sycp1, and E) merged Dmc1, Sycp1, and DAPI. Dmc1 foci are clearly visible only in the nucleus and associate closely with Sycp1.

In contrast to the findings in mouse, immunostaining Dmc1 in platypus revealed a clear and consistent staining pattern (Fig. 32, 34). Little to no background staining was observed and Dmc1 foci consistently associated with the chromosome cores. Due in part to the seasonal reproductive cycle of platypuses and the time when the platypus testis material was collected, most prophase cells observed were in pachytene or later in spermatogenesis. Specific and abundant Dmc1 foci were not expected later outside early prophase I because it contrasted with previous mouse studies that observed Dmc1 foci numbers decrease until the protein was all but absent by pachytene. It was possible to estimate the prophase stage using the state of the synaptonemal complex; because Sycp1 filaments begin to assemble along chromosome cores in zygotene and appear fully synapsed (represented by unbroken filaments) in mid

pachytene, it was possible to confirm the majority of the Dmc1-positive cells as early to mid-pachytene.

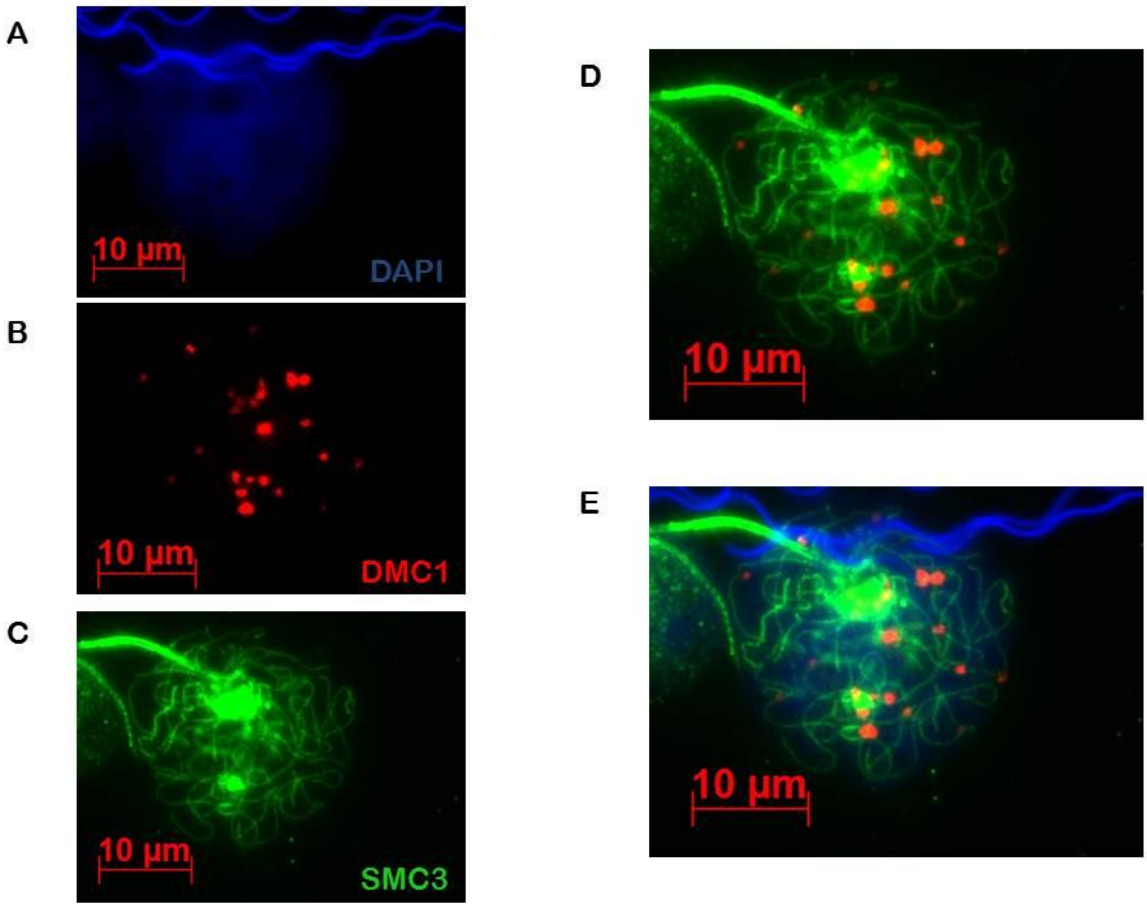

Figure 33: Localisation of Dmc1 and Smc3 in platypus pachytene cells Immunofluorescent imaging of A) DAPI, B) Dmc1, C) Smc3, D) merged Smc3 and Dmc1, and E) merged DAPI, Smc3, and Dmc1. Some Dmc1 foci associate closely with the Smc3 filaments.

The observed Dmc1 foci in platypus appeared to vary in size: on one extreme they were discrete pinpoint foci while on the other they were larger, globular masses (Fig. 34). This finding seems to suggest that Dmc1 accumulates at specific regions in platypus late-zygotene and early-pachytene. In general Dmc1 foci averaged a surface area of about 0.33 μm^2; larger, globular accumulation of Dmc1 (as large as 3.06 μm^2)—while a frequent occurrence—was not the most commonly observed size (most foci measured ~0.33 μm^2; see Section S0.6, pg. 8 of Supplemental Data on accompanying CD for details of measurement procedure).

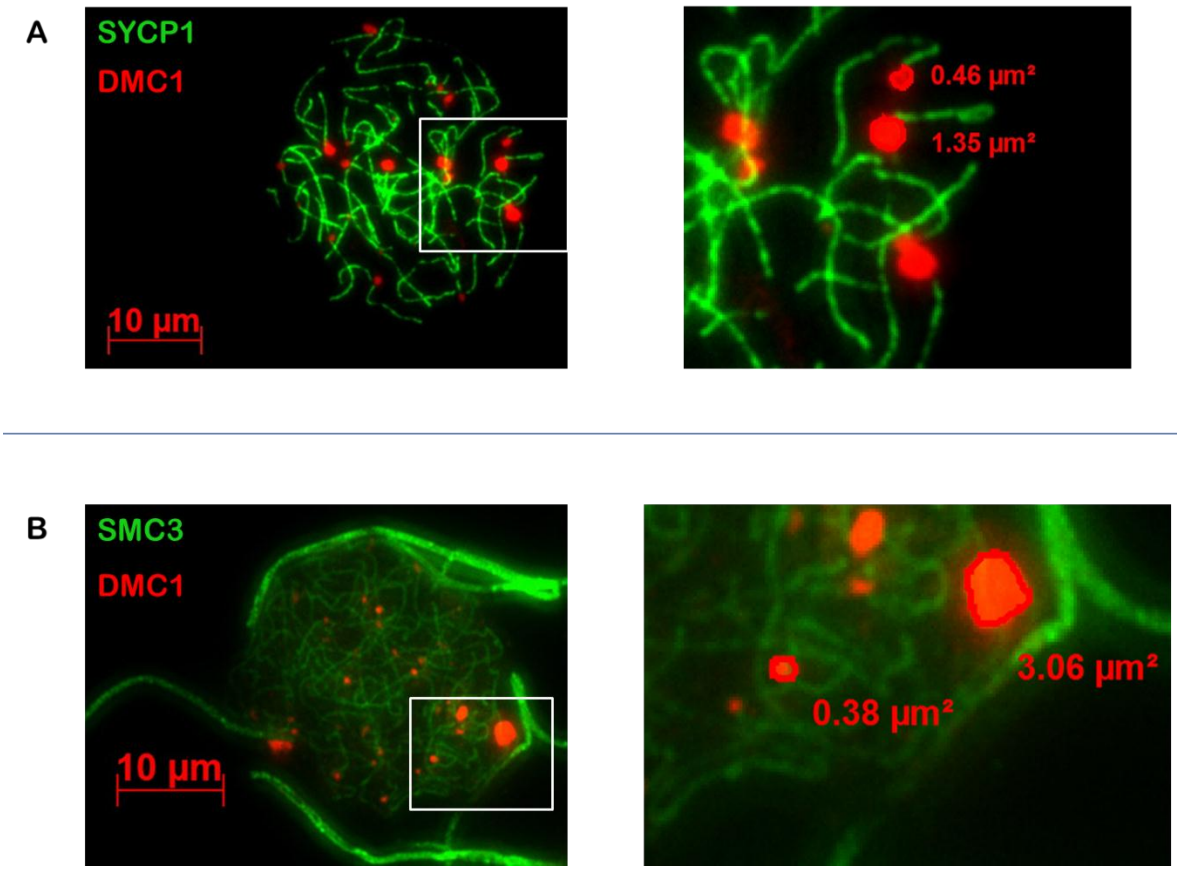

Figure 34: Dmc1 foci in platypus pachytene cells On the right are zoomed-in reproductions of the areas confined in the white boxes. In these zoomed regions, numbers adjacent to Dmc1 foci indicate the measured foci area. Typically Dmc1 foci averaged 0.33 µm^2; however there was occasional variation in this size, ranging as large as 3.06 µm^2

It was also observed that Dmc1 foci consistently associated with chromosome cores, but not always co-localised with the visible SC filaments (Fig. 35). Although in some cases the apparent absence of an SC may be the result of an out of focus SC (due to less efficient spreading typical for platypus meiotic material). Upon close examination it became clear that the majority of the Dmc1 foci seem to localise at the ends of Scp1 filaments (Fig. 35). While many foci did co-localise with Smc3 filaments and occasionally with Scp1, overall Dmc1 was observed at the ends of the SC. The SCs and the DAPI staining furthermore do not appear to indicate overly spread cells, therefore it was concluded that the Dmc1 foci are localised at the ends of synapsed chromosome regions. This pattern was consistently observed in testis samples from three platypus males captured in three different years, but for the purposes of this study only P07 and P09 platypus materials were used ("07" and "09" correspond to the years the specimens were captured). To that end, Dmc1 foci from 560 cells divided evenly between two platypus individuals were scored (full foci counts in Tables S3.1 and S3.2 on accompanying CD).

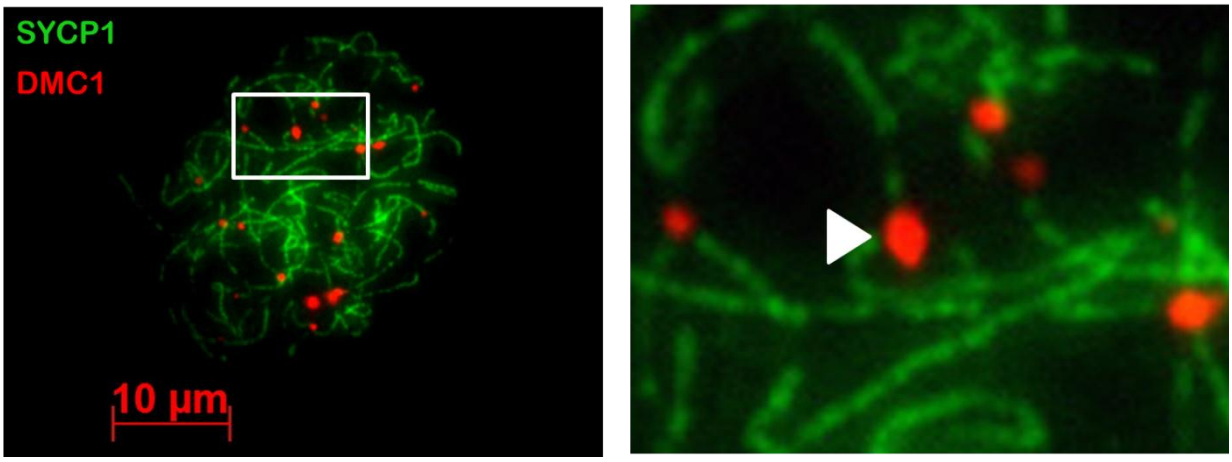

Figure 35: Dmc1 foci localise at the ends of Scp1 filaments On the right is a zoomed-in image of the area boxed in white. While many Dmc1 foci cross over the SC, many foci (e.g. indicated by the white arrow in the right panel) appear to localise at the end of the SC filaments.

Using Microsoft Excel, it was calculated that each nucleus had, on average approximately 24 Dmc1 foci (with an average standard deviation of 3.51) (Table 4). The platypus has a total of 52 chromosomes, including ten sex chromosomes—which translates to 21 autosome pairs and five sex chromosome pairs that pair via 9 PARs at meiosis. It is hypothesised, based on the obligate crossover paradigm, that each autosome pair and each PAR will have at least one crossover—as it has been observed in other animals that homologous chromosomes need to be joined by at least one crossover to ensure proper meiotic segregation, i.e. it is hypothesised that there will be a minimum of 30 crossovers in platypus male pachytene cells (that is, autosomal bivalents are expected to have a minimum of 21 foci—at least one foci per bivalent—and if each PAR has a crossover there would be a minimum of 30 foci; however, given there are some sex chromosomes that have minute or no predicted PAR, this number of expected foci could be less with a possibility of some achiasmate sex chromosomes). If the observed Dmc1 foci are related to crossovers, there are ~ 16% less foci observed than expected; however, several factors have to be considered that could affect these counts. Platypus pachytene cells are characterised as having a large nucleolar-like structure that is extremely robust. This structure tends to make it very difficult to flatten cells on a slide, and as such some Dmc1 foci may have been missed due to location in different focal planes. Overall, this is not likely—the vast majority of foci are within a single focal plane and have strong signal, but in some cells Dmc1 foci near nucleolar-like structures appears to be out of focus. Additionally, in many captured cells Dmc1 foci tended to accumulate around the nucleolar-like structure, making them more difficult to count. Last, due to the compact nature of the platypus pachytene cells, it is also possible some foci were so close together as to appear to be a single focus. Despite these caveats, intensity and number of Dmc1 foci is

surprising given that Dmc1 does not typically persist so late into pachytene in mouse (Oliver-Bonet et al., 2005). In addition, an average number of 24 foci makes it tempting to speculate that there is about 1 foci per bivalent and that these foci might be associated with crossover events.

Table 4: Average number Dmc1 foci in P07 and P09 platypus animals Averages presented here represent measurements collected over a total of 560 cells collected between two animals.

	Average number Dmc1 Foci
P07.1	24.37
P07.2	25.33
P07.3	23.90
P07.4	23.06
P07.5	22.80
Average	**23.89**
P09.4	25.06
P09.17	24.08
P09.18	23.14
P09.19	23.55
P09.20	22.18
P09.21	22.32
Average	**23.39**
Average of P09 and P07	**23.64**

Chapter 4: Analysis of Dmc1 localisation with pseudoautosomal regions (PARs) of the platypus sex chromosome chain

As previously stated, to date there have been no published analyses of meiotic recombination in platypus, and this is significant because the complex platypus sex chromosome chain poses numerous problems based on published ideas regarding crossover management. It has been hypothesised that the sex chromosome chain is held together with a series of terminal chiasmata, resulting in one chiasma per PAR. Platypus sex chromosomes and PARs vary greatly in size; for instance, PAR1 spans nearly an entire arm of X1/Y1 while PAR5 represents only a very small portion of X3/Y3. Some PARs (PAR9 and PAR7) located on the smaller members of the chain still have yet to be identified. Assuming crossover interference is present in platypus meiosis, extensive regulation and promotion of crossover in platypus PARs would be necessary for this model to be realised. Alternatively it is possible the platypus sex chromosomes could be held together via a dense plate-like structure as has been observed in marsupials (Solari & Bianchi, 1975) or that the monotreme chain uses a mixture of strategies.

Based on the assumption that Dmc1 has some role in the recombination pathway at meiotic prophase I, co-localisation of the Dmc1 foci observed with sex chromosomes should be investigated further along with the distribution of Dmc1 on autosomes versus sex chromosomes. To accomplish this task this study used bacterial artificial chromosome (BAC) probes and a chromosome paint as markers of different autosomes and sex chromosomes in a series of sequential fluorescent *in situ* hybridisation (FISH) experiments after Dmc1 immunostaining.

Five BAC clones and one chromosome paint were selected as probes for FISH (Fig. 36), five of which hybridise to specific positions in the sex chromosome chain. The paint probe

hybridises to chromosome 6 (Rens et al., 2004), which served as the autosomal control group that will be used as a point of reference for all other co-localisations of Dmc1 and FISH signals. The selection of sex chromosome specific BAC probes in this study aims to analyse a large number of features particular to the chain: PAR vs. unpaired sex chromosomal region vs. autosome; smaller PARs vs. larger PARs; and known PARs vs. Y chromosomes without confirmed PARs. Of the sex chromosome BAC clones, the X1-specific (CH236-804 001) and PAR1 (CH236-286 H10) probes, specifically, will be used to highlight differences between XY shared and X-specific regions. These two probes are immediately juxtaposed in the sex chromosome chain, and PAR1 furthermore covers much of one of the X1 and Y1 arms. Also selected was a BAC containing the platypus major histocompability complex (MHC) (Oa_Bb-462C1), which has been mapped to the pairing region between X3 and Y3 (PAR5). This region is significant not only because it is a PAR, but more importantly the MHC is one of the most significant recombination hotspots in mouse and human (Yauk, Bois, & Jeffreys, 2003; Kauppi, Sajantila, & Jeffreys, 2002). As a crossover hotspot in other species and a PAR region in platypus it was hypothesised this BAC would likely highlight a region containing a crossover event in platypus. The last two BAC probes, Y2 (145P9) and Y5 (Oa_Bb-152P15), are Y-specific. Due to the small size of these Y chromosomes and abundant repeats these BAC probes cover the entire Y chromosome. The Y2 probe acts as a reference for an internally-located PAR while the Y5 is representative of the end of the chain, the smallest Y chromosome, and a sex chromosome on which so far no PAR has been identified.

Figure 36: Map of BAC FISH probes in the platypus sex chromosome chain Localisation of BAC clones on platypus sex chromosome chain used in this study (modified from Veyrunes et al., 2008).

This study used a FISH protocol as published in Daish, Casey, and Grützner 2009, with slight modification (See section S0.5, pg. 7 of Supplemental Data on accompanying CD). For X1 and PAR1 probes it was possible to analyse a total of 74 cells each; however, for the other probes it was only possible to hybridise and analyse approximately 30 cells each due to an inability to sufficiently denature many of the cells (Fig. 37). Despite these limitations, this study was able to observe a clear trend in the data.

In order to co-localise DNA probes with Dmc1 foci, cells were immunostained with Dmc1. Cells were then photographed and recorded before conducting a series of FISH experiments. To accurately co-localise, overlaid cell images were made by matching up distinct features of DAPI staining. This virtual representation of FISH results juxtaposed with immunofluorescence images allowed a counting of how many cells showed co-localisation of Dmc1 foci with FISH signals.

Table 5: Frequency in % co-localisation of Dmc1 with FISH probes

	% Co-localisation with DMC1					
Slide	**Y2**	**Y5**	**PAR1**	**X1**	**MHC**	**6**
P07.2	N/A	N/A	76.19%	23.81%	N/A	N/A
P09.4	77.42%	80.65%	68.75%	21.88%	79.31%	90.32%
Average	**77.42%**	**80.65%**	**72.47%**	**22.84%**	**79.31%**	**90.32%**
n =	31	31	74	74	29	31

Using this methodology it was possible to calculate the frequency of co-localisation between Dmc1 and FISH signals (Table 5). This shows that Dmc1 foci co-localises with the chromosome 6 paint approximately 90% of the time. This result supports the possibility that Dmc1 might associate with crossovers and that the platypus meiotic recombination system operates under the obligate crossover paradigm. It is likely that the autosomal co-localisation percentage is so high because this study used a paint probe that hybridised along the entire length of the chromosome, making any correspondence with Dmc1 easier to identify. In contrast the PAR1 probe only hybridises with a small section of the PAR. Therefore small co-localisation frequencies were expected. Surprisingly, the PARs co-localised with Dmc1 foci approximately 72-80% of the time. Of particular note, Y5 had a co-localisation percentage of 80.65% while the MHC on PAR5 was 79.31% (contrasted with the 72.42% for PAR1). The relatively higher frequency of correspondence in Y5 is likely due to the size of the chromosome; because Y5 is so small it is more likely that a Dmc1 focus will directly co-

localise or be immediately adjacent to the FISH probe. Likewise, Y2 has a 77.42% co-localisation with Dmc1 foci; this higher level of correspondence is, like Y5, likely due to the size of the chromosome.

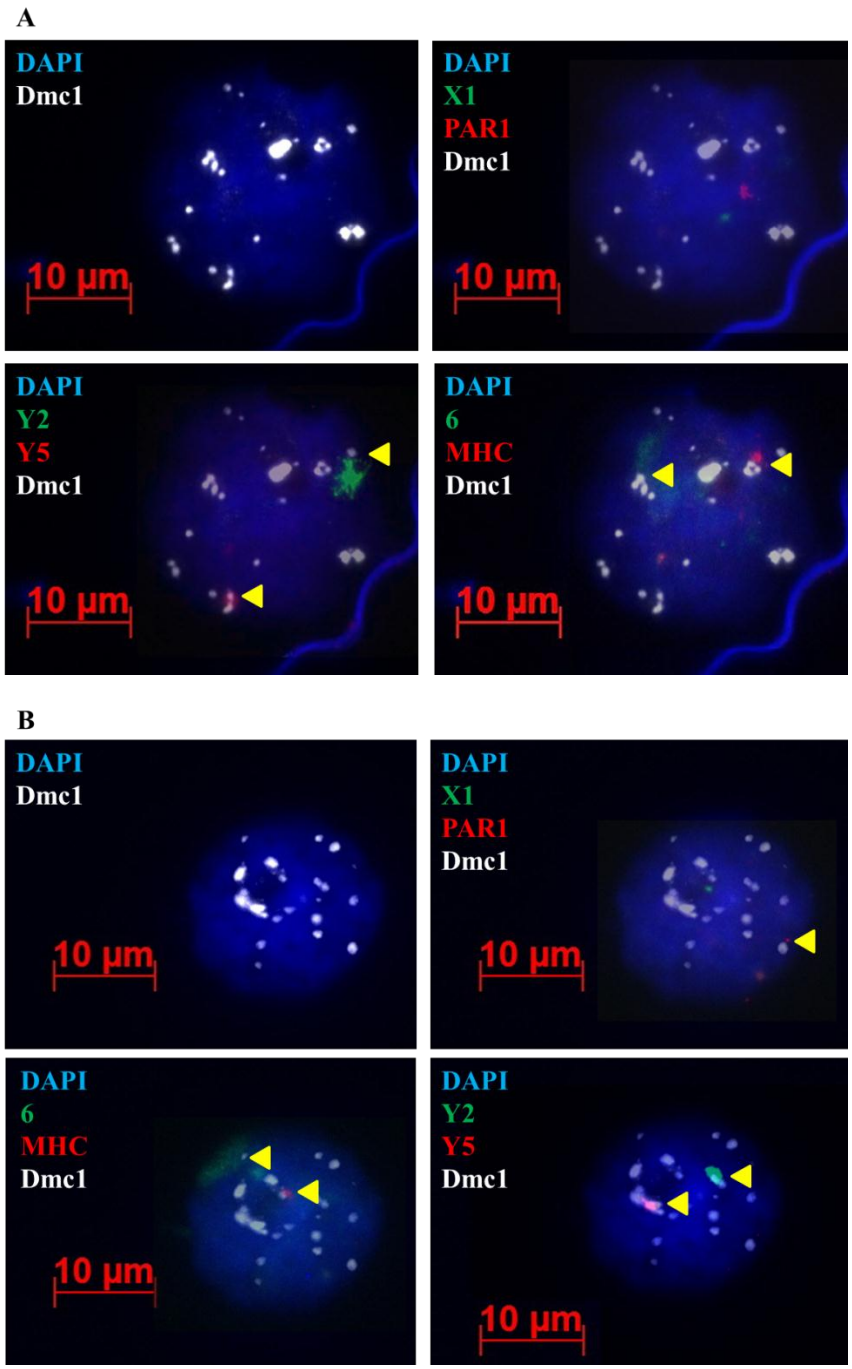

Figure 37: Co-localisation of Dmc1 with specific DNA clones representing sex chromosomes and autosomes in male platypus pachytene cells In figure (A) is an example FISH experiment using animal P09 while figure (B) uses animal P07. The upper left of each shows the immunofluorescence experiment consisting of staining for DAPI (blue), and Dmc1 (white). The upper right of each is the first FISH experiment using BAC probes for X1-specific (green) and PAR1 (red). The lower left of each is the second FISH experiment, using BACs for Y2 (green) and Y5 (red). Last, in the lower right of each is the final FISH, using a chromosome 6 painting probe (green) and a BAC of the MHC domain on PAR5 (red). All FISH experiments were done on the same cell (the same cell in the upper left), and all experiments were performed in sequence. Yellow arrows indicate co-localisation of FISH signals with Dmc1 foci.

In the case of the MHC probe it is likely that the increased percentage of co-localisation is due to MHC being a crossover hotspot. In direct contrast with the high correlations between Dmc1 foci and PAR FISH signals, the X1-specific probe showed a much lower percentage of co-localisation (22.84%). To some extend this low co-localisation frequency could be due to the small region represented by the BAC. This also indicates that the X1-specific region shows a significantly lower number of Dmc1 foci compared to other BAC clones, in particular X1pY1. It must also be noted that the higher than expected frequency of Dmc1 co-localisation with the X1-specific region may be due to the BAC on X1 being on proximal X1q close to the PAR.

To correct for size variations among the FISH signals, measurements of signal surface area were recorded (Table 6; a complete account of measurements can be found in Table S3.3 on pg. 37 on accompanying CD). It was observed that the chromosome 6 FISH signal, as expected, had the largest surface area, ~17 μm^2, while the MHC domain had the smallest, ~0.6 μm^2. Dividing the average number of Dmc1 foci per FISH probe by the size of the FISH signal, it was possible to normalise the data to average Dmc1 foci per μm^2.

Table 6: Average number of Dmc1 foci per area of FISH signal

	X1	**PAR1**	**Y2**	**Y5**	**MHC**	**6**
average number Dmc1 foci	0.23	0.72	0.77	0.81	0.79	0.90
Average surface area (μm^2)	0.73	0.75	3.77	1.31	0.59	16.67
average number Dmc1 foci per μm^2	**0.31**	**0.96**	**0.21**	**0.62**	**1.33**	**0.05**

This revealed several interesting results. It confirms a much lower correlation of the X-specific region with Dmc1 foci on sex chromosomes, and Y2 showed a lower Dmc1 co-localisation frequency. It was found that, per μm^2, the MHC domain had by far the highest number of Dmc1 foci (1.33), followed closely by PAR1 (0.96) and Y5 (0.62). Overall, Dmc1 foci were more commonly associated (per FISH signal surface area) with members of the sex chromosome chain than with chromosome 6. Using the same surface area values, it was also possible to calculate an expected value of co-localisation of Dmc1 foci with specific FISH

signals. In order to calculate the probability of any co-localisation—even partial co-localisation—the following equation was used (personal communication with Dr. Sheila Horan, March 2011; derived using principles discussed in Ch. 1, specifically Theorem 1.7, of *Probability and Stochastic Processes, Second Edition*, Yates & Goodman, 2005, p. 15):

$$P_{(\text{co-localisation})} = 1 - \prod_{n=0}^{23}\left(1 - \frac{FISH\ surface\ area}{500.22 - 0.33n}\right)$$

In this equation, the value 500.22 represents the average surface area of the DAPI-stained region of a platypus pachytene cell (in μm^2) and 0.33 represent the average surface area of a Dmc1 focus (in μm^2). The ratio of FISH surface area to the DAPI area (minus the collective surface area of all Dmc1 foci) represents the assumption that no FISH signal randomly overlaps with a Dmc1 signal. This equation, then, represents the product of a series of probabilities of zero co-localisations of 1 to 24 Dmc1 foci with a given FISH surface area. Specifically, to calculate the probability of one event (i.e. the co-localisation of any Dmc1 focus with a given FISH signal), the collective probability for zero co-localisation was calculated and subsequently subtracted from one. Using this equation and surface area data collected from 35 cells (Table S3.3), probabilities for random co-localisation of Dmc1 with each FISH signal were calculated (Fig. 38, Table 7). With the exception of Y2 and chromosome 6, all the probabilities fell under a 10% chance, with the MHC representing the smallest probability, a 2.8% chance of co-localisation. This is particularly striking as the MHC domain had the second highest frequency of observed co-localisation and the highest number of Dmc1 foci per μm^2 FISH signal. For all except chromosome 6, the observed frequency of co-localisation was several times larger than the expected probability—and for PAR1, Y5, and the MHC domain, there was over an order of magnitude difference (Table 7). Even for chromosome 6, where the probability of random co-localisation was ~56%, there was a dramatically higher observed co-localisation (~90%, 1.5 times more than expected). A chi-square statistical analysis (assuming one degree of freedom and a P value of 0.05) found the differences between the observed and expected co-localisations were significant for PAR1, Y5, and the MHC domain (Table 7). For those three regions, the hypothesis of random distribution of Dmc1 foci must be rejected. On the other hand, the X1-specific region, Y2, and chromosome 6 regions do not show a statistically significant frequency of co-localisation with Dmc1 foci. This is the expected result for the X1-specific region, though it is not the expected result for chromosome 6 or Y2. These data, therefore, reinforce that the arrangement of the observed Dmc1 foci is specific and much more abundant on sex chromosomes.

Table 7: Probability of co-localisation of Dmc1 foci with FISH signals

	X1	PAR1	Y2	Y5	MHC	Chromosome 6
Frequency co-localisation of Dmc1 foci with FISH signal	0.23	0.72	0.77	0.81	0.79	0.90
Probability of chance co-localisation of Dmc1 foci with FISH signal	0.03	0.04	0.17	0.06	0.03	0.56
Fold change	6.6	20.4	4.6	13.1	28.2	1.6
X^2 value (P = 0.05)	1.08	**13.34**	2.20	**9.04**	**20.83**	0.21

As the exact relationship between Dmc1 and COs or DSBs is currently unknown in platypus, it remains speculation if DSBs repair and crossover formation is preferentially localised to the PARs. That said, this study does support the hypothesis that Dmc1 is present at the chromosome cores of platypus PARs, and therefore supports the hypothesis that Single End Invasion and the formation of Holliday junctions does occur at the PARs of platypus with higher frequency compared to autosomes. Moreover, the higher number of Dmc1 foci per surface area of FISH signal in the sex chromosome chain also supports the hypothesis proposed in Chapter 3 that these foci could represent Rad51 accumulation holding paired chromosomes (in this case, members of the chain) together via telomeric association.

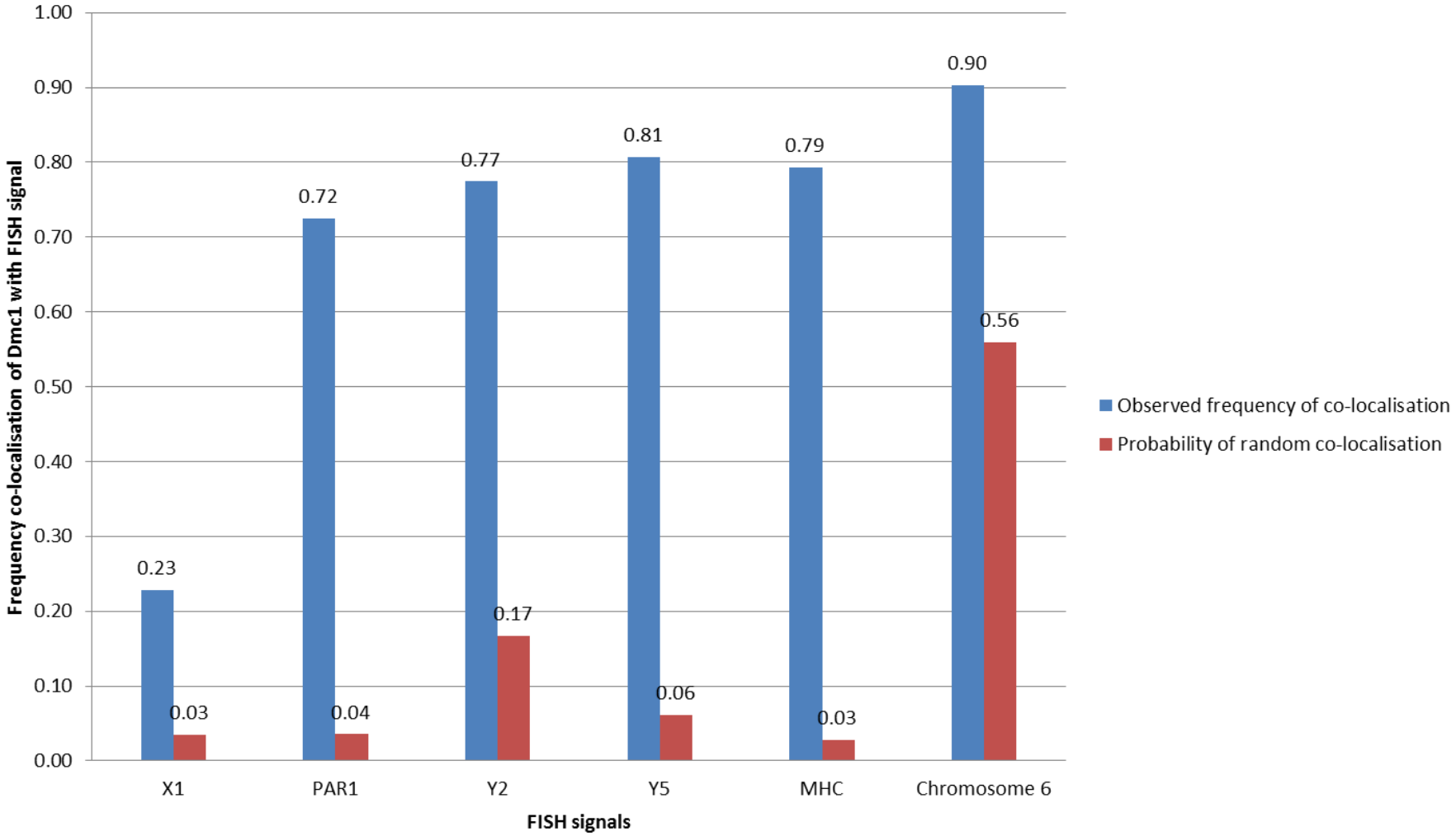

Figure 38: Observed co-localisation of Dmc1 with FISH signals versus the probability of random co-localisation The blue bars represent the observed co-localisation of Dmc1 with various BAC clone FISH signals while red bars represent the average probability of Dmc1 randomly co-localising with the same FISH signals. This study showed a general trend of co-localisation of Dmc1 at significantly higher frequencies than expected by chance.

Conclusions and future directions

Characterisation of meiotic recombination machinery in platypus

A first analysis of fifteen genes representing all major steps of the meiotic recombination pathway revealed generally high levels of conservation in terms of sequence, domain prediction, and expression in testis. Exceptions to the expected high conservation were observed in *Mei4*, *Rec114*, *Blm*, *Rad51*, *Msh4*, and *Prdm9*. Blm, Rad51, and Msh4 proteins are predicted to be missing single functional domains each, but this is likely due to inaccuracies or gaps in the genome assembly or sequence divergence in particular where these domains are essential to protein function. For Rad51 the missing monomer-monomer interface domain would inhibit the formation of the Rad51 filament and thus inhibit single-end invasion and the formation of Holliday junctions. Similarly, the Blm protein, as it is characterised in this study, is predicted to be missing the BDHCT domain, which is critical to Blm's helicase function. In the case of Msh4, it is predicted that the connector domain is missing, meaning it would be unable to effectively resolve Holliday junctions. Future work utilising cDNA amplification (RACE PCR) could be used to obtain additional sequence which might reveal the presence or absence of these domains in platypus. In terms of gene expression, it is likely that all the characterised genes—with possible exceptions of *Mei4* and *Rec114*—have conserved functions in platypus meiosis.

The changes found in the platypus *Prdm9* gene, important for recombination hotspot determination, raise some interesting questions. While the eutherian Prdm9 protein is characterised by four key protein domains (the SET domain, the Krueppel Box, the SSRX domain, and the zinc finger array), the platypus Prdm9 is more eutherian-like, missing the Krueppel Box, while the opossum Prdm9 features only the SSRX and SET domains. The absence of the zinc finger array in opossum certainly suggests a different function than is observed in eutherians; however, it is unclear whether or not the absence of a Krueppel Box in platypus will result in an alternate function of the platypus protein. According to InterPro, the Krueppel Box is associated with transcription repression, and whether or not it is significant in eutherian Prdm9 function to regulate crossover hotspots is unclear. In contrast to all other mammals (where sequence information is available) platypus has undergone

duplication of the *Prdm9* gene. Whether that is related to its physical localisation on an X chromosome which might lead to a dosage reduction in males is unclear. The domain profile of the platypus Prdm9 protein closely resembles that of zebrafish, and the conservation on the SET domain suggests that the platypus protein is likely to have a similar histone methyltransferase activity. Furthermore, the relative conservation of a zinc finger array in platypus suggests the DNA-binding capability of Prdm9; however, the platypus array is considerably shorter than those of mouse and human. It is unclear what effect this may have on platypus Prdm9 function. Functional studies are limited in this species, but it may be possible to do *in vitro* imaging of Prdm9 association with chromatin and attempt to measure correlation with hotspots as has been done in mouse.

While this study also found significant differences between platypus and other mammalian Mei4 and Rec114 protein motifs, it remains difficult to determine what effects these changes have in platypus. The motifs previously described as critical to the protein function in mouse appear to be conserved in platypus, but there is limited knowledge about the mechanism by which these proteins work to assist in the formation of DSBs. Based on studies in mouse and the bioinformatics characterisation, this study concludes that it is possible the platypus Mei4 and Rec114 proteins could have conserved function in platypus; however, this finding is undermined by the possible lack of expression data in platypus testis which needs to be investigated further.

In future studies it would be worthwhile to extend the approach used here and to include *Eme1* and *Mus81*, as these genes have been implicated in an alternative recombination pathway that is not subject to crossover interference. Additionally, other members of the MRX-sub-complex and Spo11-sub-complex (e.g. *Mre11*) would be necessary in order to further characterise the DSB formation mechanisms of platypus.

Cytological approaches to study recombination in platypus meiosis

Cytological approaches to establish physical recombination maps in monotremes are limited by the divergence of this species. This study has established improved protocols to spread meiotic cells and preliminary evidence suggests that Mlh1 antibodies do cross hybridise in monotremes. Future work with a range of different antibodies preferably raised against a monotreme peptide in combination with SC antibodies will allow visualisation of recombination nodules in platypus. Analysis of Dmc1 in platypus prophase cells yielded consistent and unexpected staining patterns. While it is highly unusual to see Dmc1 after

zygotene, the consistency and clarity observed in platypus along with the co-localisation of foci to chromosome cores suggest that the foci represent Dmc1 distributions. It may be possible that Dmc1 is localising at the telomeres or centromeres, and may have a novel function in those regions in platypus. Alternatively, it is possible that the observed foci represent a delayed platypus DSB repair mechanism; however, the results of this study suggest this is unlikely as evidence of Mlh1 foci have been observed in the same prophase stages as the Dmc1 foci. The presence of Mlh1 shows that DSBs have been repaired or matured into crossovers, therefore it is not expected that DSB repair machinery, like Dmc1, would simultaneously be expressed.

It is possible that Dmc1, having been associated with Single End Invasion and the initiation of Holliday junctions, has acquired other functions in the platypus extending its presence at prophase I. In light of the Western blot results, it is possible the Dmc1 antibody is detecting Rad51. In a 1995 study, Ashley et al. reported several observations regarding Rad51 expression in mouse spermatogenesis that closely resemble the data reported here. In early mouse male pachytene Rad51 is localised largely on the unpaired (unsynapsed) region of the X chromosome and, as pachytene progresses, Rad51 number drop dramatically and most foci are localised to the two ends of the bivalents (Ashley et al., 1995). If the Dmc1 antibody in this study is detecting Rad51, then the observed foci pattern match the observations of Ashley et al. (1995); the observed foci occur largely at what appear to be the ends of SCs. Ashley et al. further documented that after diakenesis, Rad51 in mouse spermatocytes co-localised with kinetochores (Ashley et al., 1995); it is possible that Rad51 then has in mouse—as well as platypus—a structural role in holding homologous chromosomes together or stabilising telomeres through metaphase I.

In platypus, Dmc1 protein expression was observed in testis; however there is a significant contradiction in the data as cDNA expression analysis showed Dmc1 has a meiosis-specific expression while the protein was detected not only in testes, but in kidney and liver as well. It is suspected that the antibody may be detecting Rad51 (in addition to Dmc1) in the Western blot analysis. Though the antibody suppliers assert that these antibodies do not cross-react with Rad51, there is approximately a 50% identity between the two proteins, and the antibody suppliers did not reveal the epitope sequence. Cross-reaction with Rad51 would explain the Western blot results as well as the similarity of the phenotype observed in platypus with earlier work published by Ashley et al. 1995. One way of testing for cross-reaction is to perform an immunoprecipitation reaction using tagged Dmc1 proteins; alternatively meiotic expression could be investigated by generation of an antibody specific for platypus Dmc1.

However, these additional experiments, while necessary to further study of platypus Dmc1 activity, could not be conducted at this time due to time constraints and the challenges of optimising experimental protocols for use in platypus. It should be noted that Western blot validation is not always consistent with the specificity or the successful application of an antibody on a fixed specimen. This is due in large part to the fact that Western blot analysis tests an antibody's specificity to a denatured epitope which may not be the same epitope structure post-4% PFA fixation. In light of these concerns and keeping in mind that the antibody company guaranteed the specificity of the Dmc1 antibody, this study (hesitantly) suggests that the antibody used in this study detected Dmc1 in immunofluorescence analysis.

The observations of cells immunostained against Dmc1 raise the possibility that the Dmc1 protein has been adapted for some additional or prolonged function in the repair of DSBs. The number of observed Dmc1 foci nearly matches the hypothesised minimum number of crossovers in platypus meiosis and, as discussed in Chapter 3, it is possible that more Dmc1 foci are obscured by the three-dimensional layout of the cells; however, it is equally likely that by early to mid-pachytene Dmc1 protein is dissociating from chromosome cores, and this could account for a decreased number of foci relative to expected crossover sites.

In future meiotic studies it would be ideal to gain a broader view of the recombination machinery across platypus prophase. Unfortunately, however, antibodies suitable for use in platypus are limited as most commercially available antibodies are specific for human and mouse. With this in mind it would be a worthwhile investment to design antibodies specific for platypus proteins. Immunofluorescence studies of these proteins would greatly complement these Dmc1 findings and further help unravel the complexities particular of the sex chromosomes during platypus meiosis. Additional studies will likewise need to be undertaken in echidna in order to determine if the two monotremes have developed similar or different strategies of meiotic recombination.

While the presence of Dmc1 in pachytene was unexpected, the observations of the localisation of Dmc1 foci on the sex chromosome chain were supportive of the hypothesis that the platypus meiotic multiple is held together via terminal chiasmata. The FISH experiments indicated a co-localisation of Dmc1 foci with the PARs of various members of the sex chromosome chain at frequencies similar to that of an autosome (chromosome 6). While the issue has been raised that different cell spreading techniques could influence the size of the FISH surface area measurements and, thereby, influence the calculated probabilities of Dmc1 co-localisation. While it is true that the 2-dimensional surface area of spread cells varies dependent on spreading techniques, it also follows that the 2-dimensional

surface areas of the FISH signals would likewise be dependent on spreading technique. Given that the two are directly proportional, it is unlikely that the cell spreading techniques utilised in this study had any undue influence on the rate of co-localisation. This study further concludes that the estimates of co-localisation frequencies are likely underestimates of actual frequencies as the estimates are largely reliant on the proximity of Dmc1 foci to FISH signals. It should be noted that Dmc1 foci along unpaired X- or Y-specific regions is not uncommon in other species, and the DSBs that occur in unpaired chromosomal regions typically undergo intersister repair. Significant to this study, however, is that Dmc1 appears to preferentially co-localise with the PARs, indicating not only that the PARs preferentially undergo interhomologue DSB repair (and, as a result, are more likely to form chiasmata), but also that DSBs, themselves, appear to form preferentially in the PARs as opposed to the X-specific regions. This, therefore, marks the first time that evidence of DSB repair and possible meiotic recombination has been observed in the platypus sex chromosome chain.

This study cannot confirm the presence of terminal chiasmata holding the sex chromosome chain together, which needs to be demonstrated by co-localisation of Mlh1 foci with the PARs. Given the current limitations with available Mlh1 antibodies, this is not yet possible as the commercially available antibodies tested produce too much background staining to allow for adequate scoring of platypus prophase cells. For this reason future studies in monotreme meiotic recombination will require better Mlh1 antibodies, possibly even antibodies designed to be specific for the platypus Mlh1 protein. Yet, there are other ways of visualising chiasmata in the sex chromosome chain; it may well be favourable to examine the sex chromosome chain using the “old fashion” methods of electron microscopy and silver staining.

This study does, however, raise the possibility of an alternative role for Dmc1 in platypus meiosis. The data shows that Dmc1 significantly and non-randomly associate with platypus sex chromosomes in pachytene. The exact implications of this finding are still unknown, though it is possible Dmc1 is involved either in crossovers or a stabilisation of centromeres and telomeres, thus playing a structural role in holding homologous chromosomes together through prophase I.

Conclusion

Overall this study has taken the first steps to study meiotic recombination in monotremes. This analysis has investigated the sequence conservation and expression of a broad range of recombination proteins. Newly identified sequence together with data from the platypus genome project demonstrated an overall conservation but also unravelled some potentially interesting changes in genes involved in meiotic recombination. Towards establishing physical recombination maps, major experimental approaches have been established and produced the first images of recombination machinery in platypus prophase cells. The data have also uncovered unexpected results that raise interesting questions about platypus meiosis, namely the potential persistence of Dmc1 into pachytene. Together these findings provide experimental and scientific directions for subsequent investigations of platypus meiosis.

Works cited

Aboussekhra, A., Chanet, R., Adjiri, A., & Fabre, F. (1992). Semi-dominant suppressors of Srs2 helicase mutations of *Saccharomyces cerevisiae* map in the *RAD51* gene, whose sequence predicts a protein with similarities to prokaryotic RecA proteins. *Mol. Cell Biol., 12*, 3224-3234.

Adams, M.D., McVey, M., & Sekelsky, J.J. (2003). *Drosophila* BLM in double-strand break repair by synthesis-dependent strand annealing. *Science, 299*, 265-267.

Agarwal, S. & Roeder, G.S. (2000). Zip3 provided a link between recombination enzymes and synaptonemal complex proteins. *Cell, 102*, 245-255.

Alani, E., Padmore, R., & Kleckner, N. (1990). Analysis of wild-type and *rad50* mutants of yeast suggests an intimate relationship between meiotic chromosome synapsis and recombination. *Cell, 61*, 419-436.

Allers, T. & Lichten, M. (2001). Differential timing and control of noncrossover and crossover recombination during meiosis. *Cell, 106*, 47-57.

Anderson, D.E., Trujillo, K.E., Sung, P., & Erickson, H.P. (2001). Structure of the Rad50 × Mre11 DNA repair complex from *Saccharomyces cerevisiae* by electron microscopy. *J Biol Chem., 276*, 37027–37033.

Anderson, L.K., Reeves, A., Webb, L.M., & Ashley, T. (1999). Distribution of crossing over on mouse synaptonemal complexes using immunofluorescent localization of MLH1 protein. *Genetics, 151*, 1569-1579

Aran, B., Blanco, J., Vendrell, J.M., Egozcue, S., Barri, P.N., Egozcue, J., & Veiga, A. (1999). Screening for abnormalities of chromosomes X, Y, and 18 and for diploidy in spermatozoa from infertile men participating in an *in vitro* fertilization-intracytoplasmic sperm injection program. *Fertil. Steril., 72*, 696-701.

Aravind L. & Koonin E.V. (1998). The HORMA domain: a common structural denominator in mitotic checkpoints, chromosome synapsis and DNA repair. *Trends Biochem Sci., 23*, 284–286.

Argueso, J.L., Wanat, J., Gemici, Z., & Alani, E. (2004). Competing crossover pathways act during meiosis in *Saccharomyces cerevisiae. Genetics, 168*, 1805-1816.

Arora, C., Kee, K., Maleki, S. & Keeney, S. (2004). Antiviral protein Ski8 is a direct partner of Spo11 in meiotic DNA break formation, independent of its cytoplasmic role in RNA metabolism. *Mol. Cell, 13*, 549–559.

Ashley, T. & Moses, M.J. (1980). End association and segregation of the achiasmatic X and Y chromosomes of the sand rat, *Psammomys obesus. Chromosoma, 78*, 203-210.

Ashley, T., Plug, A.W., Xu, J., Solari, A.J., Reddy, G., Golub, E.I. & Ward, D.C. (1995). Dynamic changes in Rad51 distribution on chromatin during meiosis in male and female vertebrates. *Chromosoma, 104*, 19–28.

Bachrati, C.Z., Borts, R.H., & Hickson, I.D. (2006). Mobile D-loops are a preferred substrate for the Bloom's syndrome helicase. *Nucleic Acids Res., 34*, 2269-2279.

Bailis J.M., Smith A.V., & Roeder G.S. (2000). Bypass of a meiotic checkpoint by overproduction of meiotic chromosomal proteins. *Mol Cell Biol., 20*, 4838–4848.

Baker, S.M., Plug, A.W., Prolla, T.A., *et al.* (1996). Involvement of mouse Mlh1 in DNA mismatch repair and meiotic crossing over. *Nat. Genet., 13*, 336-342.

Barchi, M., Roig, I., Giacomo, M.D., de Rooij, D.G., Keeney, S., & Jasin, M. (2008). ATM promotes the obligate XY crossover and both crossover control and chromosome axis integrity on autosomes. *PLOS Genet., 4*, e1000076.

Baudet, F. & Nicolas, A. (1997). Clustering of meiotic double-strand breaks on yeast chromosomes III. *Proc. Natl. Acad. Sci. U. S. A.* **94**, 5213-5218.

Baudet, F., Buard, J., Fledel-Alon, A., Ober, C., Przeworski, M., Coop, G., & de Massy, B. (2010). PRDM9 Is a Major Determinant of Meiotic Recombination Hotspots in Humans and Mice. *Science, 327*, 836-840.

Beamish, H., Kedar, P., Kaneko, H., *et al.* (2002). Functional link between BLM defective in Bloom's syndrome and the ataxia-telangiectasia-mutated protein, ATM. *J. Biol. Chem., 277*, 30515-30523.

Bellani, M.A., Romanienko, P.J., Cairatti, D.A., & Camerini-Otero, R.D. (2005). SPO11 is required for sex-body formation, and Spo11 heterozygosity rescues the prophase arrest of *ATM*$^{-/-}$ spermatocytes. *J. Cell Sci., 118*, 3233-3245.

Bergerat A., de Massy, B., Gadelle, D., Varoutas, P., Nicolas, A., & Forterre, P. (1997). An atypical topoisomerase II from Archaea with implications for meiotic recombination. *Nature, 386*, 414-417.

Bhagat, R., Manheim, E.A., Sherizen, D.E., & McKim, K.S. (2004). Studies on crossover-specific mutants and the distribution of crossing over in *Drosophila* females. *Cytogenet. Genome Res., 107*, 160-171.

Bishop, D.K. (1994). RecA homologues Dmc1 and Rad51 interact to form multiple nuclear complexes prior to meiotic chromosome synapsis. *Cell, 79*, 1081-1092.

Bishop, D.K., Nikolski, Y., Oshiro, J., Chon, J., Shinohara, M., & Chen, X. (1999). High copy number suppression of the meiotic arrest caused by a *dmc1* mutation: REC114 imposes an early recombination block and RAD54 promotes a DMC1-independent DSB repair pathway. *Genes Cells, 4*, 425-444.

Bishop, D.K., Park, D., Xu, L., & Kleckner, N. (1992). *DMC1:* a meiosis-specific yeast homologue of *E. coli recA* required for recombination, synaptonemal complex formation, and cell cycle progression. *Cell, 69*, 439-456.

Blat, Y., Protacio, R.U., Hunter, N., & Kleckner, N. (2002). Physical and functional interactions among basic chromosome organizational features govern early steps of meiotic chiasma formation. *Cell, 111*, 791–802.

Boddy, M.N., Gaillard, P.L., McDonald, W.H., Shanahan, P., Yates, J.R., & Russell, P. (2001). Mus81-Eme1 are essential components of a Holliday junction resolvase. *Cell, 107*, 537-548.

Borde, V. (2007). The multiple roles of the Mre11 complex for meiotic recombination. *Chromosome Res., 15*, 551–563.

Borde, V., Lin, W., Novikov, E., Petrini, J.H., Lichten, M., & Nicolas, A. (2004). Association of Mre11p with double-strand break sites during yeast meiosis. *Mol. Cell, 13*, 389-401.

Borde, V., Robine, N., Lin, W., Bonfils, S., Géli, V., & Nicolas, A. (2009). Histone H3 lysine 4 trimethylation marks meiotic recombination initiation sites. *EMBO J., 28*(2), 81-3.

Börner, G.V., Kleckner, N., & Hunter, N. (2004). Crossover/noncrossover differentiation, synaptonemal complex formation, and regulatory surveillance at the leptotene/zygotene transition of meiosis. *Cell, 117*, 29-45.

Brendel, V., Brocchieri, L., Sandler, S.J., Clark, A.J., & Karlin, S. (1997). Evolutionary comparisons of RecA-like proteins across all major kingdoms of living organisms. *J. Mol. Evol., 44*, 528-541.

Broman, K.W., Murray, J.C., Sheffield, V.C., White, R.L., & Weber, J.L. (1998). Comprehensive human genetic maps: individual and sex-specific variation in recombination. *Am. J. Hum. Genet., 63*, 861-869.

Brush, G.S. & Kelly, T.J. (2000). Phosphorylation of the replication protein A large subunit in the *Saccharomyces cerevisiae* checkpoint response. *Nucleic Acids Res., 28*, 3725–3732.

Brush, G.S., Anderson, C.W., & Kelly, T.J. (1994). The DNA-activated protein kinase is required for the phosphorylation of replication protein A during simian virus 40 DNA replication. *Proc Natl Acad Sci USA., 91*, 12520–12524.

Brush, G.S., Clifford, D.M., Marinco, S.M., & Bartrand, A.J. (2001). Replication protein A is sequentially phosphorylated during meiosis. *Nucleic Acids Res., 29*, 4808–4817.

Buard, J., Barthès, P., Grey, C., & de Massy, B. (2009). Distinct histone modifications define initiation and repair of meiotic recombination in the mouse. *EMBO J., 28*, 2616 – 2624.

Bugreev, D.V. & Mazin, A.V. (2004). Ca^{2+} activates human homologous recombination protein Rad51 by modulating its ATPase activity. *Proc. Natl. Acad. Sci., 101*, 9988-9993.

Bugreev, D.V., Golub, E.I., Stasiak, A.Z., Stasiak, A., & Mazin, A.V. (2005). Activation of human meiosis-specific recombinase Dmc1 by Ca2+. *J. Biol. Chem.., 280*, 26886–26895.

Bugreev, D.V., Hanaoka, F., & Mazin, A.V. (2007). Rad54 dissociates homologous recombination intermediates by branch migration. *Nat. Struct. Mol. Biol., 14*, 746-753.

Bugreev, D.V., Mazina, O.M., & Mazin, A.V. (2006). Analysis of branch migration activities of proteins using synthetic DNA substrates. *Nat. Protoc.* doi: 2010.1038/nprot.2006.2217

Burgoyne, P.S. (1982). Genetic homology and crossing over in the X and Y chromosomes of mammals. *Hum Genet., 61*, 85-90.

Calogero, A.E., Burrello, N., De Palma, A., Barone, N., D'Agata, R., & Vicari, E. (2003). Sperm aneuploidy in infertile men. *Reprod. BioMed. Online, 6*, 310-317.

Carballo, J.A., Johnson, A.L., Sedgwick, S.G., & Cha, R.S. (2008). Phosphorylation of the axial element protein Hop1 by Mec1/Tel1 ensures meiotic interhomologue recombination. *Cell, 132*, 758–770.

Carvalho, A.B. (2003). The advantages of recombination. *Nat. Genet., 34*, 128-129.

Caryl, A.P., Armstrong, S.J., Jones, G.H., & Franklin, F.C. (2000). A homologue of the yeast *HOP1* gene is inactivated in the Arabidopsis meiotic mutant *asy1*. *Chromosoma, 109*, 62–71.

Catlett, M.G. & Forsburg, S.L. (2003). *Schizosaccharomyces pombe Rdh54 (TIDI)* acts with *Rhp54 (RED54)* to repair meiotic double-strand breaks. *Mol. Biol. Cell, 14*, 4707-4720.

Cervantes, M.D., Farah, J.A., & Smith, G.R. (2000). Meiotic DNA breaks associated with recombination in *S. Pombe. Mol Cell, 5*, 883-888.

Charlesworth, B. & Charlesworth, D. (1978). The degradation of Y chromosomes. *Phil.Trans. R. Soc. Lond.* B., *355*, 1563-1572

Chen, X.B., Melchionna, R., Denis, C.M., *et al.* (2001). Human Mus81-assocaited endonuclease cleaves Holliday junctions *in vitro. Mol. Cell, 8*, 1117-1127.

Cheng, Z., Liu, Y., Wang, C., Parker, R., & Song, H. (2004). Crystal structure of Ski8p, a WD-repeat protein with dual roles in mRNA metabolism and meiotic recombination. *Protein Sci., 13*, 2673–2684.

Chowdhurry, R., Bois, P.R., Feingold, E., Sherman, S.L., & Cheung, V.G. (2009). Genetic analysis of variation in human meiotic recombination. *PLoS Genetics, 5*(9), e1000648.

Chua, P.R. & Roeder, G.S. (1998). Zip2, a meiosis-specific protein required for the initiation of chromosome synapsis. *Cell, 93*, 349-359.

Clifford, D.M., Marinco, S.M., & Brush, G.S. (2004). The meiosis-specific protein kinase Ime2 directs phosphorylation of replication protein A. *J Biol Chem., 279*, 6163–6170

Cobb, J. & Handel, M.A. (1998). Dynamics of meiotic prophase I during spermatogenesis, from pairing to division. *Semin Cell Dev Biol., 9*, 445-450.

Cohen, P.E. & Pollard, J.W. (2001). Regulation of meiotic recombination and prophase I progression in mammals. *BioEssays, 23*, 996-1009.

Connelly, J.C. & Leach, D.R.F. (1996). The sbcC *and* sbcD genes of *Escherichia coli* encode a nuclease involved in palindrome inviability and genetic recombination. *Genes Cells, 1*, 285-291.

Couteau, F. & Zetka, M. (2005). HTP-1 coordinates synaptonemal complex assembly with homologue alignment during meiosis in *C. elegans. Genes Dev., 19*, 2744–2756.

Cromie, G.A. & Smith, G.R. (2007). Branching out, meiotic recombination and its regulation. *Trends Cell Biol., 17*, 448-455.

Cromie, G.A., Hyppa, R.W., Cam, H.P., Farah, J.A., Grewal, S.I.S., & Smith, G.R. (2007). A discrete class of intergenic DNA dictates meiotic DNA break hotspots in fission yeast. *PLOS Genetics, 3*, e141.

Cromie, G.A., Hyppa, R.W., Taylor, A.F., Zakharyevich, K., Hunter, N., & Smith, G.R. (2006). Single Holliday junctions are intermediates of meiotic recombination. *Cell, 127*, 1167-1178.

Daish, T., Casey, A., & Grützner, F. (2009). Platypus chain reaction, directional and ordered meiotic pairing of the multiple sex chromosome chain in *Ornithorhynchus anatinus*. *Reprod. Fert. Dev., 21*, 976-984.

Daley, J.M., Palmbos, P.L., Wu, D., & Wilson, T.E. (2005). Nonhomologous end joining in yeast. *Annu. Rev. Genet., 39*, 431-451.

de Jager, M., van Noort, J., van Gent, D.C., Dekker, C., Kanaar, R., & Wyman, C. (2001). Human Rad50/Mre11 is a flexible complex that can tether DNA ends. *Mol Cell., 8*, 1129-1135.

de la Fuente, R., Parra, M.T., Viera, A., Calvente, A., Gómez, R., Suja, J.A., Rufas, J.S., & Page, J. (2007). Meiotic pairing and segregation of achiasmate sex chromosomes in eutherian mammals: The role of SYCP3 protein. *PLOS Genet., 3*, e198.

de los Santos, T., Hunter, N., Lee, C., Larkin, B., Loidl, J., & Hollingsworth, N.M. (2003). The Mus81/Mms4 endonuclease acts independently of double-Holliday junction resolution to promote a distinct subset of crossovers during meiosis in budding yeast. *Genetics, 164*, 81-94.

de Massey, B. (2003). Distribution of meiotic recombination sites. *Trends Genet., 19*, 514-522.

de Vries, S.S., Baart, E.B., Dekker, M., Siezen, A., de Rooij, D.G., de Boer, P., & te Riele, H. (1999). Mouse MutS-like protein Mlh is required for proper chromosome synapsis in male and female meiosis. *Genes Dev., 13*, 523-531.

Dernburg A.F., McDonald, K., Moulder, G., Barstead, R., Dresser, M., & Villeneuve, A.M. (1998). Meiotic recombination in *C.elegans* initiates by a conserved mechanism and is dispensable for homologous chromosome synapsis. *Cell, 94*, 387–398.

Dohm, J.C., Tsend-Ayush, E., Reinhardt, R., Grützner, F., & Himmelbauer, H. (2007). Disruption and pseudoautosomal localization of the major histocompatibility complex in monotremes. *Genome Biology, 8*:R175

Donis-Keller, H., Green, P., Helms, C., *et al.* (1987). A genetic linkage map of the human genome. *Cell, 51*, 319-337.

Doutriaux, M.-P., Couteau, F., Bergounioux, C., & White, C. (1998). Isolation and characterisation of the RAD51 and DMC1 homologs from *Arabidopsis thaliana. Mol. Gen. Genet., 257*, 283-291.

Dresser, M.E., Ewing, D.J., Conrad, M.N., Dominguez, A.M., Barstead, R., Jiang, H., & Kodadek, T. (1997). *DMC1* functions in a *Saccharomyces cerevisiae* meiotic pathway that is largely independent of the *RAD51* pathway. *Genetics, 147*, 533-544.

Drummond, A.J., Ashton, B., Buxton, S., *et al.* (2011). Geneious v5.4, Available from http://www.geneious.com/

Edelmann, W., Cohen, P.E., Kneitz, B., Winand, N., Lia, M., Heyer, J., Kolodner, R., Pollard, J.W., & Kucherlapati, R. (1999). Mammalian MutS homologue 5 is required for chromosome pairing in meiosis. *Nat. Genet., 21*, 123-127.

Edelmann, W.. Cohen, P.E., Kane, M., *et al.* (1996). Meiotic Pachytene arrest in MLH-1-deficient mice. *Cell, 85*, 1125-1134.

Edgar, R.C. (2004). MUSCLE: multiple sequence alignment with high accuracy and high throughput.*Nucleic Acids Res. 32*(5):1792-1797. doi:10.1093/nar/gkh340

Engelman, E.H. (2001). Does a stretched DNA structure dictate the helical geometry of RecA-like filaments? *J. Mol. Biol., 309*, 539-542.

Esposito, M.S. & Esposito, R.E. (1969). The genetic control of sporulation *Saccharomyces.* I. The isolation of temperature-sensitive sporulation-deficient mutants. *Genetics, 61*, 79-89.

Flicek, P. M., Amode, R., Barrell, D., *et al.* (2011). Ensembl 2011 Nucleic Acids Research 2011 39 Database issue:D800-D806 doi:10.1093/nar/gkq1064

Froenicke, L., Anderson, L.K., Wienberg, J., & Ashley, T. (2002). Male mouse recombination maps for each autosome identified by chromosome painting. *Am. J. Hum. Genet., 71*, 1353-1368.

Fujita, P. A., Rhead, B., Zweig, A.S., *et al.* (2010). The UCSC Genome Browser database: update 2011. *Nucleic Acids Res.*

Fukuda, T., Kugou, K., Sasanuma, H., Shibata, T., & Ohta, K. (2008). Targeted induction of meiotic double-strand breaks reveals chromosomal domain-dependent regulation of Spo11 and interactions among potential sites of meiotic recombination. *Nucleic Acids. Res., 36*, 984-997.

Fung, J.C., Rockmill, B., Odell, M., & Roeder, G.S. (2004). Imposition of crossover interference through the non-random distribution of synapsis initiation complexes. *Cell, 116*, 795-802.

Gaillard, P.H., Noguchi, E., Shanahan, P., & Russell, P. (2003). The endogenous Mus81-Eme1 complex resolved Holliday junctions by a nick and counter nick mechanism. *Mol. Cell, 12*, 747-759.

Gaskell, L.J., Osman, F., Gilbert, R.J.C., & Whitby, M.C. (2007). Mus81 cleavage of Holliday junctions: a failsafe for processing meiotic recombination intermediated? *EMBO J., 26*, 1891-1901.

German, J. (1993). Bloom syndrome: A mendelian prototype of somatic mutational disease. *Medicine (Baltimore), 72*, 393-406.

Gerton, J.L., DeRisi, J., Shroff, R., Lichten, M., Brown, P.O., & Petes, T.D. (2000). Global mapping of meiotic recombination hotspots and coldspots in the yeast *Saccharomyces cerevisiae. Proc. Natl. Acad. Sci. U.S.A., 97*, 11383-11390.

Gonzalez-Barrera, S., Cortes-Ledesma, F., Wellinger, R.E., & Aguilera, A. (2003). Equal sister chromatid exchange is a major mechanism of double-strand break repair: From mechanistic understanding to cancer treatment. *DNA Repair (Amst.), 6*, 923-935.

Goodyer, W., Kaitna, S., Couteau, F., *et al*. (2008). HTP-3 links DSB formation with homologue pairing and crossing over during *C. elegans* meiosis. *Dev Cell, 14*, 263–274.

Graves, J.A. (1996). Mammals that break the rules: Genetics of marsupials and monotremes. A*nnu. Rev. Genet., 30*, 233-260.

Grey, C., Baudat, F., & de Massy, B. (2009). Genome-wide control of the distribution of meiotic recombination. *PLOS Biol., 7*, 327-339.

Grützner F., Deakin, J., Rens, W., El-Mogharbel, N., & Marshall Graves, J.A. (2003). The monotreme genome, a patchwork of reptile, mammal and unique features? *Comp Biochem Physiol A Mol Integr Physiol., 136*, 867–881.

Grützner, F., Ashley, T., Rowell, D.M., & Marshall Graves, J.A. (2006). How did the platypus get its sex chromosome chain? A comparison of meiotic multiples and sex chromosomes in plants and animals. *Chromosoma, 115*, 75-88.

Guillon, H., Baudat, F., Grey, C., Liskay, M.R., & de Massy, B. (2005). Crossover and noncrossover pathways in mouse meiosis. *Mol Cell, 20*, 563-573.

Gupta, R.C., Golub, E., Bi, B., & Radding, C.M. (2001). The synaptic activity of Hs Dmc1, a human recombination protein specific to meiosis. *Proc. Natl. Acad. Sci. USA, 98*, 8433-8439.

Habu, T., Taki, T., West, A., Nishimune, Y., & Morita, T. (1996). The mouse and human homologues of *DMC1*, the yeast meiosis-specific homologous recombination gene, have a common unique form of exon-skipped transcript in meiosis. *Nucleic Acids Res., 24*, 470-477.

Haring, S.J., Lautner, L.J., Comeron, J.M., & Malone, R.E. (2004). A test of the CoHR motif associated with meiotic doublestrand breaks in *Saccharomyces cerevisiae*. *EMBO Rep*., *5*, 41–46.

Hassold, T. & Hunt, P.A. (2001). To err (meiotically) is human, studies of the genesis of human aneuploidy. *Nat Rev Genet, 2*, 280-291.

Hassold, T., Judis, L., Chan, E.R., Schwartz, S., Seftel, A., & Lynn, A. (2004). Cytological studies of meiotic recombination in human males. *Cytogenet. Genome Res*., *107*, 249-255.

Hayashi, K.., Yoshida, K.., & Matsui, Y. (2005). A histone H3 methyltransferase controls epigenetic events required for meiotic prophase. *Nature, 438*, 374-378

Henderson, K.A. & Keeney, S. (2004). Tying synaptonemal complex initiation to the formation and programmed repair of DNA double-strand breaks. *Proc. Natl. Acad. Sci. U. S. A., 101*, 4519-4524.

Henderson, K.A., Kee, K., Maleki, S., Santini, P.A., & Keeney, S. (2006). Cyclin-dependent kinase directly regulates initiation of meiotic recombination. *Cell, 125*, 1321–1332.

Henke, A., Fischer, C., & Rappold, G.A. (1993). Genetic map of the human pseudoautosomal region reveals a high rate of recombination in female meiosis at the Xp telomere. *Genomics, 18*, 478-485.

Hillers, K.J. & Villeneuve, A.M. (2003). Chromosome-wide control of meiotic crossing over in *C. elegans. Curr. Biol., 13*, 1641-1647.

Hillers, K.J. (2004). Crossover interference. *Curr. Biol., 14*, R1036-1037.

Hong, E.L., Shinohara, A., & Bishop, D.K. (2001). *Saccharomyces cerevisiae* Dmc1 protein promoted renaturation of single-stranded DNA (ssDNA) and assimilation of ssDNA into homologous super-coiled duplex DNA. *J. Biol. Chem., 276*, 41906-41912.

Hopfner, K.P., Craig, L., Moncalian, G., *et al.* (2002). The Rad50 zinc-hook is a structure joining Mre11 complexes in DNA recombination and repair. *Nature, 418*, 562-566.

Huelsenbeck, J. P. & Ronquist, F. (2001). MRBAYES: Bayesian inference of phylogeny. *Bioinformatics 17*, 754-755.

Hulten, M. (1974). Chiasma distribution at Diakinesis in the normal human male. *Hereditas, 76*, 55-78.

Hunt, P.A. & Hassold T. (2002). Sex matters in meiosis. *Science, 296*, 2181.

Hunter, N. & Kleckner, N. (2001). The single-end invasion: an asymmetric intermediate at the double-strand break to double-Holliday junction transition of meiotic recombination. *Cell, 106*, 59-70.

Hunter, S., Apweiler, R., Attwood, T.K., *et al.* (2009). InterPro: the integrative protein signature database *Nucleic Acids Res. 37* (Database Issue):D211-D215.

Jantsch, V., Pasierbek, P., Mueller, M., Dieter, S., Jantsch, M., & Loidl, J. (2004). Targeted gene knockout reveals a role in meiotic recombination for *ZHP-3*, a *Zip3*-related protein in *Caenorhabditis elegans*. *Mol. Cell. Biol., 24*(18), 7998-8006.

Jiao, K.., Salem, L., & Malone, R. (2003). Support for a meiotic recombination initiation complex: interactions among Rec102p, Rec104p, and Spo11p. *Mol. Cell. Biol., 23*, 5928–5938.

Johzuka, K. & Ogawa, H. (1995). Interaction of Mre11 and Rad50: two proteins required for DNA repair and meiosis-specific double-strand break formation in *Saccharomyces cerevisiae. Genetics, 139*, 1521-1532.

Jones, G.H. & Franklin, F.C. (2006). Meiotic crossing-over; obligation and interference. *Cell, 126*, 246-248.

Jun, J., Mandoiu, I.I., & Nelson, C.E. (2009). Identification of mammalian orthologs using local synteny. *BMC Genomics, 10*, 630.

Karow, J.K., Constantinou, A., Li, J., West, S.C., & Hickson, I.D. (2000). The Bloom's syndrome gene product promotes branch migration of Holliday junctions. *Proc. Natl. Acad. Sci, 97*, 6504-6508.

Kauppi, L., Sanjantila, A., & Jeffreys, A.J. (2002). Recombination hotspots rather than population history dominate linkage disequilibrium in the MHC class II region. *Hum. Mol. Genet., 12*(1), 33-40.

Kee, K., & Keeney, S. (2002). Functional interactions between SPO11 and REC102 during initiation of meiotic recombination in *Saccharomyces cerevisiae*. *Genetics, 160*, 111–122.

Kee, K., Protacio, R.U., Arora, C., & Keeney, S. (2004). Spatial organization and dynamics of the association of Rec102 and Rec104 with meiotic chromosomes. *EMBO J., 23*, 1815–1824.

Keeney, S. (2001). Mechanism and control of meiotic recombination initiation. *Curr. Top. Dev. Biol., 52*, 1–53.

Keeney, S. (2007). Spo11 and the formation of DNA double-strand breaks in meiosis. *Genome Dyn Stab.*, *2*, 81-123.

Keeney, S., Giroux, C.N., & Kleckner, N. (1997). Meiosis-specific DNA double-strand breaks are catalysed by Spo11, a member of a widely conserved protein family. *Cell*, *88*, 375-384.

Kent, W. J. (2002). BLAT - the BLAST-like alignment tool. *Genome Res.*, *4*, 656-664.

Klapholz, S., Waddell, C.S., & Esposito, R.E. (1985). The role of the SPO11 gene in meiotic recombination in yeast. *Genetics*, *110*, 187-216.

Kleckner, N., Zickler, D., Jones, G.H., Dekker, J., Padmore, R., Henle, J., & Hutchinson, J. (2004). A mechanical basis for chromosome function. *Proc. Natl. Acad. Sci. U.S.A.*, *101*, 12592-12597.

Kneitz, B., Cohen, P.E., Avdievich, E., *et al.* (2000). MutS homologue 4 localization to meiotic chromosomes is required for chromosome pairing during meiosis in male and female mice. *Genes Dev.*, *14*, 1085-1097.

Koehn, D. R., Haring, S.J., Williams, J.M., & Malone, R.E. (2009). Tethering recombination initiation proteins in *Saccharomyces cerevisiae* promotes double strand break formation. *Genetics*, *182*, 447-458.

Koller, P.C. & Darlington, C.D. (1934). The genetical and mechanical properties of the sex chromosomes. I. *Rattus norvegicus. J. Genet.*, *29*, 159-173.

Kong, A., Gudbjartsson, D.F., Sainz, J., *et al.* (2002). A high-resolution recombination map of the human genome. *Nat Genet.*, *31*(3), 241-247.

Kong, A., Thorleifsson, G., Stefansson, H., *et al.* (2008). Sequence variants in the *RNF212* gene associate with genome-wide recombination rate. *Science*, *319*, 1398-1401.

Kumar, R., Bourbon, H., & de Massy, B. (2010). Functional conservation of Mei4 for meiotic DNA double-strand break formation from yeast to mice. *Genes Dev.*, *24*, 1266-1280.

Lahn, B.T. & Page, D.C. (1999). Four evolutionary strata on the human X chromosome. *Science*, *286*, 964-967.

Lawson-Handley, L.J., Ceplitis, H., & Ellegren, H. (2004). Evolutionary strata on the chicken Z chromosome: Implications for sex chromosome evolution. *Genetics*, *167*, 367-376.

Lee, M.H., Chang,Y.C., Hong,E.L., Grubb,J., Chang,C.S., Bishop,D.K. & Wang,T.F. (2005). Calcium ion promotes yeast Dmc1 activity via formation of long and fine helical filaments with single-stranded DNA. *J. Biol. Chem..*, *280*, 40980–40984.

Li, J., Hooker, G.W., & Roeder, G.S. (2006). *Saccharomyces cerevisiae* Mer2, Mei4 and Rec114 form a complex required for meiotic double-strand break formation. *Genetics*, *173*, 1969–1981.

Lin, Y. & Smith, G.R. (1994). Transient, meiosis-induced expression of the rec6 and rec12 genes of *Schizosaccharomyces pombe. Genetics*, *136*, 769-779.

Lin, Y.J. (1980). Chromosome behaviour in *Rhoeo spathacea* var. *variegata. Cytobios.*, *27*, 113-128.

Lipkin, S.M., Moens, P.B., Wang, V., *et al.* (2002) Meiotic arrest and aneuploidy in MLH3-deficience mice. *Nat. Genet. 31*, 385-390.

Lipkin, S.M., Wang, V., Jacoby, R., Banerjee-Basu, S., Baxevanis, A.D., Lynch, H.T., Elliott, R.M., & Collins, F.S. (2000). MLH3: a DNA mismatch repair gene associated with mammalian microsatellite instability. *Nat. Genet.*, *24*, 27-35.

Lynn, A., Koehler, K.E., Judis, L., Chan, E.R., Cherry, J.P., Schwartz, S., Seftel, A., Hunt, P.A., & Hassold, T.J. (2002). Covariation of Synaptonemal Complex Length and Mammalian Meiotic Exchange Rates. *Science.*, *21*(296), 2222-2225.

Mahadevaiah, S.K., Turner, J.M.A., Baudat, F., *et al.* (2001). Recombinational DNA double-strand breaks in mice precede synapsis. *Nat Genet.*, *27*, 271-276.

Maleki, S., Neale, M.J., Arora, C., Henderson, K.A., & Keeney, S. (2007). Interactions between Mei4, Rec114, and other proteins required for meiotic DNA double-strand break formation in *Saccharomyces cerevisiae. Chromosoma*, *116*, 471–486.

Mao-Draayer, Y., Galbraith, A.M., Pittman, D.L., Cool, M. & Malone, R.E. (1996). Analysis of meiotic recombination pathways in the yeast Saccharomyces cerevisiae. *Genetics, 144*, 71–86.

Marcon, E. & Moens, P. (2003). MLH1p and MLH3p localize to precociously induced chiasmata of okadaic-acid-treated mouse spermatocytes. *Genetics, 165*, 2283-2287.

Marcon, E. & Moens, P.B. (2005). The evolution of meiosis: recruitment and modification of somatic DNA-repair proteins. *BioEssays, 27*, 795-808.

Martinez-Perez E., Schvarzstein, M., Barroso, C., Lightfoot, J., Dernburg, A.F., & Villeneuve, A.M. (2008). Crossovers trigger a remodelling of meiotic chromosome axis composition that is linked to two-step loss of sister chromatid cohesion. *Genes Dev*., *22*, 2886–2901.

Martinez-Perez, E. & Villeneuve, A.M. (2005). HTP-1-dependent constraints coordinate homologue pairing and synapsis and promote chiasma formation during *C. elegans* meiosis. *Genes Dev*., *19*, 2727–2743.

Masson, J.Y., Davies, A.A., Hajibagheri, N., Van Dyck, E., Benson, F.E., Stasiak, A.Z., Stasiak, A., & West, S.C. (1999). The meiosis-specific recombinase hDmc1 forms ring structures and interacts with hRad51. *EMBO J.*, *18*, 6552-6560.

McIlwraith, M.J., Van Dyck, E., Masson, J.Y., Stasiak, A.Z., Stasiak, A., & West, S.C. (2000). Reconstitution of the strand invasion step of double-strand break repair using human Rad51 Rad52 and RPA proteins. *J Mol Biol*., *304*, 151–164.

McKee, A.H.Z., & Kleckner, N. (1997). A general method for identifying recessive diploid-specific mutations in *Saccharomyces cerevisiae*, its application to the isolation of mutants blocked at intermediate stages of meiotic prophase and characterization of a new gene *SAE2. Genetics, 146*, 797-816.

McKim, K.S. & Hayashi-Hagihara, A. (1998). mei-W68 in Drosophila melanogaster encodes a Spo11 homologue: evidence that the mechanism for initiating meiotic recombination is conserved. *Genes Dev., 12*, 2932-2942.

McPherson, J.P., Lemmers, B., Chahwan, R., *et al.* (2004). Involvement of mammalian Mus81 in genome integrity and tumour suppression. *Science*, *304*, 18220-1826.

Meneely, P.M., Farago, A.F., & Kauffman, T.M. (2002). Crossover distribution and high interference for both the X chromosome and an autosome during oogenesis and spermatogenesis in *Caenorhabditis elegans. Genetics*, *162*, 1169-1177.

Mieczkowski, P.A., Dominska, M., Buck, M.J., Gerton, J.L., Lieb, J.D., & Petes, T.D. (2006). Global analysis of the relationship between the binding of the Bas1p transcription factor and meiosis-specific double-strand DNA breaks in *Saccharomyces cerevisiae. Mol. Cell Biol., 26*, 1014-1027.

Mihola O., Trachtulec, Z., Vlcek, C., Schimenti, J.C., & Forejt, J. (2008). A mouse speciation gene encodes a meiotic histone H3 methyltransferase. *Science*, *323*(5912), 373-375.

Mimitou, E.P. & Symington, L.S. (2009). DNA end resection: many nucleases make light work. *DNA Repair (Amst), 8*(9), 983-995.

Moens, P.B., Kolas, N.K., Tarsounas, M., Marcon, E., Cohen, P.E., & Spyropoulos, B. (2002). The time course and chromosomal localization of recombination-related proteins at meiosis in the mouse are compatible with models that can resolve the early DNA-DNA interactions without reciprocal recombination. *J. Cell Sci., 115*, 1611-1622.

Moosani, N., Pattinson, H.A., Carter, M.D., Cox, D.M., Rademaker, A.W., & Martin, R.H. (1995). Chromosomal analysis of sperm from men with idiopathic infertility using sperm karyotyping and fluorescence in situ hybridization. *Fertil. Steril., 64*, 811-817.

Morton, N.E. & Collins, A. (1990). Standard maps of chromosome 10. *Ann. Hum. Genet., 54*, 235-251.

Nabeshima, K., Villeneuve, A.M., & Hillers, K.J. (2004). Chromosome-wide regulation of meiotic crossover formation in *aenorhabditis elegans* requires properly assembled chromosome axes. *Genetics*, *168*, 1275-1292.

Nairz, K. & Klein, F. (1997). *mre11S*—A yeast mutation that blocks double-strand break processing and permits nonhomologous synapsis in meiosis. *Genes & Dev., 11*, 2272-2290.

Neale, M.J., Pan, J., & Keeney, S. (2005). Endonucleolytic processing of covalent protein-linked DNA double-strand breaks. *Nature*, *436*, 1053-1057.

Neyton, S., Lespinasse, F., Moens, P.B., Paul, R., Gaudray, P., Paguis-Flucklinger, V., Santucci-Darmanin, S. (2004). Association between MSH4 (MutS homologue 4) and the DNA strand-exchange RAD51 and DMC1 proteins during mammalian meiosis. *Mol. Hum. Reprod., 10*, 917-924

Niu, H., Wan, L., Baumgartner, B., Schaefer, D., Loidl, J., & Hollingsworth, N.M. (2005). Partner choice during meiosis is regulated by Hop1-promoted dimerization of Mek1. *Mol. Biol. Cell, 16*, 5804-5818.

Nonomura, K.I., Nakano, M., Murata, K., *et al*. (2004). An insertional mutation in the rice *PAIR2* gene, the ortholog of *Arabidopsis ASY1*, results in a defect in homologous chromosome pairing during meiosis. *Mol Genet Genomics*, *271*, 121–129.

Novak, J.E., Ross-Macdonald, P.B., & Roeder, G.S. (2001). The budding yeast Msh4 protein functions in chromosome synapsis and the regulation of crossover distribution. *Genetics*, *158*, 1013-1025.

Ogawa, T., Yu, X., Shinohara, A., & Egelman, E.H. (1993). Similarity of the yeast RAD51 filament to the bacterial RecA filament. *Science, 259*, 1896-1899.

Oh, S.D., Lao, J.P., Hwang, P.Y., Taylor, A.F., Smith, G.R., & Hunter, N. (2007). BLM ortholog, Sgs1, prevents aberrant crossing-over by suppressing formation of multichromatid joint molecules. *Cell, 130*, 259-272.

Ohno, S., Kaplan, W.D., & Kinositar (1959). Do XY- and O-sperm occur in *Mus musculus*? *Exp. Cell. Res., 18*, 382-384.

Oliver, P.L., Goodstadt, L., Bayes, J.J., *et al.* (2009). Accelerated evolution of the *Prdm9* speciation gene across diverse metazoan taxa. *PLoS Genetics., 5*(12), e1000753

Oliver-Bonet, M., Turek, P.J., Sun, F., Ko, E., & Martin, R.H. (2005). Temporal progression of recombination in human males. *Mol. Hum. Rep., 11*, 517-522.

Osman, F., Dixon, J., Doe, C.L., & Whitby, M.C. (2003). Generating crossovers by resolution of nicked Holliday junctions, a role for Mus81-Eme1 in meiosis. *Mol Cell, 12*, 761-774.

Page, D.C., Bieker, K., Brown, L.G., *et al.* (1987). Linkage, physical mapping and DNA sequence analysis of pseudoautosomal loci on the human X and Y chromosomes. *Genetics, 1*, 243-256.

Page, J., Berríos, S., Parra, M.T., Viera, A., Suja, J.A., Prieto, I., Barbero, J.L., Rufas, J.S., & Fernández-Donoso, R. (2005). The program of sex chromosome pairing in meiosis is highly conserved across marsupial species: Implications for sex chromosome evolution. *Genetics*, *170*, 793-799.

Page, J., Berrios, S., Rufas, J.S., Parra, M.T., Suja, J.A., Heyting, C., & Fernández-Donoso, R. (2003). The pairing of X and Y chromosomes during meiotic prophase in the marsupial species *Thylamys elegans* is maintained by a dense plate developed from their axial elements. *J. Cell Sci., 116*, 551-560.

Page, J., Viera, A., Parra, M.T., *et al.* (2006). Involvement of synaptonemal complex proteins in sex chromosome segregation during marsupial male meiosis. *PLOS Genet., 2*, e136.

Page, S.L. & Hawley, R.S. (2003). Chromosome choreography: the meiotic ballet. *Science*, *301*, 785-789.

Pagni, M., Ioannidis, V., Cerutti, L., Zahn-Zabal, M., Jongeneel, C.V., Hau, J., Martin, O., Kuznetsov, D., & Falguet, L. (2007). MyHits: improvements to an interactive resource for analyzing protein sequences. *Nuc. Acid. Res., 35*, W433–W437 doi:10.1093/nar/gkm352.

Pasco, L. & Morton, N.E. (1987). The use of map functions in multipoint mapping. *Am. J. Hum. Genet., 40*, 174-183.

Passy, S.I., Yu, X., Li, Z., Radding, C.M., Masson, J., West, S.C., & Egelman, E.H. (1999). Human Dmc1 protein binds DNA as an octameric ring. *Proc. Natl. Acad. Sci. USA, 96*, 10694-10688.

Pawlowski, W.P. & Cande, W.Z. (2005). Coordinating the events of the meiotic prophase *Trends Cell Biol., 15*, 674-681.

Pearson, P.L. & Bobrow, M. (1970). Definitive evidence for the short arm of the Y chromosome associating with the X during meiosis in the human male. *Nature, 226*, 959-961

Peciña, A., Smith, K.N., Mézard, C., Murakami, H., Ohta, K., & Nicolas, A. (2002). Targeted stimulation of meiotic recombination. *Cell, 111*, 173–184.

Perry, J., Palmer, S., Gabriel, A., & Ashworth, A. (2001). A short pseudoautosomal region in laboratory mice. *Genome Res., 11*, 1826-1832.

Petes, T. D. (2001). Meiotic recombination hot spots and cold spots. *Nat. Rev. Genet., 2*, 360–369.

Petkov, P.M., Broman, K.W., Szatkiewicz, J.P., & Paigen, K. (2007). Crossover interference underlies sex differences in recombination rates. *Trends Genet., 23*, 529-542.

Pigozzi, M.I. & Solari, A.J. (1997). Extreme axial equalization and wide distribution of recombination nodules in the primitive ZW pair of *Rhea Americana* (Aves, Ratitae). *Chromosome Res., 5*, 421-428.

Pigozzi, M.I. & Solari, A.J. (2005). Meiotic recombination in the ZW pair of a trinamid bird shows a differential pattern compared with neognaths. *Genome, 48*, 286-290.

Pigozzi, M.I. (2001). Distribution of MLH1 foci on the synaptonemal complexes of chicken oocytes. *Cyt. Cell Genet., 95*, 129-133.

Pittman, D.L., Cobb, J., Schimenti, K.J., Wilson, L.A., Cooper, D.M., Brignull, E., Handel, M.A., & Schimenti, J.C. (1998). Meiotic prophase arrest with failure of chromosome synapsis in mice deficient for Dmc1, a germ-line-specific RecA homologue. *Mol. Cell, 1*, 697-705.

Plug A.W., Peters, A.H., Keegan, K.S., Hoekstra, M.F., de Boer, P., & Ashley, T. (1998). Changes in protein composition of meiotic nodules during mammalian meiosis. *J Cell Sci., 111*, 413–423.

Prieler, S., Penkner, A., Borde, V., & Klein, F. (2005). The control of Spo11's interaction with meiotic recombination hotspots. *Genes Dev., 19*, 255-269.

Prinz, S., Amon, A., & Klein, F. (1997). Isolation of *COM1*, a new gene required to complete meiotic double-strand break induced recombination in *Saccharomyces cerevisiae. Genetics, 146*, 781-795.

Qin, J., Richardson, L.L., Jasin, M., Handel, M.A., & Arnheim, N. (2004). Mouse strains with an active H2-Ea meiotic recombination hot spot exhibit increased levels of H2-Ea-specific DNA breaks in testicular germ cells. *Mol Cell Biol., 24*, 1655-1666.

Rappold, G.A., Klink, A., Weiss, B., & Fischer, C. (1994). Double crossover in the human Xp/Yp pseudoautosomal region and its bearing on interference. *Hum. Mol. Genet., 3*, 1337-1340.

Ratomponirina, C., Viegas-Péguignot, E., Dutrillaux, B., Petter, F., & Rumpler, Y. (1986). Synaptonemal complexes in the Gerbillidae: probable role of intercalated heterochromatin in genosome-autosome translocations. *Cytogenet. Cell Genet., 43*, 161-167.

Rens, W., Grützner, F., O'brien, P.C., Fairclough, H., Graves, J.A., & Ferguson-Smith, M.A. (2007). The multiple sex chromosomes of platypus and echidna are not completely identical and several share homology with the avian Z. *Genome Biol., 8*, R243.

Rens, W., Grützner, F., O'brien, P.C., Fairclough, H., Graves, J.A., & Ferguson-Smith, M.A. (2004). Resolution and evolution of the duckbilled platypus karyotype with an X1Y1X2Y2X3Y3X4Y4X5Y5 male sex chromosome constitution. *Proc. Natl Acad. Sci., 101*, 16257-16261.

Rickards, G.K. (1983). Orientation behaviour of chromosome multiples of interchange (reciprocal translocation) heterozygotes. *Annu. Rev. Genet., 17*, 443-498.

Roca, A.I. & Cox, M.M. (1997). RecA protein: structure, function, and role in recombinational DNA repair. *Prog Nuclcic. Acid Res. Mol. Biol., 56*, 129-223.

Roche, L., Seluja, G., & Wettstein, R. (1986). The meiotic behaviour of the XY pair in *Lutreolina crassicaudata* (Marsupialia: Didelphoidea). *Genetica, 71*, 213-224.

Rockmill, B. Fung, J.C., Branda, S.S., & Roeder, G.S. (2003). The Sgs1 helicase regulates chromosome synapsis and meiotic crossing over. *Curr. Biol., 13*, 1954-1962.

Rockmill,B. & Roeder,G.S. (1990). Meiosis in asynaptic yeast. *Genetics, 126*, 563–574.

Roderick, T.H., Davisson, M.T., & Doolittle, D.P. (1996). Recombination Percentages and chromosomal assignments. In *Genetic Variants and Strains of the Laboratory Mouse* (Lyon, M.F. and Searly, A.G., eds), pp.929-1255, Oxford University Press.

Roeder, G.S. (1997). Meiotic chromosomes, it takes two to tango. *Genes Dev*., *11*, 2600-2621.

Romanienko, P.J. & Camerini-Otero, R.D. (2000). The mouse *Sp11* gene is required for meiotic chromosome synapsis. *Mol. Cell*, *6*, 975-987.

Ronquist, F. & Huelsenbeck, J.P. (2003). MRBAYES 3: Bayesian phylogenetic inference under mixed models. *Bioinformatics, 19*, 1572-1574.

Rouyer, F., Simmler, M., Johnsson, C., Vergnaud, G., Cooke, H.J., & Weissenbach, J. (1986). A gradient of sex linkage in the pseudoautosomal region of the human sex chromosomes. *Nature*, *319*, 291-295.

Salem, L., Walter, N., & Malone, R. (1999). Suppressor analysis of the *Saccharomyces cerevisiae* gene REC104 reveals a genetic interaction with REC102. *Genetics*, *151*, 1261–1272.

Sanchez-Moran, E., Santos, J.L., Jones, G.H., & Franklin, F.C. (2007). ASY1 mediates AtDMC1-dependent interhomologue recombination during meiosis in *Arabidopsis. Genes Dev*., *21*, 2220–2233.

Sandler, S.J., Hugenholtz, P., Schleper, C., DeLong, E.F., Pace, N.R., & Clark, A.J. (1999). Diversity of radA genes from cultured and uncultured archaea: comparative analysis of putative RadA proteins and their use as a phylogenetic marker. *J. Bacteriol*, *181*, 907-915.

Santucci-Darmanin, S., Neyton, S., Lespinasse, F., Saunièrer, A., Gaudray, P., & Paquis-Flucklinger, V. (2002). The DNA mismatch-repair MLH3 protein interacts with MSH4 in meiotic cells, supporting a role for this MutL homologue in mammalian meiotic recombination. *Hum. Mol. Genet., 11*, 1697-1706.

Santucci-Darmanin, S., Walpita, D., Lespinasse, F., Desnuelle, C., Ashley, T., & Paguis-Flucklinger, V. (2000). MSH4 acts in conjunction with MLH1 during mammalian meiosis. *Faseb J., 14*, 1539-1547.

Sasanuma, H., Hirota, K., Fukuda, T., Kakusho, N., Kugou, K., Kawasaki, Y., Shibata, T., Masai, H., & Ohta, K. (2008). Cdc7-dependent phosphorylation of Mer2 facilitates initiation of yeast meiotic recombination. *Genes Dev*., *22*, 398–410.

Sauvageau, S., Stasiak,A.Z., Banville, I., Ploquin, M., Stasiak, A. & Masson, J.Y. (2005). Fission yeast rad51 and dmc1, two efficient DNA recombinases forming helical nucleoprotein filaments. *Mol. Cell. Biol*., *25*, 4377–4387.

Schmitt, K., Lazzeroni, L.C., Foote, S., Vollrath, D., Fisher, E.M.C., Goradia, T.M., Lange, K., Page, D.C., & Arnheim, N. (1994). Multipoint linkage map of the human pseudoautosomal region, based on single-sperm typing: Do double crossovers occur during male meiosis? *Am. J. Hum. Genet., 55*, 423-430.

Schwacha A. & Kleckner, N. (1994). Identification of joint molecules that form frequently between homologues but rarely between sister chromatids during yeast meiosis. *Cell, 76*, 51–63.

Schwacha, A. & Kleckner, N. (1995). Identification of double Holliday junctions as intermediates in meiotic recombination. *Cell*, *83*, 783-791.

Schwacha, A. & Kleckner, N. (1997). Interhomologue bias during meiotic recombination: meiotic functions promote a highly differentiated interhomologue-only pathway. *Cell, 90*, 1123-1135.

Sehorn, M.G., Sigurdsson, S., Bussen, W., Unger, V.M., & Sung, P. (2004). Human meiotic recombinase Dmc1 promotes ATP-dependent homologous DNA strand exchange. *Nature, 429*, 433–437.

Sekelsky, J.J., Brodsky, M.H., & Brutis, K.C. (2000). DNA repair in Drosophila: insights from the *Drosophila* genome sequence. *J. Cell Biol., 150*, F31-F36.

Seluja, G.A., Roche, L., & Solari, A.J. (1987). Male meiotic prophase in *Didelphis albiventris. J. Heredity, 78*, 218-222.

Shannon, M., Richardson, L., Christian, A., Handel, M.A., & Thelen, M.P. (1999). Differential gene expression of mammalian SPO11/TOP6A homologues during meiosis. *FEBS Lett., 462*, 329-334.

Sharma, S., Doherty, K.M., & Brosh, R.M. (2006). Mechanisms of RecQ helicases in pathways of DNA metabolism and maintenance of genomic stability. *Biochem. J., 398*, 319-337.

Sharp, P. (1982). Sex chromosome pairing during male meiosis in marsupials. *Chromosoma, 86*, 27-47.

Sharples, G.J. & Leach, D.R.F. (1995). Structural and functional similarities between the SbcCD proteins of *Escherichia coli* and the Rad50 and Mre11 (Rad32) recombination and repair proteins of yeast. *Mol. Microbiol., 17*, 1215-1220.

Sheridan, S.D., Yu, X., Roth, R., Heuser, J.E., Sehorn, M.G., Sung, P., Egelman, E.H., & Bishop, D.K. (2008). A comparative analysis of Dmc1 and Rad51 nucleoprotein filaments. *Nucleic Acids Research, 36*, 4057-4066.

Shields, D.C., Collins, A., Buetow, K.H., & Morton, N.E. (1991). Error filtration, interference, and the human linkage map. *Proc. Natl. Acad. Sci. U. S. A., 88*, 6501-6505.

Shim, K.S., Schmutte, C., Tombline, G., Heinen, C.D., & Fishel, R. (2004). hXRCC2 enhances ADP/ATP processing and strand exchange by hRAD51. *J. Biol. Chem., 279*, 30385-30394.

Shinohara, A. & Shinohara, M. (2004). Roles of RacA homologues Rad51 and Dmc1 during meiotic recombination. *Cytogenet. Genome Res., 107*, 201-207.

Shinohara, A., Gasior, S., Ogawa, T., Kleckner, N., & Bishop, D.K. (1997). *Saccharomyces cerevisiae recA* homologueues *RAD51* and *DMC1* have both distinct and overlapping roles in meiotic recombination. *Genes Cells, 2*, 615-629.

Shinohara, A., Ogawa, H., & Ogawa, T. (1992). Rad51 protein involved in repair and recombination in *S. cerecisiae* is a RecA-like protein. *Cell, 69*, 457-470.

Shinohara, A., Ogawa, H., Matsuda, Y., Ushio, N., Ikeo, K., & Ogawa, T. (1993). Cloning of human, mouse, and fission yeast recombination genes homologous to *RAD51* and *recA*. *Nat. Genet., 4*, 239-243.

Shinohara, M., Gasior, S.L., Bishop, D.K., & Shinohara, A. (2000). Tid1/Rdh54 promotes colocalization of Rad51 and Dmc1 during meiotic recombination. *Proc. Natl. Acad. Sci. USA, 97*, 10814-10819.

Smith, G.R., Boddy, M.N., Shanahan, P., & Russell, P. (2003). Fission yeast Mus81-Eme1 Holliday junction resolvase is required for meiotic crossing over but not for gene conversion. *Genetics, 165*, 2289-2293.

Snowden, T., Acharya, S., Butz, C., Berardini, M., & Fishel, R. (2004). hMSH4-hMSH5 recognizes Holliday Junctions and forms a meiosis-specific sliding clamp that embraces homologous chromosomes. *Mol. Cell, 15*, 437-451.

Solari, A.J. & Ashley, T. (1977). Ultrastructure and behaviour of the achiasmatic telosynaptic XY pair of the sand rat (*Psammomys obesus*). *Chromosoma, 62*, 319-336.

Solari, A.J. & Bianchi, N.O. (1975). The synaptonemal behaviour of the X and Y chromosomes in the marsupial *Monodelphis dimidiate. Chromosoma, 52*, 11-25.

Solari, A.J. (1974). The behaviour of the XY pair in mammals. *Int. Rev. Cytol., 38*, 273-317.

Solari, A.J. (1980). Synaptonemal complexes and associated structures in microspread human spermatocytes. *Chromosoma, 81*, 315-337.

Sonoda, E., Sasaki, M.S., Morrison, C., Yamaguchi-Iwai, Y., Takata, M., & Takeda, S. (1999). Sister chromatid exchanges are mediated by homologous recombination in vertebrate cells. *Mol. Cell Biol., 19*, 5166-5169.

Soriano, P., Keitges, E.A., Schorderet, D.F., Harbers, K., Gartler, S.M., & Jaenisch, R. (1987). High rate of recombination and double crossovers in the mouse pseudoautosomal region during male meiosis. *Proc. Natl. Acad. Sci. U. S. A., 84*, 7218-7220

Stack, S.M. & Soulliere, D.L. (1984). The relationship between synapsis and chiasma formation in *Rhoeo spathacea. Chromosoma, 90*, 72-83.

Storlazzi, A., Tessé, S., Gargano, S., James, F., Kleckner, N., & Zickler, D. (2003). Meiotic double-strand breaks at the interface of chromosome movement, chromosome remodelling and reductional division. *Genes Dev., 17*, 2675-2687.

Sun, F., Mikhaail-Pjilips, M., Oliver-Bonet, M., Ko, E., Rademaker, A., Turek, P., & Martin, R.H. (2008). The relationship between meiotic recombination in human spermatocytes and aneuploidy in sperm. *Hum. Reprod.,* Doi:10.1093/humrep/den027.

Sun, F., Oliver-Bonet, M., Liehr, T., Starke, H., Turek, P., Ko, E., Rademaker, A., & Martin, R.H. (2006). Variation in MLH1 distribution in recombination maps for individual chromosomes from human males. *Hum. Mol. Genet., 15*(15), 2376-2391.

Sun, H., Treco, D., Schultes, N.P., & Szostak, J.W. (1989). Double-strand breaks at an initiation site for meiotic gene conversion. *Nature, 338*, 87-90.

Sung, P., Krejci, L., Van Komen, S., & Sehorn, M.G. (2003). Rad51 recombinase and recombination mediators. *J. Biol. Chem.., 278*, 42729-42732.

Svetlanov, A. & Cohen, P. (2004). Mismatch repair proteins, meiosis, and mice: understanding the complexities of mammalian meiosis. *Exp. Cell Res., 296*, 71-79.

Sym, M. & Roeder, G.S. (1994). Crossover interference is abolished in the absence of synaptonemal complex protein. *Cell, 79*, 283-292.

Symington, L.S. (2002). Role of *RAD52* epistasis group genes in homologous recombination and double-strand break repair. *Microbiol. Mol. Biol. Rev., 66*, 630-670.

Szostak, J.W., Orr-Weaver, T.L., Rothstein, R.J., & Stahl, F.W. (1983). The double-strand-break repair model for recombination. *Cell, 33*,25-35.

Tarounas, M., Morita, T., Pearlman, R.E., & Moens, P.B. (1999). RAD51 and DMC1 form mixed complexes associated with mouse meiotic chromosome cores and synaptonemal complexes. *J. Cell Biol., 147*, 207-220.

Tease, C. & Hulten, M.A. (2004). Inter-sex variation in synaptonemal complex lengths largely determine the different recombination rates in male and female germ cells. *Cytogenet. Genome Res., 107*, 208-215.

Terasawa, M., Ogawa, H., Tsukamoto, Y., Shinohara, M., Shirahige, K., Kleckner, N., & Ogawa, T. (2007). Meiotic recombination-related DNA synthesis and its implications for cross-over and non-cross-over recombinant formation. *Proc. Natly. Acad. Sci. U. S. A., 104*, 5965-5970.

Terasawa,M., Shinohara, A., Hotta, Y., Ogawa, H., & Ogawa, T. (1995). Localization of RecA-like recombination proteins on chromosomes of the lily at various meiotic stages. *Genes Dev., 9*, 925-934.

Toder, R., Wakefield, M.J., & Graves, J.A. (2000). The minimal mammalian Y chromosome—the marsupial Y as a model system. *Cytogenet. Cell Genet., 91*, 285-292.

Uetz, P., Giot, L., Cagney, G., *et al*. (2000). A comprehensive analysis of protein-protein interactions in *Saccharomyces cerevisiae*. *Nature, 403*: 623–627.

van Brabant, A.J. (2000). Binding and melting of D-loops by the Bloom syndrome helicase. *Biochemistry, 39*, 14617-14625.

Van Brink J. (1959) L'expression morphologique de la diagametie chez les sauropsids et les monotremes. *Chromosoma, 10*, 1–72.

Veyrunes, F., Watersm P.D., Miethke, P,, *et al.* (2008). Bird-like sex chromosomes of platypus imply recent origin of mammalian sex chromosomes. *Genome Res., 18*, 965-973.

Wan, L., de los Santos, T., Zhang, C., Shokat, K., & Hollingsworth, N.M. (2004). Mek1 kinase activity functions downstream of RED1 in the regulation of meiotic double strand break repair in budding yeast. *Mol. Biol. Cell, 15*, 11-23.

Wang, H., Guan, J., Perrault, A.R., Wang, Y., & Iliakis, G. (2001). Replication protein A2 phosphorylation after DNA damage by the coordinated action of ataxia telangiectasia-mutated and DNA-dependent protein kinase. *Cancer Res., 61*, 8554–8563.

Ward, J.O., Reinholdt, L.G., Motley, W.W., *et al.* (2007). Mutation in mouse hei10, an e3 ubiquitin ligase, disrupts meiotic crossing over. *PLoS Genet.***,** *3*(8), e139.

Warren W.C., Hillier L.W., Graves J.A.M., *et al.* (2008). Genome analysis of the platypus reveals unique signatures of evolution. *Nature, 453*, 175–183.

Whitby, M.C. (2001). Making crossovers during meiosis. *Biochem. Soc. Trans., 33*, 1451-1455.

Whitby, M.C., Osman, F., & Dixon, J. (2003). Cleavage of model replication forks by fission yeast Mus81-Eme1 and budding yeast Mus81-Mms4. *J Biol. Chem., 278*, 6928-2935.

Wiltshire, T., Park, C., Caldwell, K.A., & Handel, M.A. (1995). Induced premature G2/M-phase transition in Pachytene spermatocytes includes events unique to meiosis. *Dev. Biol., 169*, 557-567.

Wiltzius J.J., Hohl, M., Fleming, J.C., & Petrini, J.H. (2005). The Rad50 hook domain is a critical determinant of Mre11 complex functions. *Nat Struct Mol Biol*., *12*, 403–407.

Wojtasz, L., Daniel, K., Roig, I., *et al.* (2009). Mouse HORMAD1 and HORMAD2, two conserved meiotic chromosomal proteins, are depleted from synapsed chromosomal axes with the help of TRIP13 AAA-ATPase. *Plos Genetics., 5*(10): e1000702

Wold MS. (1997). Replication protein A: a heterotrimeric, single-stranded DNA-binding protein required for eukaryotic DNA metabolism. *Annu Rev Biochem*., *66*:61–92.

Wolf, K.W., Baumgart, K., & Winking, H. (1988). Meiotic association and segregation of the giant sex chromosomes in male field vole (*Microtus agrestis*). *Chromosoma*, *97*, 124-133.

Woltering D., Baumgartner, B., Bagchi, S., Larkin, B., Loidl, J., de los Santos, T., & Hollingsworth, N.M. (2000). Meiotic segregation, synapsis, and recombination checkpoint functions require physical interaction between the chromosomal proteins Red1p and Hop1p. *Mol Cell Biol*., *20*, 6646–6658.

Wu, L. & Hickson, I.D. (2003). The Bloom's syndrome helicase suppresses crossing over during homologous recombination. *Nature, 426*, 870-874.

Wu, L. & Hickson, I.D. (2006). DNA helicases required for homologous recombination and repair of damaged replication forks. *Annu. Rev. Genet., 40*, 279-306.

Yates, R.D. & Goodman, D.J. (2005). *Probability and Stochastic Processes, Second Edition*. John Wiley and Sons, Inc. Chapter 1: p. 15.

Yauk, C.L., Bois, P.R.J., & Jeffreys, A.L. (2003). High-resolution sperm typing of meiotic recombination in the mouse MHC E_β gene. *EMBO Journal*, *22*, 1389-1397.

Yoshida, K., Kondoh, G., Matsuda, Y., Habu, T., Nishimune, Y., & Morita, T. (1998). The mouse RecA-like gene Dmc1 is required for homologous chromosome synapsis during meiosis. *Mol. Cell, 1*, 707-718.

Young, J.A., Schreckhise, R.W., Steiner, W.W., & Smith, G.R. (2002). Meiotic recombination remote from prominent DNA break sites in *S. pombe. Mol. Cell*, *9*, 253-263.

Zalevsky, J., MacQueen, A.J., Duffy, J.B., Kemphues, K.J., & Villeneuve, A.M. (1999). Crossing over during *Caenorhabditis elegans* meiosis requires a conserved MutS-based pathway that is partially dispensable in budding yeast. *Genetics, 153*, 1271-1283.

Zetka, M.C., Kawasaki, I., Strome, S., & Muller, F. (1999). Synapsis and chiasma formation in *Caenorhabditis elegans* require HIM-3, a meiotic chromosome core component that functions in chromosome segregation. *Genes Dev*., *13*, 2258–2270.

Zickler, D. & Kleckner, N. (1999). Meiotic chromosomes: integrating structure and function. *Annu. Rev. Genet., 33*, 603-754.